ISSN 1881-7831 Online ISSN 1881-784X

DD&T

Drug Discoveries & Therapeutics

Volume 17, Number 3
June, 2023

IRCA BSSA
IACMHR

www.ddtjournal.com

DD&T
Drug Discoveries & Therapeutics

ISSN: 1881-7831
Online ISSN: 1881-784X
CODEN: DDTRBX
Issues/Year: 6
Language: English
Publisher: IACMHR Co., Ltd.

Drug Discoveries & Therapeutics is one of a series of peer-reviewed journals of the International Research and Cooperation Association for Bio & Socio-Sciences Advancement (IRCA-BSSA) Group. It is published bimonthly by the International Advancement Center for Medicine & Health Research Co., Ltd. (IACMHR Co., Ltd.) and supported by the IRCA-BSSA.

Drug Discoveries & Therapeutics publishes contributions in all fields of pharmaceutical and therapeutic research such as medicinal chemistry, pharmacology, pharmaceutical analysis, pharmaceutics, pharmaceutical administration, and experimental and clinical studies of effects, mechanisms, or uses of various treatments. Studies in drug-related fields such as biology, biochemistry, physiology, microbiology, and immunology are also within the scope of this journal.

Drug Discoveries & Therapeutics publishes Original Articles, Brief Reports, Reviews, Policy Forum articles, Case Reports, Communications, Editorials, News, and Letters on all aspects of the field of pharmaceutical research. All contributions should seek to promote international collaboration in pharmaceutical science.

Editorial Board

Editorial and Head Office:

Pearl City Koishikawa 603,
2-4-5 Kasuga, Bunkyo-ku,
Tokyo 112-0003, Japan
E-mail: office@ddtjournal.com

Drug Discoveries & Therapeutics

Editorial and Head Office

Pearl City Koishikawa 603, 2-4-5 Kasuga, Bunkyo-ku,
Tokyo 112-0003, Japan

E-mail: office@ddtjournal.com
URL: www.ddtjournal.com

Editorial Board Members

CONTENTS

Volume 17, Number 3, 2023

Review

Original Article

Brief Report

Correspondence

Letter to the Editor

Review

DOI: 10.5582/ddt.2022.01097

A systematic review on anti-diabetic action of 7-*O*-galloyl-D-sedoheptulose, a polyphenol from Corni Fructus, in type 2 diabetic mice with hepatic and pancreatic damage

Chan Hum Park[1,*], Jeong Sook Noh[2], Jin Pyeong Jeon[3,*], Takako Yokozawa[4,*]

[1] Institute of New Frontier Research Team, Research Institute of Medical-Bio Convergence, Hallym University, Chuncheon, Republic of Korea;
[2] Department of Food Science and Nutrition, Tongmyong University, Busan, Republic of Korea;
[3] Department of Neurosurgery, College of Medicine, Hallym University, Chuncheon, Republic of Korea;
[4] Graduate School of Science and Engineering for Research, University of Toyama, Toyama, Japan.

SUMMARY Traditional medicines are recently being focused on to treat diabetes and its complications because of their lack of toxic and/or side effects. This report describes the effects of 7-*O*-galloyl-D-sedoheptulose (GS), a polyphenolic compound isolated from Corni Fructus, on type 2 diabetic *db/db* mice with hepatic and pancreatic damage. We examined several biochemical factors and oxidative stress- and inflammation-related markers. In the serum, levels of glucose, leptin, insulin, C-peptide, resistin, tumor necrosis factor-α, and interleukin-6 were down-regulated, while adiponectin was augmented by GS treatment. In addition, GS suppressed the reactive oxygen species and lipid peroxidation in the serum, liver, and pancreas, but increased the pancreatic insulin and pancreatic C-peptide contents. These results were derived from attenuating the expression of nicotinamide adenine dinucleotide phosphate oxidase subunit proteins, Nox-4 and $p22^{phox}$. Augmented nuclear factor (NF)-E2-related factor 2 and heme oxygenase-1 were reduced with a decrease in oxidative stress during GS treatment. NF-κB-related pro-inflammatory factors were also alleviated in hepatic tissue. Moreover, GS modulated the protein expressions of pro-inflammatory NF-κB, cyclooxygenase-2, inducible nitric oxide synthase, c-Jun N-terminal kinase (JNK), phosphor-JNK, activator protein-1, transforming growth factor-β_1, and fibronectin. Based on these results, we demonstrated that the anti-diabetic action of GS may be due to its anti-oxidative stress property and anti-inflammatory action.

Keywords 7-*O*-galloyl-D-sedoheptulose, type 2 diabetes, liver, pancreas, oxidative stress, inflammation, fibrosis

1. Introduction

Changes in lifestyle and diet have resulted in increasing rates of obesity, and obesity has been considered as a causative factor for several diseases, such as type 2 diabetes, hypertension, cardiovascular disease, various infectious diseases, and cancer. Among these problems related to obesity, the most devastating may be type 2 diabetes. Type 2 diabetes, a complex metabolic disorder, is a major health problem associated with high morbidity, mortality, and health-care costs (*1*). Therefore, prevention and the implementation of intervention for people with type 2 diabetes should become a public health priority worldwide.

Type 2 diabetes is a systematic multi-organ dysfunction caused by dynamic interplay among different organs (*2*). It is characterized by reduced responsiveness to normal circulating concentrations of insulin through a long period of insulin resistance (*3*). In particular, hepatic insulin resistance is a principal component of type 2 diabetes. Decreased insulin sensitivity in the liver leads to elevated hepatic glucose production, hyperinsulinemia, β-cell stress, and hyperglycemia (*4*). Additionally, insulin resistance is accompanied by the intracellular production of free radicals, consequently causing elevated oxidative stress in the tissues of various organs (*5*). This indicates that there is a strong association between the degree of oxidative stress and risk of developing insulin resistance.

Increased oxidative stress induced by hyperglycemia is associated with type 2 diabetes. Reactive oxygen species (ROS) activate stress-sensitive intracellular signaling pathways, such as the transcription of nuclear factor-kappa B (NF-κB), which plays a central role in inflammation-related disease (*6*), and mitogen-activated

protein kinase (MAPK), which mediates the induction of NF-E2-related factor 2 (Nrf2) (*7,8*). Several researchers have demonstrated that ROS generation induced by nicotinamide adenine dinucleotide phosphate (NADPH) oxidase and the mitochondrial electron transport chain occurs in an early stage of diabetic development (*9,10*). In addition, oxidative stress activates different processes involving protein kinase C, cytokines, and others (*6*). Therefore, novel approaches are necessary to identify therapeutic agents that can act with a pleiotropic effect, including antioxidant properties, to prevent and treat diabetic development.

Marked effort has been made to identify safe and effective therapeutic agents from natural sources for metabolic disorders such as obesity and diabetes mellitus. Traditional medicines have been touted for their potential therapeutic actions in diabetes and its complications due to their lack of toxicity and side effects. Accordingly, previous studies from our group have reported that Corni Fructus (*Cornus officinalis* SIEB. *et* ZUCC.), which is used as a traditional medicine, exhibited antidiabetic effects by ameliorating glucose-mediated metabolic disorders as well as aminoguanidine, an inhibitor of advanced glycation endproduct (AGE) formation, in streptozotocin-induced diabetic rats (*11*). Furthermore, we screened out an iridoid glycoside fraction containing morroniside, loganin, mevaloside, loganic acid, and 5-hydroxymethyl-2-furfural, and a low-molecular-weight polyphenol fraction containing 7-*O*-galloyl-D-sedoheptulose (GS) from Corni Fructus. These components may be important contributors to prevent or delay the onset of diabetic kidney disease (*12*). In particular, GS has only been isolated from Corni Fructus as far as we know (*13*), and the biological activity of GS has been poorly understood until now. For these reasons, we decided to clarify the mechanisms of GS in type 2 diabetes using *db/db* mice as a model, especially in the liver and pancreas.

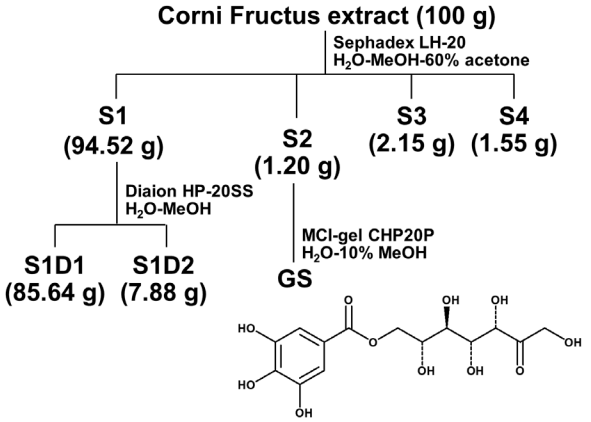

Figure 1. Fractionation of Corni Fructus.

2. Purification of GS from Corni Fructus

As shown in Figure 1, a water extract of Corni Fructus (100 g) was fractionated by Sephadex™ LH-20 column chromatography (32 × 5 cm) with water containing increasing proportions of methanol (0-100%, 10% stepwise gradient elution) and finally with 60% acetone to obtain four fractions: S1 (94.52 g), S2 (1.20 g), S3 (2.15 g), and S4 (1.55 g). The fraction S1 was further separated by Diaion™ HP-20SS column chromatography (28 × 5 cm) with water-methanol (0-100%, 10% stepwise gradient elution) to obtain S1D1 (85.64 g) and S1D2 (7.88 g). TLC and HPLC analyses showed that S1D1 and S1D2 mainly contained sugars and iridoid glycosides, and S2, S3, and S4 contained phenolic substances. A portion of S2 (150 mg) was further purified by MCI-gel CHP20P column chromatography (28 × 2 cm) with 0-10% methanol to obtain GS (98 mg). A white amorphous powder was analyzed by HR-FAB-MS; *m/z*: 363.0903, $C_{14}H_{19}O_{11}$ [M+H] requires 363.0927. ^{1}H-NMR (acetone-d_6 + D_2O) of major anomer δ: 7.13 (s, galloyl-H), 4.36 (m, H-4, H-7a), 4.23 (dd, J = 6.6, 11.7 Hz, H-7b), 4.09 (d, J = 6.4 Hz, H-3), 4.05 (m, H-6), 3.88 (t, J = 5.5 Hz, H-5), 3.5 (2H, br s, H-1), ^{1}H-NMR (acetone-d_6 + D_2O) of major anomer δ: 167.0 (galloyl C-7), 145.9 (galloyl C-3,5), 138.7 (galloyl C-4), 121.5 (galloyl C-1), 109.8 (galloyl C-2,6), 103.7 (C-2), 83.3 (C-5), 78.0 (C-3), 77.1 (C-4), 71.1 (C-6), 66.2 (C-7), 64.4 (C-1). Other anomeric carbon signals were observed at δ 98.2, 103.7, and 109.0. Assignments of the signals were achieved by COSY, HSQC, and HMBC spectral analysis. The structure was further confirmed by the formation of an osazone derivative: a mixture of the compound (10 mg), phenylhydrazine hydrochloride (20 mg), and sodium acetate (30 mg) in water (0.5 mL) was heated at 80°C for 25 min, and the resulting precipitates were collected by filtration. The ^{1}H-NMR spectral data (in DMSO-d_6) and $[\alpha]_D$ value coincided with the data for the osazone derivative of GS (*14,15*).

3. General characteristics

Compared with the vehicle-treated *db/db* mice, the body weights were not changed by GS treatment throughout the experimental periods. However, the administration of GS led to a significant decrease of food intake in a dose-dependent manner. The water intake showed a tendency toward a slight decrease (without significance) by 20 and 100 mg of GS treatment for 6 weeks (*14*). Type 2 diabetes causes characteristics such as hyperglycemia, hyperleptinemia and hyperinsulinemia, in *db/db* mice compared with *m/m* mice. GS administration significantly reduced the serum leptin and insulin levels at a dose of 100 mg/kg, and the C-peptide level at doses of 20 and 100 mg/kg, while the serum glucose level was slightly decreased without significance (*16,17*). Thus, GS administration can prevent diabetes in *db/db* mice, as evidenced by improved insulin sensitivity

through the maintenance of insulin and glucose levels and preservation of insulin and C-peptide levels in the pancreas, revealing that GS can ameliorate impaired glucose and insulin tolerance in *db/db* mice. In addition, the resistin, tumor necrosis factor-alpha (TNF-α), and interleukin-6 (IL-6) levels in serum were increased in the *db/db* control group compared with *m/m* group, and reduced by GS administration (*17*). Regarding the adiponectin level, the oral administration of GS at a dose of 100 mg/kg to *db/db* mice significantly enhanced the reduction. Moreover, oxidative stress-related biomarkers, such as ROS and thiobarbituric acid-reactive substance (TBARS), in the serum of *db/db* mice were higher than those in *m/m* mice. However, ROS and TBARS in the serum of GS-treated *db/db* mice were markedly reduced in a dose-dependent manner (*17*). Concerning hepatic functional parameters, the serum alanine aminotransferase (ALT) and aspartate aminotransferase (AST) levels were increased compared with *m/m* mice, and these augmented levels showed a significant decrease at a dose of 100 mg/kg (*16*).

4. GS attenuates diabetes-induced hepatic damage through regulation of oxidative stress and inflammation

4.1. Oxidative stress-related protein expressions in the liver

As a major source of ROS generation, the Nox family of NADPH oxidase strongly contributes to the initial step and development of oxidative stress. Nox-derived ROS play a physiological role in stimulating various growth factors, cytokines, and hormones, including insulin (*18*), and have pathophysiological roles in endothelial dysfunction, inflammation, apoptosis, fibrosis, and angiogenesis, and important processes underlying diabetes and tissue injury (*19*). Structurally, NADPH oxidase comprises a membrane-associated cytochrome, *b*558, composed of one $p22^{phox}$ and one $gp91^{phox}$ subunit and at least four cytosolic subunits ($p47^{phox}$, $p67^{phox}$, $p40^{phox}$, and the small GTP_{ase} *rac*1 or *rac*2) (*20*). Especially, Nox-4 and $p22^{phox}$ were found to be major sources of ROS production and play roles in pathological conditions (*21-23*). Therefore, we performed immunoblotting analyses of Nox-4 and $p22^{phox}$ in hepatic tissue of *db/db* mice. GS administration to *db/db* mice significantly attenuated oxidative stress by reducing ROS and TBARS levels in hepatic tissue, showing similar levels as those of normal *m/m* mice (*16*). These results suggest that the effect of GS involved the control of oxidative stress-induced hepatic injury, without serum glucose adjustment. Additionally, the increased expressions of hepatic Nox-4 and $p22^{phox}$ were significantly reduced by the administration of GS, which is also related to the reduction of hepatic ROS and TBARS levels (*16*). Therefore, the efficacy of GS may be related to the suppression of ROS-generating NADPH oxidase triggered by hyperglycemia, which is a potential source of oxidative stress in diabetes.

Oxidative stress also induces alterations in the Nrf2 complex, and its gene transcription, such as that of heme-oxygenase-1 (HO-1), is enhanced (*24*). Under physiological conditions, Nrf2 is sequestered in the cytoplasm by Keap1, which facilitates its ubiquitination and proteasomic degradation (*25*). Upon exposure to oxidative stress, the sequestration complex breaks down and dissociated Nrf2 translocates into the nucleus, where it binds to cis-acting antioxidant response elements and promotes the transcription of numerous cytoprotective genes (*26,27*). NADPH oxidase-derived superoxide and the consequently induced activation of intracellular protein kinase cascades, such as mitogen-activated protein kinase, can mediate the induction of Nrf2 and HO-1 expression (*7,8*). Therefore, increased Nrf2-HO-1 pathway activation may be a biomarker of oxidative stress and an adaptive response under pathological conditions. In our results, type 2 diabetic *db/db* mice showed enhanced expressions of Nrf2 and HO-1 in the liver compared with normal *m/m* mice; however, GS treatment significantly reduced these expressions (*16*). These results suggest that GS administration effectively alleviates oxidative stress and results in the down-regulation of Nrf2 and HO-1.

4.2. Inflammation-related protein expression in the liver

Chronic hyperglycemia also favors the increased expression of cyclooxygenase-2 (COX-2) and inducible nitric oxide synthase (iNOS) mediated by the activation of NF-κB, which is also involved in ROS generation and inflammatory responses (*28*). Following inflammatory stimuli, both COX-2 and iNOS have been reported to induce deleterious effects on the liver (*29*). Among them, iNOS inhibitor improved hepatic insulin signaling at the levels of insulin receptor substrate-1 and -2 and protein kinase B in the liver of genetically obese diabetic mice (*30*). Excess nitric oxide (NO) generation, most of which is attributable to iNOS expression, often occurs under pathogenic conditions. High NO production by iNOS in macrophages and other cells is an inflammatory mediator (*31*). In *db/db* mice, NADPH oxidase-derived ROS and iNOS-produced NO were augmented together, suggesting that the type 2 diabetic condition augmented oxidative and nitrosative stress in the liver. In the present study, GS significantly suppressed hepatic NF-κB, COX-2, and iNOS protein expressions in a type 2 diabetic *db/db* mouse model, which was probably the result of reduced ROS and TBARS in the hepatic tissue. Additionally, these results suggest that GS can effectively prevent oxidative and nitrosative stress and their related inflammatory responses by attenuating the expression of NADPH oxidase subunits and NF-κB-related protein (*16*).

5. The role of GS in ameliorating hyperglycemia-mediated oxidative damage to the pancreas

The pancreas is a complex of exocrine and endocrine glands that controls many homeostatic functions. In the development of diabetes, chronic hyperglycemia can exert deleterious effects on β-cell function (*32,33*), and the mechanisms of glucotoxicity involve several transcriptional factors and are, at least in part, mediated by the generation of chronic oxidative stress (*34,35*). Furthermore, β-cell dysfunction caused by glucotoxicity has been reported to be potentially reversible with the restoration of metabolic control (*36*). Thus, an effective remedy to attenuate the decline in pancreatic function by suppressing oxidative stress with the restoration of glucose metabolism may help to prevent the development of diabetic complications, whereas attempts to stimulate insulin secretion and improve insulin action with drug therapies are temporarily helpful but are ultimately unable to prevent progressive β-cell dysfunction.

The destruction of β-cells and disorder of insulin secretion in the diabetic state generally causes physico-metabolic abnormalities such as a decrease in body weight gain and an increase in the pancreatic weight, food intake, and water intake. The diabetic mice in this study also showed these changes. However, the administration of GS slightly, but not significantly, decreased these diabetes-induced physiological changes and led to a decrease in the pancreatic weight (*17*).

A number of mechanisms contribute to the development of pancreatic disorders such as glucotoxicity, oxidative stress, AGE accumulation, fibrogenesis, and cytokine production (*37*). ROS play an important role in insulin resistance and pancreatic β-cell dysfunction, a highly prevalent condition implicated in the development of diabetes (*38,39*). Under diabetic conditions, hyperglycemia may induce large amounts of ROS that are responsible for the progressive dysfunction of β-cells, worsening insulin resistance and further promoting relative insulin deficiency (*40*). In particular, β-cells are sensitive to ROS because they are low in free radical quenching (anti-oxidant) enzymes (*41*). The excess ROS may also indirectly damage cells by activating a variety of stress-sensitive intracellular signaling pathways, including NF-κB and MAPK. In the present study, GS administration suppressed pancreatic ROS and TBARS in addition to c-Jun N-terminal kinase (JNK), p-JNK, and activator protein-1 (AP-1) oxidative stress-related proteins (*17*).

Since inflammation is considered a major factor contributing to type 2 diabetes (*42*), we examined the pro-inflammatory markers TNF-α and IL-6 in serum, and found that GS treatment inhibited serum TNF-α and IL-6 (*17*), showing that the anti-diabetic action occurred due to an inhibition of inflammation. We further examined pro-inflammatory NF-κBp65, COX-2, and iNOS protein levels in the pancreas of *db/db* mice, and found that GS treatment down-regulated these levels (*17*).

6. Hepatic and pancreatic histological examination

The present study showed that in the results of histological examination using HE staining, which detects hepatocellular damage. The level of

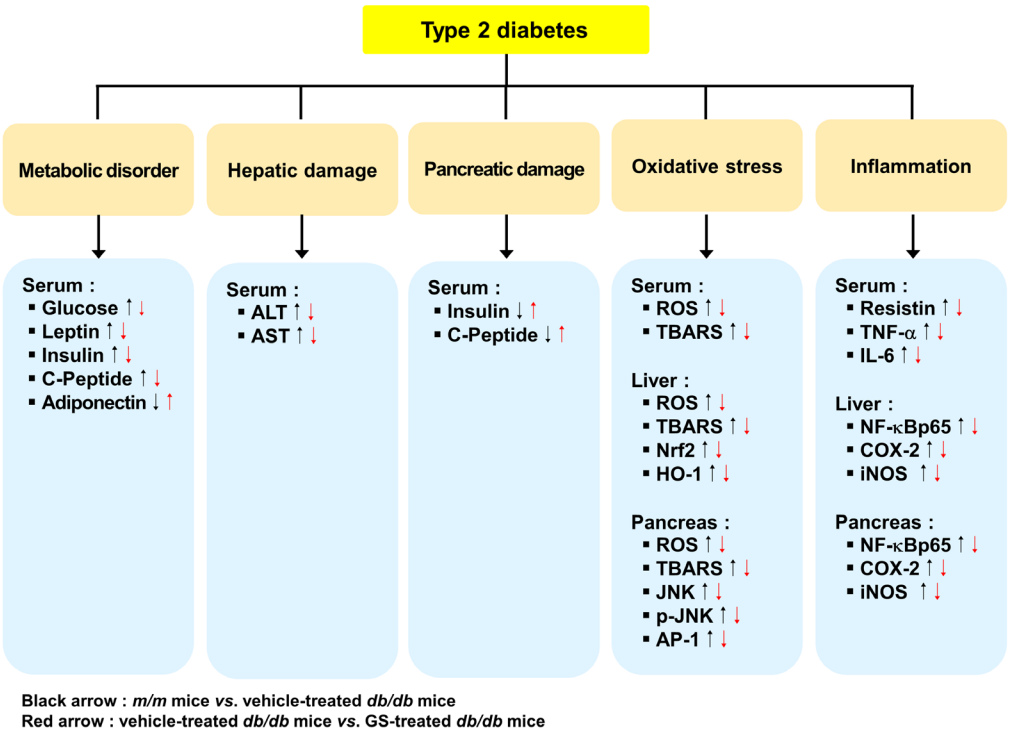

Figure 2. The effect of 7-*O*-galloyl-D-sedoheptulose against *db/db* mice.

hepatocellular damage was higher in the liver of *db/db* mice compared with *m/m* mice. However, GS-treated *db/db* mice clearly showed decreased hepatocellular damage (*16*). To evaluate pancreatic fibrosis, sections of pancreatic tissue obtained from *m/m* and *db/db* mice were stained with Azan, along with representative blue-stained fibrotic tissue sections from vehicle-treated *db/db* and GS-treated mice. The administration of GS showed a reduction of the blue-stained section (*17*).

7. Conclusion

Traditional medicine has been used widely in the treatment of diabetic mellitus in East Asia, including Japan, China, and Korea. In traditional medicine, Corni Fructus is the main ingredient for the treatment and prevention of diabetes. In our previous study, we analyzed the bioactive compounds of Corni Fructus, and morroniside, GS, and loganin were isolated (*12*). Notably, GS has only been found in Corni Fructus as far as we know, and the biological activity of GS has been poorly understood until now. The present study showed that GS treatment protected mice against type 2 diabetes due to its ameliorating effects on oxidative stress, inflammation, and fibrosis, as summarized in Figure 2. We provided experimental evidence of GS as an anti-diabetic agent, which warrants further clinical investigation.

Funding: This work was supported by a grant from Hallym University.

Conflict of Interest: The authors have no conflicts of interest to disclose.

References

1. Narayan KM, Gregg EW, Fagot-Campagna A, Engelgau MM, Vinicor F. Diabetes – a common, growing, serious, costly, and potentially preventable public health problem. Diabetes Res Clin Pract. 2000; 50:S77-S84.
2. Tao T, Deng P, Wang Y, Zhang X, Guo Y, Chen W, Qin J. Microengineered multi-organoid system from hiPSCs to recapitulate human liver-islet axis in normal and type 2 diabetes. Adv Sci. 2022; 9:2103495.
3. Weyer C, Funahashi T, Tanaka S, Hotta K, Matsuzawa Y, Pratley RE, Tataranni PA. Hypoadiponectinemia in obesity and type 2 diabetes: close association with insulin resistance and hyperinsulinemia. J Clin Endocrinol Metab. 2001; 86:1930-1935.
4. Michael MD, Kulkarni RN, Postic C, Previs SF, Shulman GI, Magnuson MA, Kahn CR. Loss of insulin signaling in hepatocytes leads to severe insulin resistance and progressive hepatic dysfunction. Mol Cell. 2000; 6:87-97.
5. Evans JL, Goldfine ID, Maddux BA, Grodsky GM. Are oxidative stress-activated signaling pathways mediators of insulin resistance and β-cell dysfunction? Diabetes. 2003; 52:1-8.
6. Hotamisligil GS. Inflammation and metabolic disorders. Nature. 2006; 444:860-867.
7. Anwar KN, Fazal F, Malik AB, Rahman A. RhoA/Rho-associated kinase pathway selectively regulates thrombin-induced intercellular adhesion molecule-1 expression in endothelial cell *via* activation of I κB kinase β and phosphorylation of RelA/p65. J Immunol. 2004; 173:6965-6972.
8. He M, Siow RCM, Sugden D, Gao L, Cheng X, Mann GE. Induction of HO-1 and redox signaling in endothelial cells by advanced glycation end products: a role for Nrf2 in vascular protection in diabetes. Nutr Metab Cardiovasc Dis. 2011; 21:277-285.
9. Li JM, Shah AM. ROS generation by nonphagocytic NADPH oxidase: potential relevance in diabetic nephropathy. J Am Soc Nephrol. 2003; 14:S221-S226.
10. Newsholme P, Haber EP, Hirabara SM, Rebelato ELO, Procopio J, Morgan D, Oliveira-Emilio HC, Carpinelli AR, Curi R. Diabetes associated cell stress and dysfunction: role of mitochondrial and non-mitochondrial ROS production and activity. J Physiol. 2007; 583:9-24.
11. Yamabe N, Kang KS, Goto E, Tanaka T, Yokozawa T. Beneficial effect of Corni Fructus, a constituent of Hachimi-jio-gan, on advanced glycation end-product-mediated renal injury in streptozotocin-treated diabetic rats. Biol Pharm Bull. 2007; 30:520-526.
12. Yamabe N, Kang KS, Matsuo Y, Tanaka T, Yokozawa T. Identification of antidiabetic effect of iridoid glycosides and low molecular weight polyphenol fractions of Corni Fructus, a constituent of Hachimi-jio-gan, in streptozotocin-induced diabetic rats. Biol Pharm Bull. 2007; 30:1289-1296.
13. Zhang Y, Chen Y, Zhao S. A sedoheptulose gallate from the fruits of *Cornus officinalis*. Acta Pharm Sin. 1999; 34:153-155.
14. Yamabe N, Kang KS, Park CH, Tanaka T, Yokozawa T. 7-*O*-Galloyl-D-sedoheptulose is a novel therapeutic agent against oxidative stress and advanced glycation endproducts in the diabetic kidney. Biol Pharm Bull. 2009; 32:657-664.
15. Lee SH, Tanaka T, Nonaka G, Nishioka I. Sedoheptulose digallate from *Cornus officinalis*. Phytochemistry. 1989; 28:3469-3472.
16. Noh JS, Park CH, Tanaka T, Yokozawa T. 7-*O*-Galloyl-D-sedoheptulose attenuates oxidative stress-induced diabetic injury *via* decreasing expression of nuclear factor-κB- and apoptosis-related protein in the liver. Biol Pharm Bull. 2012; 35:950-956.
17. Park CH, Tanaka T, Yokozawa T. Anti-diabetic action of 7-*O*-galloyl-D-sedoheptulose, a polyphenol from Corni Fructus, through ameliorating inflammation and inflammation-related oxidative stress in the pancreas of type 2 diabetics. Biol Pharm Bull. 2013; 36:723-732.
18. Goldstein BJ, Mahadev K, Wu X. Redox paradox: insulin action is facilitated by insulin-stimulated reactive oxygen species with multiple potential signaling targets. Diabetes. 2005; 54:311-321.
19. Bedard K, Krause KH. The NOX family of ROS-generating NADPH oxidases: physiology and pathophysiology. Physiol Rev. 2007; 87:245-313.
20. Babior BM, Lambeth JD, Nauseef W. The neutrophil NADPH oxidase. Arch Biochem Biophys. 2002; 397:342-344.
21. Geiszt M, Kopp JB, Várnai P, Leto TL. Identification of renox, an NAD(P)H oxidase in kidney. Proc Natl Acad Sci USA. 2000; 97:8010-8014.
22. Etoh T, Inoguchi T, Kakimoto M, Sonoda N, Kobayashi K,

Kuroda J, Sumimoto H, Nawata H. Increased expression of NAD(P)H oxidase subunits, NOX4 and p22phox, in the kidney of streptozotocin-induced diabetic rats and its reversibity by interventive insulin treatment. Diabetologia. 2003; 46:1428-1437.
23. Gorin Y, Block K, Hernandez J, Bhandari B, Wagner B, Barnes JL, Abboud HE. Nox4 NAD(P)H oxidase mediates hypertrophy and fibronectin expression in the diabetic kidney. J Biol Chem. 2005; 280:39616-39626.
24. Tong KI, Katoh Y, Kusunoki H, Itoh K, Tanaka T, Yamamoto M. Keap1 recruits Neh2 through binding to ETGE and DLG motifs: characterization of the two-site molecular recognition model. Mol Cell Biol. 2006; 26:2887-2900.
25. Niture SK, Kaspar JW, Shen J, Jaiswal AK. Nrf2 signaling and cell survival. Toxicol Appl Pharmacol. 2010; 244:37-42.
26. de Vries HE, Witte M, Hondius D, Rozemuller AJM, Drukarch B, Hoozemans J, van Horssen J. Nrf2-induced antioxidant protection: a promising target to counteract ROS-mediated damage in neurodegenerative disease? Free Radic Biol Med. 2008; 45:1375-1383.
27. Kaspar JW, Niture SK, Jaiswal AK. Nrf2:INrf2 (Keap1) signaling in oxidative stress. Free Radic Biol Med. 2009; 47:1304-1309.
28. Spitaler MM, Graier WF. Vascular targets of redox signalling in diabetes mellitus. Diabetologia. 2002; 45:476-494.
29. García-Mediavilla V, Crespo I, Collado PS, Esteller A, Sánchez-Campos S, Tuñón MJ, González-Gallego J. The anti-inflammatory flavones quercetin and kaempferol cause inhibition of inducible nitric oxide synthase, cyclooxygenase-2 and reactive C-protein, and down-regulation of the nuclear factor kappaB pathway in Chang Liver cells. Eur J Pharmacol. 2007; 557:221-229.
30. Fujimoto M, Shimizu N, Kunii K, Martyn JAJ, Ueki K, Kaneki M. A role for iNOS in fasting hyperglycemia and impaired insulin signaling in the liver of obese diabetic mice. Diabetes. 2005; 54:1340-1348.
31. Moncada S, Palmer RM, Higgs EA. Nitric oxide: physiology, pathophysiology, and pharmacology. Pharmacol Rev. 1991; 43:109-142.
32. Moran A, Zhang HJ, Olson LK, Harmon JS, Poitout V, Robertson RP. Differentiation of glucose toxicity from beta cell exhaustion during the evolution of defective insulin gene expression in the pancreatic islet cell line, HIT-T15. J Clin Invest. 1997; 99:534-539.
33. Gleason CE, Gonzalez M, Harmon JS, Robertson RP. Determinants of glucose toxicity and its reversibility in the pancreatic islet β-cell line, HIT-T15. Am J Physiol Endocrinol Metab. 2000; 279:E997-E1002.
34. Kaneto H, Xu G, Song KH, Suzuma K, Bonner-Weir S, Sharma A, Weir GC. Activation of the hexosamine pathway leads to deterioration of pancreatic β-cell function through the induction of oxidative stress. J Biol Chem. 2001; 276:31099-31104.
35. Laybutt DR, Kaneto H, Hasenkamp W, Grey S, Jonas JC, Sgroi DC, Groff A, Ferran C, Bonner-Weir S, Sharma A, Weir GC. Increased expression of antioxidant and antiapoptotic genes in islets that may contribute to β-cell survival during chronic hyperglycemia. Diabetes. 2002; 51:413-423.
36. LeRoith D. β-Cell dysfunction and insulin resistance in type 2 diabetes: role of metabolic and genetic abnormalities. Am J Med. 2002; 113:3S-11S.
37. Tikellis C, Cooper ME, Thomas MC. Role of the renin-angiotensin system in the endocrine pancreas: implications for the development of diabetes. Int J Biochem Cell Biol. 2006; 38:737-751.
38. Evans JL, Maddux BA, Goldfine ID. The molecular basis for oxidative stress-induced insulin resistance. Antioxid Redox Signal. 2005; 7:1040-1052.
39. Houstis N, Rosen ED, Lander ES. Reactive oxygen species have a causal role in multiple forms of insulin resistance. Nature. 2006; 440:944-948.
40. Robertson RP, Harmon J, Tran PO, Tanaka Y, Takahashi H. Glucose toxicity in β-cells: type 2 diabetes, good radicals gone bad, and the glutathione connection. Diabetes. 2003; 52:581-587.
41. Evans JL. Antioxidants: do they have a role in the treatment of insulin resistance? Indian J Med Res. 2007; 125:355-372.
42. de Luca C, Olefsky JK. Inflammation and insulin resistance. FEBS Lett. 2008; 582:97-105.

Received November 2, 2022; Revised May 2, 2023; Accepted May 14, 2023.

Address correspondence to:
Takako Yokozawa, Graduate School of Science and Engineering for Research, University of Toyama, 3190 Gofuku, Toyama 930-8555, Japan.
E-mail: yokozawa@inm.u-toyama.ac.jp

Jin Pyeong Jeon, Department of Neurosurgery, College of Medicine, Hallym University, Chuncheon 24252, Republic of Korea.
E-mail: jjs6553@hanmail.net

Chan Hum Park, Institute of New Frontier Research Team, Research Institute of Medical-Bio Convergence, Hallym University, Chuncheon, Republic of Korea.
E-mail: ptman123@naver.com

Released online in J-STAGE as advance publication May 27, 2023.

Review

DOI: 10.5582/ddt.2023.01010

The association of gut microbiome with recurrent pregnancy loss: A comprehensive review

Jun Zhu[1,§], Jiaxi Jin[1,§], Qing Qi[2,3,4], Lisha Li[2,3,4], Jing Zhou[2,3,4], Liwen Cao[5], Ling Wang[2,3,4,*]

[1] The Affiliated Wenling Hospital of Wenzhou Medical University, Zhejiang, China;
[2] Laboratory for Reproductive Immunology, Obstetrics and Gynecology Hospital of Fudan University, Shanghai, China;
[3] The Academy of Integrative Medicine of Fudan University, Shanghai, China;
[4] Shanghai Key Laboratory of Female Reproductive Endocrine-related Diseases, Shanghai, China;
[5] Center for Reproductive Medicine, Zhoushan Women and Children Hospital, Zhejiang, China.

SUMMARY The steady-state gut microbiome not only promotes the metabolism and absorption of nutrients that are difficult to digest by the host itself, but also participates in systemic metabolism. Once the dynamic balance is disturbed, the gut microbiome may lead to a variety of diseases. Recurrent pregnancy loss (RPL) affects 1-2% of women of reproductive age, and its prevalence has increased in recent years. According to the literature review, the gut microbiome is a new potential driver of the pathophysiology of recurrent abortion, and the gut microbiome has emerged as a new candidate for clinical prevention and treatment of RPL. However, few studies have concentrated on the direct correlation between RPL and the gut microbiome, and the mechanisms by which the gut microbiome influences recurrent miscarriage need further investigation. In this review, the effects of the gut microbiome on RPL were discussed and found to be associated with inflammatory response, the disruption of insulin signaling pathway and the formation of insulin resistance, maintenance of immunological tolerance at the maternal-fetal interface due to the interference with the immune imbalance of Treg/Th17 cells, and obesity.

Keywords gut microbiome, recurrent pregnancy loss, inflammation, insulin resistance, immunity, obesity

1. Introduction

Recurrent pregnancy loss (RPL), whose definition has still remained controversial, was traditionally defined as multiple spontaneous abortions with the same spouse. The American Society for Reproductive Medicine (ASRM) defined two or more pregnancy failures and explicitly excluded biochemical pregnancies in 2020 (*1*). In addition, the European Society of Human Reproduction and Embryology (ESHRE) defined two or more pregnancy failures before 24 weeks of gestation, including biochemical pregnancies (*2*). RPL could affect 1-2% of women of reproductive age, and its prevalence has increased in recent years (*2*). Hence, RPL is a disease that impairs patients' physical and mental health and their families' stability. The etiology of RPL is complex, and the main recognized factors include chromosomal abnormalities, inflammation, insulin resistance (IR), immunity, obesity, *etc*.

In an individual, the gut microbiome is composed of more than 1,000 species of bacteria, including approximately 3.8×10^{13} bacterial cells and 3.3 million genes (*3*). Compared with human genes, the gut microbiota contains 150 times more genes than the human genes (*3,4*), which are essential for the survival of these organisms in the gut and confer different functions to various bacteria that play important roles in regulating metabolism, immunity, and inflammation. Over time, this dynamic population evolves with the host, including bacteria, fungi, parasites, archaebacteria, and viruses. Metagenomic analyses of volunteers and lean mice have shown that the microbiome was comprised of two main primary phyla, *Bacteroides* and *Firmicutes*, and *Bacteroidetes* can be commonly found in healthy hosts, making them superior to *Firmicutes* (*4*).

Gut microbiome can attach to the intestinal mucosal surface, forming a protective barrier and participating in the maintenance of homeostasis within the tissues to prevent the growth and invasion of pathogenic bacteria (*5*). The steady-state gut microbiome not only promotes the metabolism and absorption of nutrients that are difficult to digest by the host itself, but also participates in systemic metabolism (*6*). The intestinal barrier, primarily consisting of a mucus layer, an

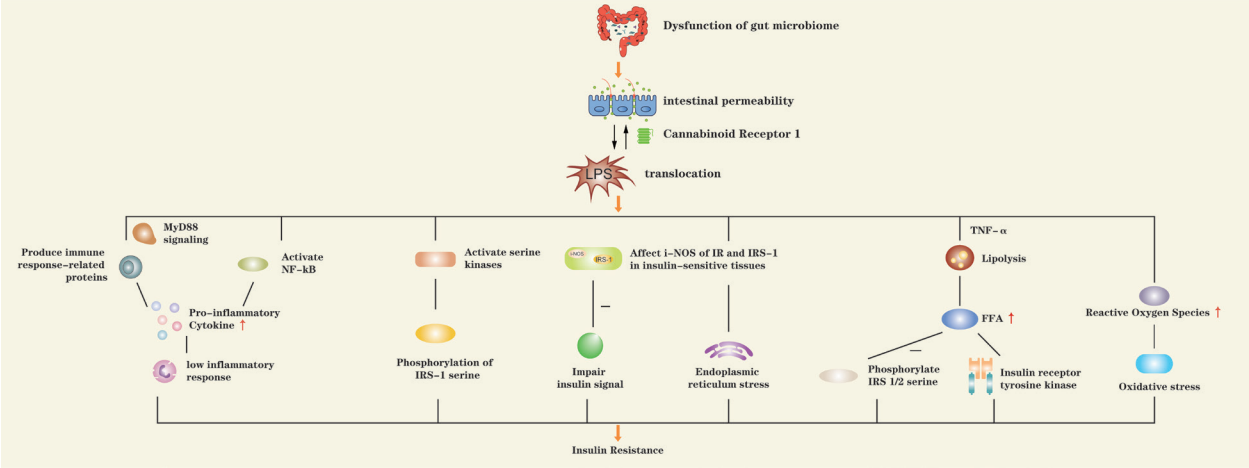

Figure 1. The possible mechanisms of RPL based on the effects of LPS by regulating gut microbiome. ↑: increase; ↓: decrease; -: inhibit.

epithelial barrier, and a gut vascular barrier, limits the transport of intestinal contents into systemic circulation by providing a physical and functional barrier. First, the tight junctions between the epithelial cells restrict the entry of bacteria and their products into the systemic circulation. Second, the mucin layer consists of the highly glycated protein mucin secreted by goblet cells, which does not allow bacteria to penetrate by firmly adhering to the epithelial cells (*5*). The thickness and composition of the mucus layer are mainly affected by the gut microbiome. Consequently, the interaction between the intestinal mucus layer and microorganisms is of great significance for maintaining healthy intestinal homeostasis. In addition, the gut microbiome participates in the establishment of mucosal immunity, and the glycine-rich structural domains on mucins can provide binding sites for certain microorganisms secreting specific lectins or glycosides for selective adhesion (*7*). In germ-free animals, there are fewer goblet cells, a thinner mucus layer, and a higher proportion of neutral mucin. Whereas the intestinal mucus layer of germ-free animals is restored rapidly after feeding on the bacterial products, which also promotes the maturation of the immune system through the mucosal system and protects the host from the attack of opportunistic pathogens (*8*). In general, the gut microbiome is in dynamic balance, while it is susceptible to the environmental factors, such as long-term dietary habits and medications. Once the dynamic balance is disturbed, the gut microbiome may lead to a variety of diseases.

According to the available literature, the gut microbiome is a new potential driver of the pathophysiology of recurrent abortion, and the gut microbiome has emerged as a new candidate for clinical prevention and treatment of RPL. However, few studies have concentrated on the direct correlation between RPL and the gut microbiome, and the mechanisms by which the gut microbiome influences recurrent miscarriage need further investigation. The present review aimed to discuss the relationship between RPL and gut microbiome.

2. Effects of gut microbiome on RPL

2.1. Insights into inflammation and gut microbial imbalance

Few studies have directly shown that gut microbes are associated with RPL, while there is strong evidence to support the correlation between the gut microbiome and the increased risk of inflammation, which in turn leads to IR. Dysfunction of intestinal microbiome involves abnormal production of cytokines, which may be at the risk of inflammation. There is significant evidence supporting that the increased risk of pro-inflammation is associated with a decrease in the diversity of the gut microbiome (*9*). In addition to the loss of diversity, Liu *et al*. reported a significant reduction in the dominant microbiota beneficial to human health and an increase in the proportion of *Firmicutes* in patients with abortion (*10*).

2.1.1. Lipopolysaccharide (LPS)

LPS, known as endotoxin, is considered one of the initiators of inflammatory responses and apoptosis. Although the development of inflammation may be caused by several factors, according to studies on mice, the gut microbiome is one of the important causes, and the LPS is one of the best-studied inflammation inducers (*5,11*). In general, the intestinal barrier prevents the entry of LPS from the gut into systemic circulation. The toxicity of LPS is present in the portion of Lipid A moiety, which allows LPS to bind to toll-like receptor-4 (TLR4), and then enter the systemic circulation. Intestinal alkaline phosphatase produced by epithelial cells catalyzes the dephosphorylation of Lipid A moiety to detoxify bacterial endotoxin, thereby preventing the translocation of LPS into the systemic circulation (*5*). However, changes in the ratio of *Bacteroides* to *Firmicutes* make LPS to translocate and move into the systemic circulation by the junctions (Figure 1).

There is a specific interaction between LPS and TLR4. LPS-binding protein binds to LPS and delivers it to the TLR4/myeloid differentiation protein-2 complex, which then induces the early activation of nuclear factor-kappa B (NF-κB), Interferon regulatory factor 3, and mitogen-activated protein kinase (MAPK) pathways, which can be mediated by the adapters myeloid differentiation primary response 88 (MyD88) and MyD88 adaptor-like. After the subsequent activation and phosphorylation of interleukin-1 receptor-associated kinase, tumor necrosis factor (TNF) receptor-associated factor 6 becomes activated (*12*), which gives rise to the expression of pro-inflammatory genes. Then, inflammatory cytokines lead to a low inflammatory response and IR (*13*). A contender for the MyD88-independent branch of signaling pathways induced by LPS is dsRNA-dependent protein kinase (PKR), which has been shown to be associated with MyD88 adaptor-like. The translocation of LPS also activates serine kinases, which induces serine phosphorylation of insulin receptor substrate 1 (IRS-1) and promotes IR formation. Moreover, LPS entering to the gut through a compromised intestinal barrier also affects S-nitrosation of IR and IRS-1 in insulin-sensitive tissues, leading to the impaired insulin signal (*14,15*). In addition, S-nitrosylation/S-nitrosylation has been shown to be a central phenomenon induced by endoplasmic reticulum stress, which could also be an important molecular mechanism of IR (*16*).

Changes in the gut microbiome can activate the endocannabinoid system. LPS can exacerbate the inflammatory response by binding to cannabinoid receptor 1 to increase intestinal permeability and promote its absorption into the blood (*17*). LPS can also promote lipolysis directly, or indirectly through TNF-α, significantly increasing the production of free fatty acids (FFAs). The increased levels of FFAs can phosphorylate IRS1/2 serine and inhibit the activity of insulin receptor tyrosine kinase, leading to IR (*18*). In addition, LPS promotes the production of reactive oxygen species (ROS) and induces oxidative stress, which in turn increases the risk of IR (*19*). Importantly, in mice supplemented with lipoic acid, oxidative stress was lower than in mice that did not receive lipoic acid (*20*).

2.1.2. Short-chain fatty acids (SCFAs)

Gut microbiome can metabolize dietary fiber and indigestible carbohydrates into SCFAs by producing specific enzymes (*6*). To our knowledge, SCFAs are immunomodulatory molecules that are involved in the regulation of cytokine production and T regulatory (Treg) cell expansion, activating or inhibiting of the inflammatory cascade (*21*).

With the progression of research, SCFAs can be detected in the blood circulation, suggesting a wide range of extra-gastrointestinal effects of gut microbiota-derived SCFAs. SCFAs include acetate, propionate, and butyrate (the highest level is 95%). In a study on rats, it was revealed that altering the gut microbiota was resulted in the increased acetate production, which activated the parasympathetic nervous system, thereby promoting the increased insulin secretion (*22*). Propionate is a substrate for hepatic gluconeogenesis. Several studies have shown that high levels of imidazole propionates produced by *Bacteroides* and *Prevotella* are involved in the immune activation and low inflammation (*23,24*). Besides, another study on mice showed that imidazole propionate inhibits insulin signaling at the level of IRS by activating P38 MAPKs and promoting the phosphorylation of P62 (*25*).

Another SCFA, butyrate, is the most important metabolite in colonocyte metabolism. Of note, butyrate is an anti-inflammatory metabolite that inhibits pathways, leading to the production of pro-inflammatory cytokines. A previous study has demonstrated that *Bifidobacterium bifidum* strain Bb could decrease *Prevotellaceae*, a major driver of inflammation, by modulating SCFAs, particularly butyrate (*26*). Related to this anti-inflammatory effect, butyrate induces extrathymic production of anti-inflammatory Treg cells, which in turn minimizes the risk of IR by improving insulin signaling (*21*). Besides, butyrate increases the expression levels of tight junction proteins, leading to reduced intestinal permeability (*27*) and maintenance of the intestinal barrier, thereby minimizing LPS mobility in the gut and reducing LPS-related effects.

2.1.3. Bile acids

Bile acids, metabolized by enzymes in gut microbiome, are essential for the maintenance of homeostatic metabolism, insulin sensitivity, and innate immunity. Gut microbes can convert primary bile acids to secondary bile acids *via* deconjugation, dihydroxylation, or dehydrogenation (*28*), and thus, gut microbiota can influence the synthesis of bile acids. Bile acids serve several functions, enabling lipids to be emulsified and absorbed by the body, as well as exerting their role as signaling ligands (*13*). Bile acids play an inflammatory role by activating the farnesoid X receptor signaling pathway in enterocytes (*29*). However, activation of Takeda G-protein receptor 5 by secondary bile acids activates glucagon-like peptide 1 (GLP1) secretion from L-cells in the intestine (*30*). Furthermore, GLP1 prevents IR (*31*). Meanwhile, bile acid metabolites are abundant in the intestinal tract of mammals and produce a large pool of bioactive molecules to control the differentiation of T helper 17 (Th17) cells and Treg cells (*32*). Hang *et al*. studied two different derivatives of lithocholic acid (LCA), 3-oxoLCA and isoalloLCA, and found that 3-oxoLCA was directly associated with retinoic acid γt binding that could inhibit the differentiations of Th cells, a key transcription factor in Th17 cell differentiation.

Nevertheless, isoalloLCA enhanced the differentiation of Treg cells by generating ROS (*32*).

2.1.4. Cytokines

Cytokines are signaling molecules that influence several processes in the host, such as immune regulation. As a pro-thrombotic cytokine (IL), IL-6 is involved in the differentiation process of Th17 cells, and it is closely associated with RPL (*33*). Compared with normal pregnancy, levels of Th17-related cytokines (*e.g*., TNF-α and IL-17) were significantly elevated in the decidua of RPL patients (*34*). Furthermore, a study found that miscarriage was caused by abnormally elevated IL-17 level at maternal-to-fetus interface, and administration of anti-IL-17 antibodies prevented unexplained recurrent miscarriages *(35*).

Gut microbiota can induce an imbalance in cytokine levels (*10*), and a systematic review found the abundance of *Bifidobacterium*, *Faecalibacterium*, *Ruminococcus*, and *Prevotella* was negatively correlated with IL-6 expression level (*36*). However, the underlying molecular mechanisms have not yet been fully clarified.

Bacterial overgrowth in the intestine could lead to bacterial translocation, which could exacerbate the inflammation and disrupt tight junctions, thereby facilitating intestinal permeability (*37*). For instance, *Collinia* could increase intestinal permeability by decreasing the expression levels of tight junction proteins in epithelial cells and inducing IL17 expression level (*38*). *Lactobacillus* strains can modify production of cytokines in different cells. Aline *et al*. found that *Lactobacillus* strains could reduce concentrations of pro-inflammatory cytokines, such as IL-6 and TNF-α, and significantly increase concentrations of anti-inflammatory cytokines (*39*). Importantly, in patients with miscarriage, concentrations of IL-2, IL-17, TNF-α, and interferon-γ (IFN-γ) were upregulated, and microbial diversity and the relative abundance of *Prevotella_1*, *Prevotellaceae_UCG_003* and *Selenomonas_1* were significantly reduced (*10*).

In addition, the gut microbiome metabolites modulate immunity through cytokines. Liu *et al*. found that imidazolepropionic acid and 1,4-methylimidazoleacetic acid were associated with recurrent miscarriage by Th1/Th17-mediated immunity (*10*). Histone deacetylase inhibitory activity of butyrate induces changes in gene expression in dendritic cells, including inhibition of IL-6, which contributes to the differentiation of Treg cells (*40*). Butyrate regulates the immune response of macrophages by inhibiting the transcription of precursor macrophages, such as IL-6 (*41*), contributing to the maintenance of tolerance toward commensal bacteria.

TNF-α, a cytokine known as an inflammatory driver, activates various signaling pathways to develop metabolic disorders. Additionally, elevated incidence rates of metabolic disorders have been found to be associated with IR (*42*). To successfully establish a pregnancy, extravillous trophoblast cells must invade the placental bed. Harry A found that the increased level of TNF-α in women with miscarriage could inhibit extravillous trophoblast cells invasion by increasing trophoblast apoptosis, and/or altering production of active proteases (*43*). Importantly, TNF-α level was higher in mice with intestinal enrichment of *Staphylococcus aureus* and *Danieliae* than that in normal mice (*44*). However, Mechoud *et al*. demonstrated that *Lactobacillus* could reduce TNF-α production by interfering with the ability of NF-κB to bind to DNA targets (*45*).

2.2. Insights into IR and gut microbial imbalance

The gut microbiome dysbiosis may reshape intestinal barrier functions and host metabolic and signaling pathways, which are directly or indirectly related to the IR in type 2 diabetes. Independent of obesity, insulin resistance and associated hyperglycemia trigger a rapid, drastic, and reversible intestinal dysbiosis, which contributes at least partly to enhanced gut permeability.

IR includes a series of pathological and clinical manifestations caused by a reduced or lost response of the target organs and tissues to the biological effects of insulin. During pregnancy, physiological IR is due to the high secretion of hormones, such as cortisol and progesterone, antagonizing the effects of insulin. Maternal tissue reduces blood glucose intake to maintain stable blood glucose levels to meet the needs of fetal growth. However, pathological IR is an important factor in adverse pregnancy outcomes. Destruction of intestinal barrier would destroy the symbiotic relationship between the gut microbiome and their hosts, leading to low-grade inflammation and metabolic disturbances that impair the insulin signaling pathway, alter insulin sensitivity, and ultimately lead to IR. The gut microbiome dysbiosis may reshape intestinal barrier functions and host metabolic and signaling pathways, which are directly or indirectly related to the insulin resistance in type 2 diabetes. Independent of obesity, IR and associated hyperglycemia trigger a rapid, drastic, and reversible intestinal dysbiosis, contributing at least partly to the enhanced gut permeability (*46*). Moreover, gut microbiota dysbiosis may result in IR.

Over the past decades, it was revealed that IR is one of the factors influencing the susceptibility of patients with polycystic ovarian syndrome (PCOS) to recurrent miscarriages, while the risk of IR in RPL patients remains noticeable after excluding PCOS- and diabetes-related factors. In the newly published guidelines, abnormal insulin metabolism has been recognized as an independent risk factor for RPL (*47*).

There is a relationship between IR and PRL, while the mechanism of IR inducing abortion is complex. Hyperinsulinemia increases the expression level of plasminogen activator inhibitor-1, which can induce

a hypofibrinolytic state. This promotes vascular thrombosis reduces blood supply to the placenta, which in turn leads to trophoblast dysplasia and miscarriage (*48*). Insulin directly and indirectly stimulates the production and secretion of androgens by ovarian theca cells. First, high concentrations of insulin inpatients with IR can act directly on ovarian follicular membrane cells, accelerating the transformation of intracellular progesterone into 17α-hydroxyprogesterone and promoting the conversion of 17α-hydroxyprogesterone, androstenedione, and testosterone, ultimately resulting in hyperandrogenemia. Second, high levels of insulin can increase the luteinizing hormone (LH) pulse amplitude of pituitary gland by increasing the body's sensitivity to gonadotropin-releasing hormone, followed by worsening of hyperandrogenemia. In addition, IR reduces the production of sex hormone binding globulin in the liver, which increases free testosterone and functional hyper and rogenemia in the body. Furthermore, free androgens in serum can directly damage to ovum and embryo, and even lead to PRL in severe cases (*49*). Moreover, androgen receptor mediates the regulation of androgen in structure and function of uterine tissue, and a single nucleotide polymorphism of androgen receptor (G1733A) gene changes cytoskeletal tissue and cell cycle regulation, affecting decidualization of human endometrial stromal cells, which is detrimental to embryonic implantation and increases abortion rate (*50*). Hyperandrogenemia and IR may cause mitochondria-mediated damage, cause the imbalance of oxidative stress and antioxidant stress response of the uterus, and ultimately lead to abortion (*51*).

IR or hyperinsulinemia has various deleterious metabolic effects, such as increased serum level of hyperhomocysteinemia (HHcy). HHcy increases oxidative stress in the vascular endothelium and activates platelets by interfering with endometrial blood flow and vascular integrity, leading to implantation failure or abortion (*52*). Jakubowicz *et al*. found that hyperinsulinemia at the implantation situs could decrease the concentration of insulin-like growth factor binding protein-1 (*53*), promoting the adhesion process at the maternal-fetal interface. Thus, insulin is negatively associated with insulin-like growth factor binding protein-1 concentration, increasing the risk of miscarriage. In addition, hyperinsulinemia may cause dysregulation of prokineticin 1 expression level, which inhibits endometrial stromal cell migration and trophoblast invasion, and interferes with embryonic implantation, thereby leading to miscarriage (*54*).

2.3. Insights into immunity and gut microbial imbalance

The etiology of RPL is complex and approximately 50% of the complexity is related to immune factors (*34*). Intestinal microorganisms are closely associated with Treg/Th17 cellular immune homeostasis, and gut microorganisms and their metabolites may interfere with Treg/Th17 cellular immune balance. First, Treg/Th17 cellular immune imbalance may occur when gut microbial composition changes, leading to the increase of IL-17 secretion and a shift in Treg/Th17 homeostasis to Th17 cells (*55*). Liu *et al*. also found a significant decrease in the dominant microbiota beneficial to human health and an increase in the ratio of *Firmicutes* to *Bacteroides*. Further analysis showed that these changes in the gut microbiome were related to the increase in the levels of Th1- and Th17-related cytokines (*10*). Segmented filamentous bacteria could induce the differentiation of Th17 cells by stimulating ROS and promoting the production of serum amyloid A (*56*). *Bifidobacterium* was confirmed to induce differentiation of Th17 cells (*57*). However, *Bacteroides fragilis* could promote the differentiation of $CD4^+$ T lymphocytes into Treg cells and inhibit the differentiation of $CD4^+$ T lymphocytes into Th17 cells *via* the TLR signaling pathway on the surface of T lymphocytes (*57*). Second, each bacterium could also regulate the differentiation balance of Treg/Th17 cells by its metabolites. For instance, *Clostridium* clusters XIVa and IV could also induce Treg cell proliferation through SCFAs (*58*).

2.3.1. Autoimmune diseases (AIDs)

AIDs refer to the syndromes, in which the body produces high titers of autoantibodies and/or auto-reactive lymphocytes that attack the corresponding normal cells and tissues, resulting in tissue and organ dysfunction. AIDs are characterized by disruption of immune tolerance, and they are an important cause of pregnancy-associated complications, such as RPL. Christiansen *et al*. reported that the incidence of RPL was 1.7-5.3 times higher in pregnant women with AIDs, including lupus erythematosus and autoimmune thyroid disease (AITD) than in healthy controls (*59*).

It is broadly accepted that dysfunction of the gut microbiome can cause an overactive immune system, leading to AIDs, while few *in vivo* relevant studies were conducted. In a seminal experiment performed by Min Jin *et al*. (*9*), significant differences between the positive and negative groups were identified by investigating the gut microbiota-induced recurrent miscarriages associated with immune antibody positivity. The relative abundance of Bacteroidetes was the highest in the positive group. In contrast, *Bacteroides*, *Faecalibacterium*, *Erysipelotrichaceae_UCG-003*, and *Prevotella_9* had a high relative abundance in the negative group. The results of alpha diversity analysis showed that the community richness, community diversity, and phylogenetic diversity were higher in the positive group than those in the negative group. It is speculated that there may be some relationships between the gut microbiome and RPL with positive immune antibodies. However, the mechanism has not been extensively studied.

Autoimmune factors-induced RPL refers to the presence of various autoimmune antibodies in the maternal, which attack the maternal tissues and placenta, thereby causing abortion. Autoantibodies can be classified as non-organ-specific antibodies, such as antiphospholipid antibody (aPL), antinuclear antibody (ANA), and organ-specific antibodies (*e.g*., anti-thyroid antibody).

The antiphospholipid syndrome (APS) is an autoimmune disorder mediated by T cell-dependent aPL, and it is known as an RPL-related immunological diagnosis in the world. APL is the most common autoimmune antibody that causes RPL, which is composed of heterogeneous sets of antibodies that recognize plasma or cell surface antigens, including the antibodies against proteins related to coagulation, such as β2 glycoprotein I.

The pathogenic aPLs inhibit fibrinolytic and protein C pathways and promote thrombosis in arterial vessels and microcirculation in multiple target cell types, such as endothelial cells, platelets, and monocytes. One-third of the placental tissues in patients with APS is thrombosed, resulting in fetal ischemia and hypoxia (*60*). APLs affect prostaglandin production through decidual cells and various cytokines and increase secretion and expression levels of pro-inflammatory cytokines, such as TNF-α and IL-6. APL activates the innate immunity of trophoblast cells and inhibits the proliferative activity of trophoblast cells by binding pattern recognition receptors to the surface of trophoblast cells. This reduces the migration and invasion of trophoblast cells, and promotes the release of a large number of inflammatory factors, which accelerate apoptosis of trophoblast cells and interfere with uterine spiral artery recasting (*61*). Dietary changes can alter the gut microbiome and mortality of mice with high titers of β2 glycoprotein I antibodies, and APS manifestations are markedly reduced by dietary restriction. Importantly, probiotic bacterial strain could alter aPLs in non-autoimmune animals (*62*).

RPL may be attributed to the influence of ANA on the platelet activity, coagulation or anticoagulation mechanisms, and damage of vascular endothelial cells to induce thrombosis, thereby affecting placental angiogenesis and uterine hemodynamics (*63*). Gülden *et al*. administered a combination of four antibiotics into humanized mice to treat them with ANA and found an increase in the number of effector T cells in the gut, indicating how the microbiome could influence human immune cells (*64*).

2.3.2. Autoimmune thyroid disease

AITD is an organ-specific autoimmune disorder mediated by Th1 cells. A meta-analysis showed that miscarriage was associated with a positive thyroid antibody (DR: 3.73, 95% confidence interval (CI): 1.8-7.6) and RPL (odds ratio (OR): 2.3, 95% CI: 1.5-3.5) (*65*). At present, it is widely accepted that changes in the composition and structures of the intestinal microbiota are associated with the occurrence and development of AITD. Proteins of certain strains of *Yersinia*, *Bifidobacteria*, and *Lactobacillus* have similar amino acid sequences with thyroid-stimulating hormone receptor, thyroglobulin, and thyroid peroxidase. When dysregulation of intestinal microbiota causes damage to the intestinal barrier, they can be entered into the blood by the gap, and break the immune tolerance to induce the autoimmune response through molecular simulation and other mechanisms, thereby inducing AITD (66,67). In addition, *Phyllofilamentous*, *Prevotella*, *Eubacter rectum*, and other bacteria may induce or aggravate AITD by affecting Th17/Treg axis (*68,69*).

2.3.3. Maternal-fetal immunological disorder

As patients with recurrent abortion account for more than half of the population, the procedures are sometimes referred to as some of the unexplained recurrent miscarriages that might be explained by abnormalities in maternal-fetal immunology (*34*). Pregnancy is a unique immunological phenomenon, and maternal-fetal immune tolerance is the basis of embryonic implantation and pregnancy maintenance. Hence, a normal immune response is essential to maintain pregnancy in early-stage. The foundation is the development of immunological tolerance during pregnancy, which includes reduced activity of natural killer (NK) cells, Th2 type immune response, increased activity of Treg cells, and modest trophoblast infiltration. Any abnormalities may lead to imbalance of maternal-fetal immune tolerance (*70*). Once the immune tolerance is broken, the maternal immune system may reject the embryo, failing of embryonic implantation and abortion (*34*).

Changes in the number and species of the gut microbiome and the concentrations and activities of their metabolites are important factors, affecting systemic immune response and endocrine. By interfering with the immunological balance of Treg/Th17 cells at the maternal-fetal interface, their aberrant alterations may result in IR and induce RPL (*34,58*). When Treg and Th17 cells interact with each other and tend to balance, the decidua can not only resist external infection but also prevent the embryo from being rejected by the maternal immune system. As a result, an imbalance of Treg/Th17 cells is an important cause of maternal-fetal immune intolerance (*34,70*).

In general, IFN-γ is involved in supporting uterine spiral artery remodeling and decidualization, and NK cells are beneficial to pregnancy by secretion of IFN-γ. At the maternal-fetal interface, a large number of NK cells are accumulated, and 70% of decidual lymphocytes are $CD56^{bright}CD16^{-}$ NK cells. These cells can take part in endometrial vascular remodeling, trophoblast invasion,

and the maintenance of immunological tolerance at the maternal-fetal interface, according to research conducted on animals and humans (*71*). Therefore, abnormal number and activity of NK cells are closely related to URSA. Recently, Fu *et al*. demonstrated that the decidual NK cells could prevent the Th17 cells from secreting IFN-γ, which could cause a local inflammatory reaction, and lead to tolerance. Contrarily, in RPL patients or animal models, the number of decidual Th17 could increase, and the inhibition of NK cell-mediated response could be vanish, finally leading to the loss of tolerance (*71*). Additionally, healthy decidual NK cells release large amounts of the anti-inflammatory cytokine IL-10, which is crucial for inhibiting TH17 cells (*72*). Therefore, NK cells could maintain fetal development at the maternal-fetal interface by controlling the local inflammation.

Intestinal microbiota can activate NK cells (*73*) and stimulate the development of the intestinal mucosal immune system directly or indirectly by activating helper cells (*74*). For instance, it was revealed that *Lactobacillus Eosinophilus* could promote the secretion of IL-12 by dendritic cells, activating NK cells to promote the synthesis and secretion of IFN-γ (*75*). *Lactobacillus plantarum* could also promote synthesis of NK cells and secretion of IL-22 by recognizing TLR2, upregulating the expression levels of tight junction proteins in intestinal epithelial cells (*73*). In addition, *Roseburia intestinalis* was found to be positively associated with IL-22 and IL-6, improving insulin sensitivity (*76*). It was well documented that human leukocyte antigen class I molecules could regulate the function of NK cells. Importantly, changes in human leukocyte antigen structure could be associated with distinct variations in the gut microbiome (*77*).

2.4. Obesity can be an independent risk factor for RPL

In women of reproductive age, obesity is on the rise, and it has a detrimental effect on their capacity to conceive. Obesity causes RPL through heredity, inflammation, immune imbalance, decidua damage, endocrine disorder, pre-thrombotic state, *etc*. Obesity could be an independent risk factor for RPL. However, there is a significant difference in the gut microbiome diversity between healthy individuals and obese individuals, and the diversity is related to body mass index (BMI). Hence, the gut microbiome is associated with susceptibility to obesity (Figure 2). Schele *et al*. demonstrated that the gut microbiome reduced the expression level of proglucagon, which encoded the fat-suppressing peptide GLP1 in the brain stem and contributed to the increased fat mass (*78*). A previous study showed that *Bacteroides* to *Firmicutes* ratio was altered in obese individuals and this ratio could revert to normal weight loss, suggesting that the gut microbiome might play a key role in obesity (*79*).

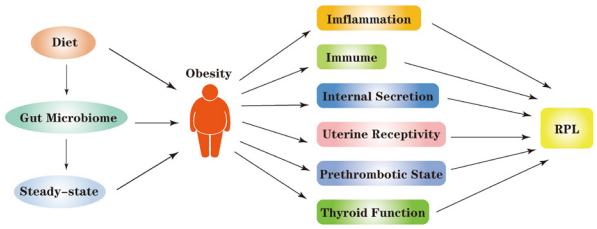

Figure 2. The possible mechanisms of the effects of diet on the gut microbiome and the relationship leading to the increased risk of the development of RPL.

2.4.1. Heredity

Clinically, RPL is highly associated with an abnormal chromosomal karyotype (*80*). Obese women were reported to be at a significantly higher risk of miscarriage, whereas at a lower risk of chromosomal abnormalities in stream products compared with women with normal BMI (*81*). Therefore, the majority of chromosomal abnormalities are irrelevant to obesity-induced RPL.

2.4.2. Obesity-induced gut microbiome promotes inflammation

The association between obesity and inflammation could be mediated by the inflammatory agents produced by gut microbiome, such as LPS and TNF-α. Wang *et al*. found that a high-fat diet (HFD) could result in an abundance of gram-negative bacteria in intestinal tracts of obese mice, which could cause damage to the mucosal barrier and increase intestinal permeability, releasing a significant quantity of LPS into the blood (*82*). Fei *et al*. used Enterobacteriaceae isolated from the gut microbiome of obese individuals to establish a genetic mouse model with only this microbiome, and it was revealed that the experimental group showed elevated LPS, developing obesity and IR, while their germ-free counterparts who were exposed to the same conditions exhibited no change (*83*). In accordance with Fei *et al*.'s findings (*83*), Just *et al*. concluded that germ-free mice would not become obese even if they were given an HFD (*84*).

Additional inflammatory products are produced by gut microbiome in obese patients than in normal individuals. Li *et al*. found that obese mice in the HFD group had significantly higher levels of LPS and TNF-α compared with those in the control group (*85*). Moreover, the relative abundance of *Firmicutes* and Proteobacteria increased, while the relative abundance of Bacteroidetes, Actinobacteria, and Verrucomicrophyla decreased, suggesting that the high levels of LPS and TNF-α could be related to the changes of intestinal microbiota. LPS stimulates the pro-inflammatory pathway and causes IR by activating TLR4 on adipocytes and upregulating NF-κB expression level (*86*). When the function of adipocytes is abnormal, it's usually macrophages in fat

tissue that may release IL-6 (*42*), downregulating the expression levels of glucose transporter-4 and IRS-1 in adipocytes. TNF-α binding to insulin receptors in liver cells and skeletal muscle cells can inhibit IRS phosphorylation and decrease its activity, which may reduce the efficiency of insulin signal transmission and lead to IR (*87*).

The gut microbiome in obese patients produces more inflammatory products. In contrast to the healthy control group, Zheng *et al*. demonstrated that obese HFD-fed mice had an intestinal microbiota that was dysregulated (88), and the bile acid content of their cecal contents had dramatically risen. Some scholars have shown that IL-18 and FFA levels were overexpressed in the endometrium of overweight patients with PCOS at the proliferative stage (*89*). Increased inflammatory substances cause reduction of ovarian blood, which may cause damage to granulosa and follicular membrane cells and lower progesterone production. The reduced progesterone production leads to attenuate endometrial secretory function, which is unconducive to embryonic implantation and growth, and it may manifest as infertility or abortion. Besides, an animal study showed that FFA could inhibit the synthesis of inflammatory kinases in pituitary gonadotropins and suppress activin-induced follicle-stimulating hormone β subunit expression level through Toll like receptor 2. The upregulated LH mRNA expression could inhibit FSH mRNA expression. In female HFD-fed mice, estrus cycle length was shortened and luteal count in the ovary was reduced, severely attenuating luteal function in early pregnancy because they did not experience the anticipated rise in LH and FSH levels before estrus (*90*).

2.4.3. Obesity-mediated alterations in immunity

The cultivation of embryos requires maternal immune tolerance. Abortion and unsuccessful embryonic implantation originate from the maternal immune system rejecting the embryo after the immunological tolerance has been compromised. Parker *et al*. found that the expression of uterine $CD8^+$ cells was reduced by nearly 40% in HFD-fed mice, suggesting that obesity could adversely affect maternal immunological adaptation (*91*). Thus, excessive fat may contribute to the development of AIDs. Long *et al*. reported that IL-18 was significantly overexpressed in the endometrium of overweight patients with PCOS at the proliferative stage (*89*), its overexpression increased IFN-γ production, and led to chronic low-grade inflammation. Parker *et al*. fed C57/BL6 mice with a high fat/sugar diet for 12 weeks to establish an obese mouse model, and mice were fed with a low fat/sugar diet as control. Progesterone and prolactin levels in plasma were measured at 7.5 days after copulation. The results showed that the percentage of NK cells and the expression level of IFN-γ were significantly reduced in obese mice. Besides, IFN-γ is involved in supporting uterine spiral artery remodeling and decidualization (*91*). Therefore, it could be hypothesized that obesity during the first trimester of pregnancy could inhibit angiogenesis by upregulating IL-18 expression level and downregulating IFN-γ expression level in NK cells.

2.4.4. Internal secretion

Leptin is an adipocytokine synthesized and secreted into the blood by lipocytes. It was demonstrated that HFD-fed mice had gut microbiota-associated diseases, which accelerated the leptin response (*78*). Leptin can not only activate adenosine-activated protein kinase (AMPK) signal transduction pathway, but also directly regulate lipid metabolism. It can also mediate phosphatidylinositol 3-kinase signaling pathway through binding to its receptor in hypothalamus, promoting insulin sensitivity. Leptin resistance can develop from a noticeable drop in the sensitivity of the leptin receptor caused by an increase in blood levels of the hormone (*92*). Leptin resistance may lead to metabolic disorders and promote IR (*93*). In addition to leptin, the dysbiosis of intestinal microbiome caused by an HFD may also lead to adiponectin resistance. Furthermore, adiponectin, an insulin-sensitizing hormone, promotes fatty acid oxidation and reduces triglyceride level in the muscle and liver of obese mice by activating the AMPK signaling pathway. Adiponectin resistance decreases fatty acid oxidation by inhibiting AMPK activity. Moreover, adiponectin resistance impairs phosphorylation of important insulin signaling proteins (Akt and AS160) in muscle. Ultimately, adiponectin resistance decreases insulin sensitivity and IR (*94*).

It is noteworthy that overweight individuals are at a lower risk of HHcy. A growing body of evidence demonstrated that the gut microbiota affects the blood homocysteine level of obese individuals, causing RPL. However, research has shown that folic acid generated by *Bifidobacterium longum* in the human intestines could lower the homocysteine level in individuals receiving hemodialysis (*95*). HHcy can damage endothelial cells by inhibiting the activity of glutathione oxidase and promoting the formation of peroxides. Further increase of the production of chemokines and cell adhesion molecules could promote platelet thrombosis, enhancing coagulation and preventing anticoagulation (*52*).

2.4.5. Uterine receptivity

Uterine receptivity is controlled by the activation of self-regulating feedback loops of decidual stromal cells in the subluminal epithelium. For pregnancy to succeed, the endometrium should engage with an embryo, and the embryo is implanted into the decidual matrix. However, obesity may cause decreased endometrial receptivity and poor endometrial decidualization during

implantation. Endometrial stromal cells in decidua after being transformed to the biosensor might cause decidual chemical harm to the PRL mechanism because they are extremely fatty to provide enough decidual response when they are implanted (*96*). Rhee *et al*. mated female mice after 12 weeks of HFD and high-sugar diet and found that the number of syncytia in decidua after fertilization was significantly lower than that in female mice with a normal diet. They performed diagnostic curettage under hysteroscopy in obese women with BMI $\geq$ 30 kg/m^2 and normal women with BMI < 25 kg/m^2. The expression levels of prolactin and insulin-like binding protein in the endometrial decidua in the obese group were lower than those in the normal weight group. These two factors are important markers for endometrial decidua (*97*). Yu *et al*. found that β-sitosterol might regulate the endometrial receptivity of patients with PCOS by changes in the structure and composition of the gut microbiome (*98*). Hence, changes in the gut microbiome can be associated with endometrial receptivity, and further relevant research should be conducted in the future.

2.4.6. Prethrombotic state (PTS)

Although there is strong evidence indicating the association of the gut microbiome with an elevated risk of obesity, which in turn increases the risk of the PTS, there is no clear, direct method in which the gut microbiota is associated with the PTS. The PTS, which has been identified as a significant contributor to RPL, is a pathological hypercoagulant condition and a pathological process of coagulation and anticoagulation system dysfunction in the body. Obesity is a risk factor for PTS and increases the expression levels of plasma plasminogen activator inhibitor-1 and tissue factor (TF). TF drives several aspects of metabolic disorders through the G-protein-coupled protein-activated receptor (PAR2, PAR1) signaling pathway. TF-PAR2 signaling pathway in adipocytes leads to diet-induced obesity by attenuating metabolism, while TF-PAR2 signaling pathway in hematopoietic and myeloid cells causes inflammation. As a result, this inflammatory effect could activate TF-induced clotting, and the two reinforce each other, leading to a vicious cycle (*99*).

3. Conclusions and future prospects

In recent years, a growing body of evidence demonstrated the association of the gut microbiota with a variety of diseases. Previous research suggested that the gut microbiome could respond to RPL, however, few studies have reported a direct correlation between RPL and intestinal microbes. Therefore, numerous physiological and pathological mechanisms need to be confirmed. In this review, the effects of the gut microbiome on RPL were discussed to be related to inflammatory response, the disruption of insulin signaling pathway and the formation of IR, maintenance of immunological tolerance at the maternal-fetal interface due to the interference with the immune imbalance of Treg/Th17 cells, and obesity. Exploring the effects of the gut microbiome on RPL is suggested *via* further research on the cytokines and signaling pathways involved in the pathogenesis of RPL caused by microorganisms, which may be beneficial for clinical prevention and treatment of RPL.

Acknowledgements

The authors wish to sincerely thank Peng Li and Suna Tian for their assistance in preparing the figures in this manuscript.

Funding: This work was supported by a project of the Taizhou Science and Technology Foundation (grant no. 1902ky154 to J Zhu), a project under the Scientific and Technological Innovation Action Plan of the Shanghai Natural Science Fund (grant no. 20ZR1409100 to L Wang), a project of the Chinese Association of Integration of Traditional and Western Medicine special foundation for Obstetrics and Gynecology-PuZheng Pharmaceutical Foundation (grant no. FCK-PZ-08 to L Wang), a project for hospital management of the Shanghai Hospital Association (grant no. X2021046 to L Wang), a clinical trial project of the Special Foundation for Healthcare Research of the Shanghai Municipal Health Commission (grant no. 202150042 to L Wang) and a project under the science and technology programs of Zhoushan, Zhejiang (grant no. 2021C31055 to WL Cao).

Conflict of Interest: The authors have no conflicts of interest to disclose.

References

1. Definitions of infertility and recurrent pregnancy loss: A committee opinion. Fertil Steril. 2020; 113:533-535.
2. RPL EGGo, Bender Atik R, Christiansen OB, Elson J, Kolte AM, Lewis S, Middeldorp S, Nelen W, Peramo B, Quenby S, Vermeulen N, Goddijn M. ESHRE guideline: Recurrent pregnancy loss. Hum Reprod Open. 2018; 2018:004.
3. Lu C, Li X, Gao Z, Song Y, Shen Y. Urolithins and intestinal health. Drug Discov Ther. 2022; 16:105-111.
4. Sender R, Fuchs S, Milo R. Are we really vastly outnumbered? Revisiting the ratio of bacterial to host cells in humans. Cell. 2016; 164:337-340.
5. Ghosh SS, Wang J, Yannie PJ, Ghosh S. Intestinal barrier dysfunction, LPS translocation, and disease development. J Endocr Soc. 2020; 4:039.
6. den Besten G, van Eunen K, Groen AK, Venema K, Reijngoud DJ, Bakker BM. The role of short-chain fatty acids in the interplay between diet, gut microbiota, and host energy metabolism. J Lipid Res. 2013; 54:2325-

2340.
7. Juge N. Microbial adhesins to gastrointestinal mucus. Trends Microbiol. 2012; 20:30-39.
8. Petersson J, Schreiber O, Hansson GC, Gendler SJ, Velcich A, Lundberg JO, Roos S, Holm L, Phillipson M. Importance and regulation of the colonic mucus barrier in a mouse model of colitis. Am J Physiol Gastrointest Liver Physiol. 2011; 300:327-333.
9. Jin M, Li D, Ji R, Liu W, Xu X, Feng X. Changes in gut microorganism in patients with positive immune antibody-associated recurrent abortion. Biomed Res Int. 2020; 2020:4673250.
10. Liu Y, Chen H, Feng L, Zhang J. Interactions between gut microbiota and metabolites modulate cytokine network imbalances in women with unexplained miscarriage. NPJ Biofilms Microbiomes. 2021; 7:24.
11. Larsen JM. The immune response to *Prevotella* bacteria in chronic inflammatory disease. Immunology. 2017; 151:363-374.
12. Guo S, Li W, Chen F, Yang S, Huang Y, Tian Y, Xu D, Cao N. Polysaccharide of Atractylodes macrocephala Koidz regulates LPS-mediated mouse hepatitis through the TLR4-MyD88-NFκB signaling pathway. Int Immunopharmacol. 2021; 98:107692.
13. Janssen AW, Kersten S. Potential mediators linking gut bacteria to metabolic health: A critical view. J Physiol. 2017; 595:477-487.
14. Saad MJ, Santos A, Prada PO. Linking gut microbiota and inflammation to obesity and insulin resistance. Physiology (Bethesda). 2016; 31:283-293.
15. Sikalidis AK, Maykish A. The gut microbiome and type 2 diabetes mellitus: Discussing a complex relationship. Biomedicines. 2020; 8:8.
16. Fu S, Yalcin A, Lee GY, Li P, Fan J, Arruda AP, Pers BM, Yilmaz M, Eguchi K, Hotamisligil GS. Phenotypic assays identify azoramide as a small-molecule modulator of the unfolded protein response with antidiabetic activity. Sci Transl Med. 2015; 7:292-298.
17. Mehrpouya-Bahrami P, Chitrala KN, Ganewatta MS, Tang C, Murphy EA, Enos RT, Velazquez KT, McCellan J, Nagarkatti M, Nagarkatti P. Blockade of CB1 cannabinoid receptor alters gut microbiota and attenuates inflammation and diet-induced obesity. Sci Rep. 2017; 7:15645.
18. Feldstein AE, Werneburg NW, Canbay A, Guicciardi ME, Bronk SF, Rydzewski R, Burgart LJ, Gores GJ. Free fatty acids promote hepatic lipotoxicity by stimulating TNF-alpha expression *via* a lysosomal pathway. Hepatology. 2004; 40:185-194.
19. Güngör N, Pennings JL, Knaapen AM, Chiu RK, Peluso M, Godschalk RW, Van Schooten FJ. Transcriptional profiling of the acute pulmonary inflammatory response induced by LPS: Role of neutrophils. Respir Res. 2010; 11:24.
20. Larsen N, Vogensen FK, van den Berg FW, Nielsen DS, Andreasen AS, Pedersen BK, Al-Soud WA, Sørensen SJ, Hansen LH, Jakobsen M. Gut microbiota in human adults with type 2 diabetes differs from non-diabetic adults. PLoS One. 2010; 5:9085.
21. Gao Z, Yin J, Zhang J, Ward RE, Martin RJ, Lefevre M, Cefalu WT, Ye J. Butyrate improves insulin sensitivity and increases energy expenditure in mice. Diabetes. 2009; 58:1509-1517.
22. Perry RJ, Peng L, Barry NA, Cline GW, Zhang D, Cardone RL, Petersen KF, Kibbey RG, Goodman AL, Shulman GI. Acetate mediates a microbiome-brain-β-cell axis to promote metabolic syndrome. Nature. 2016; 534:213-217.
23. Deiteren A, De Man JG, Pelckmans PA, De Winter BY. Histamine H4 receptors in the gastrointestinal tract. Br J Pharmacol. 2015; 172:1165-1178.
24. Yamamoto M, Pinto-Sanchez MI, Bercik P, Britz-McKibbin P. Metabolomics reveals elevated urinary excretion of collagen degradation and epithelial cell turnover products in irritable bowel syndrome patients. Metabolomics. 2019; 15:82.
25. Koh A, Molinaro A, Stahlman M, *et al*. Microbially produced imidazole propionate impairs insulin signaling through mTORC1. Cell. 2018; 175:947-961.
26. Gargari G, Taverniti V, Balzaretti S, Ferrario C, Gardana C, Simonetti P, Guglielmetti S. Consumption of a *bifidobacterium bifidum* strain for 4 weeks modulates dominant intestinal bacterial taxa and fecal butyrate in healthy adults. Appl Environ Microbiol. 2016; 82:5850-5859.
27. Peng L, He Z, Chen W, Holzman IR, Lin J. Effects of butyrate on intestinal barrier function in a Caco-2 cell monolayer model of intestinal barrier. Pediatr Res. 2007; 61:37-41.
28. Gérard P. Metabolism of cholesterol and bile acids by the gut microbiota. Pathogens. 2013; 3:14-24.
29. Jia W, Xie G, Jia W. Bile acid-microbiota crosstalk in gastrointestinal inflammation and carcinogenesis. Nat Rev Gastroenterol Hepatol. 2018; 15:111-128.
30. Halkias C, Darby WG, Feltis BN, McIntyre P, Macrides TA, Wright PFA. Marine bile natural products as agonists of the TGR5 receptor. J Nat Prod. 2021; 84:1507-1514.
31. Albaugh VL, Banan B, Antoun J, Xiong Y, Guo Y, Ping J, Alikhan M, Clements BA, Abumrad NN, Flynn CR. Role of bile acids and GLP-1 in mediating the metabolic improvements of bariatric surgery. Gastroenterology. 2019; 156:1041-1051.
32. Hang S, Paik D, Yao L, *et al*. Bile acid metabolites control T_H17 and T_{reg} cell differentiation. Nature. 2019; 576:143-148.
33. Saito S, Nakashima A, Shima T, Ito M. Th1/Th2/Th17 and regulatory T-cell paradigm in pregnancy. Am J Reprod Immunol. 2010; 63:601-610.
34. Qian J, Zhang N, Lin J, Wang C, Pan X, Chen L, Li D, Wang L. Distinct pattern of Th17/Treg cells in pregnant women with a history of unexplained recurrent spontaneous abortion. Biosci Trends. 2018; 12:157-167.
35. Arif RN MG, Mufasirin M, Lucia TS, Sunarjo, Teguh WS, Erry GD. Effects of hyperbaric oxygen therapy on IL-17, fetal body weight and total fetus in pregnant rattus norvegicus infected with tachyzoite toxoplasma gondii. Systematic Reviews in Pharmacy. 2020; 11:328-634.
36. van den Munckhof ICL, Kurilshikov A, Ter Horst R, Riksen NP, Joosten LAB, Zhernakova A, Fu J, Keating ST, Netea MG, de Graaf J, Rutten JHW. Role of gut microbiota in chronic low-grade inflammation as potential driver for atherosclerotic cardiovascular disease: A systematic review of human studies. Obes Rev. 2018; 19:1719-1734.
37. Vega-Magaña N, Delgado-Rizo V, García-Benavides L, Del Toro-Arreola S, Segura-Ortega J, Morales A, Zepeda-Nuño JS, Escarra-Senmarti M, Gutiérrez-Franco J, Haramati J, Bueno-Topete MR. Bacterial translocation is linked to increased intestinal IFN-γ, IL-4, IL-17, and mucin-2 in cholestatic rats. Ann Hepatol. 2018; 17:318-329.
38. Chen J, Wright K, Davis JM, Jeraldo P, Marietta

EV, Murray J, Nelson H, Matteson EL, Taneja V. An expansion of rare lineage intestinal microbes characterizes rheumatoid arthritis. Genome Med. 2016; 8:43.
39. Reyes-Díaz A, Mata-Haro V, Hernández J, González-Córdova AF, Hernández-Mendoza A, Reyes-Díaz R, Torres-Llanez MJ, Beltrán-Barrientos LM, Vallejo-Cordoba B. Milk fermented by specific *lactobacillus* strains regulates the serum levels of IL-6, TNF-α and IL-10 cytokines in a LPS-stimulated murine model. Nutrients. 2018; 10:691.
40. Arpaia N, Campbell C, Fan X, Dikiy S, van der Veeken J, deRoos P, Liu H, Cross JR, Pfeffer K, Coffer PJ, Rudensky AY. Metabolites produced by commensal bacteria promote peripheral regulatory T-cell generation. Nature. 2013; 504:451-455.
41. Chang PV, Hao L, Offermanns S, Medzhitov R. The microbial metabolite butyrate regulates intestinal macrophage function *via* histone deacetylase inhibition. Proc Natl Acad Sci U S A. 2014; 111:2247-2252.
42. Kusumastuti SA, Nugrahaningsih DAA, Wahyuningsih MSH. *Centella asiatica* (L.) extract attenuates inflammation and improve insulin sensitivity in a coculture of lipopolysaccharide (LPS)-induced 3T3-L1 adipocytes and RAW 264.7 macrophages. Drug Discov Ther. 2019; 13:261-267.
43. Otun HA, Lash GE, Innes BA, Bulmer JN, Naruse K, Hannon T, Searle RF, Robson SC. Effect of tumour necrosis factor-α in combination with interferon-γ on first trimester extravillous trophoblast invasion. J Reprod Immunol. 2011; 88:1-11.
44. Okada K, Matsushima Y, Mizutani K, Yamanaka K. The role of gut microbiome in psoriasis: Oral administration of *staphylococcus aureus* and *streptococcus danieliae* exacerbates skin inflammation of imiquimod-induced psoriasis-like dermatitis. Int J Mol Sci. 2020; 21:3303.
45. Mechoud MA, Mateos MV, Salvador GA, Font De Valdez G, Rodriguez AV. Signaling pathways involved in TNF-α inhibition in PBMC by *lactobacillus reuteri*. Biocell. 2010; 34:73.
46. Gueddouri D, Caüzac M, Fauveau V, Benhamed F, Charifi W, Beaudoin L, Rouland M, Sicherre F, Lehuen A, Postic C, Boudry G, Burnol AF, Guilmeau S. Insulin resistance per se drives early and reversible dysbiosis-mediated gut barrier impairment and bactericidal dysfunction. Mol Metab. 2022; 57:101438.
47. Guideline of the european society of human reproduction and embryology. Recurrent pregnancy loss. *https://www.eshre.eu/Guidelines-and-Legal/Guidelines/Recurrent-pregnancy-loss* (accessed June 5, 2023).
48. Wang Y, Zhao H, Li Y, Zhang J, Tan J, Liu Y. Relationship between recurrent miscarriage and insulin resistance. Gynecol Obstet Invest. 2011; 72:245-251.
49. Wang J, Wu D, Guo H, Li M. Hyperandrogenemia and insulin resistance: The chief culprit of polycystic ovary syndrome. Life Sci. 2019; 236:116940.
50. Porras-Dorantes Á, Brambila-Tapia AJL, Lazcano-Castellanos AB, Da Silva-José TD, Juárez-Osuna JA, García-Ortiz JE. Association between G1733A (rs6152) polymorphism in androgen receptor gene and recurrent spontaneous abortions in Mexican population. J Assist Reprod Genet. 2017; 34:1303-1306.
51. Hu M, Zhang Y, Guo X, Jia W, Liu G, Zhang J, Li J, Cui P, Sferruzzi-Perri A, Han Y, Wu X, Ma H, Brännström M, Shao L, Billig H. Hyperandrogenism and insulin resistance induce gravid uterine defects in association with mitochondrial dysfunction and aberrant reactive oxygen species production. Am J Physiol Endocrinol Metab. 2019; 316:794- 809.
52. Ispasoiu CA, Chicea R, Stamatian FV, Ispasoiu F. High fasting insulin levels and insulin resistance may be linked to idiopathic recurrent pregnancy loss: A case-control study. Int J Endocrinol. 2013; 2013:576926.
53. Jakubowicz DJ, Essah PA, Seppala M, Jakubowicz S, Baillargeon JP, Koistinen R, Nestler JE. Reduced serum glycodelin and insulin-like growth factor-binding protein-1 in women with polycystic ovary syndrome during first trimester of pregnancy. J Clin Endocrinol Metab. 2004; 89:833-839.
54. Ujvari D, Jakson I, Oldmark C, Attarha S, Alkasalias T, Salamon D, Gidlof S, Hirschberg AL. Prokineticin 1 is up-regulated by insulin in decidualizing human endometrial stromal cells. J Cell Mol Med. 2018; 22:163-172.
55. Zhou J, Wang Y, Fan Q, Liu Y, Liu H, Yan J, Li M, Dong W, Li W. High levels of fucosylation and sialylation of milk N-glycans from mothers with gestational diabetes mellitus alter the offspring gut microbiome and immune balance in mice. FASEB J. 2020; 34:3715-3731.
56. Ravindran R, Loebbermann J, Nakaya HI, Khan N, Ma H, Gama L, Machiah DK, Lawson B, Hakimpour P, Wang Y, Li S, Sharma P, Kaufman RJ, Martinez J, Pulendran B. The amino acid sensor GCN2 controls gut inflammation by inhibiting inflammasome activation. Nature. 2016; 531:523-527.
57. Cheng H, Guan X, Chen D, Ma W. The Th17/Treg cell balance: A gut microbiota-modulated story. Microorganisms. 2019; 7:583.
58. Blacher E, Levy M, Tatirovsky E, Elinav E. Microbiome-modulated metabolites at the interface of host immunity. J Immunol. 2017; 198:572-580.
59. Christiansen OB, Steffensen R, Nielsen HS, Varming K. Multifactorial etiology of recurrent miscarriage and its scientific and clinical implications. Gynecol Obstet Invest. 2008; 66:257-267.
60. Viall CA, Chamley LW. Histopathology in the placentae of women with antiphospholipid antibodies: A systematic review of the literature. Autoimmun Rev. 2015; 14:446-471.
61. Sacharidou A, Shaul PW, Mineo C. New insights in the pathophysiology of antiphospholipid syndrome. Semin Thromb Hemost. 2018; 44:475-482.
62. Ruff WE, Vieira SM, Kriegel MA. The role of the gut microbiota in the pathogenesis of antiphospholipid syndrome. Curr Rheumatol Rep. 2015; 17:472.
63. Laczik R, Soltesz P, Szodoray P, Szekanecz Z, Kerekes G, Paragh G, Rajnavolgyi E, Abel G, Szegedi G, Bodolay E. Impaired endothelial function in patients with undifferentiated connective tissue disease: A follow-up study. Rheumatology (Oxford). 2014; 53:2035-2043.
64. Gülden E, Vudattu NK, Deng S, *et al*. Microbiota control immune regulation in humanized mice. JCI Insight. 2017; 2:e91709.
65. van den Boogaard E, Vissenberg R, Land JA, van Wely M, Ven der Post JA, Goddijn M, Bisschop PH. Significance of (sub)clinical thyroid dysfunction and thyroid autoimmunity before conception and in early pregnancy: A systematic review. Hum Reprod Update. 2016; 22:532-533.
66. Martocchia A, Falaschi P. Amino acid sequence homologies between HCV polyprotein and thyroid antigens. Intern Emerg Med. 2007; 2:65-67.

67. Kiseleva EP, Mikhailopulo KI, Sviridov OV, Novik GI, Knirel YA, Szwajcer Dey E. The role of components of *Bifidobacterium* and *Lactobacillus* in pathogenesis and serologic diagnosis of autoimmune thyroid diseases. Benef Microbes. 2011; 2:139-154.
68. Cosorich I, Dalla-Costa G, Sorini C, Ferrarese R, Messina MJ, Dolpady J, Radice E, Mariani A, Testoni PA, Canducci F, Comi G, Martinelli V, Falcone M. High frequency of intestinal T_H17 cells correlates with microbiota alterations and disease activity in multiple sclerosis. Sci Adv. 2017; 3:1700492.
69. Venkataraman A, Sieber JR, Schmidt AW, Waldron C, Theis KR, Schmidt TM. Variable responses of human microbiomes to dietary supplementation with resistant starch. Microbiome. 2016; 4:33.
70. Wang WJ, Hao CF, Yi L, Yin GJ, Bao SH, Qiu LH, Lin QD. Increased prevalence of T helper 17 (Th17) cells in peripheral blood and decidua in unexplained recurrent spontaneous abortion patients. J Reprod Immunol. 2010; 84:164-170.
71. Fu B, Li X, Sun R, Tong X, Ling B, Tian Z, Wei H. Natural killer cells promote immune tolerance by regulating inflammatory T_H17 cells at the human maternal-fetal interface. Proc Natl Acad Sci USA. 2013; 110:231-240.
72. Huber S, Gagliani N, Esplugues E, O'Connor W, Jr., Huber FJ, Chaudhry A, Kamanaka M, Kobayashi Y, Booth CJ, Rudensky AY, Roncarolo MG, Battaglia M, Flavell RA. Th17 cells express interleukin-10 receptor and are controlled by $Foxp3^-$ and $Foxp3^+$ regulatory $CD4^+$ T cells in an interleukin-10-dependent manner. Immunity. 2011; 34:554-565.
73. Qiu Y, Jiang Z, Hu S, Wang L, Ma X, Yang X. *Lactobacillus plantarum* enhanced IL-22 production in natural killer (NK) cells that protect the integrity of intestinal epithelial cell barrier damaged by enterotoxigenic *Escherichia coli*. Int J Mol Sci. 2017; 18:2409.
74. Satoh-Takayama N, Vosshenrich CA, Lesjean-Pottier S, Sawa S, Lochner M, Rattis F, Mention JJ, Thiam K, Cerf-Bensussan N, Mandelboim O, Eberl G, Di Santo JP. Microbial flora drives interleukin 22 production in intestinal $NKp46^+$ cells that provide innate mucosal immune defense. Immunity. 2008; 29:958-970.
75. Sun JC, Lanier LL. NK cell development, homeostasis and function: Parallels with $CD8^+$ T cells. Nat Rev Immunol. 2011; 11:645-657.
76. Gurung M, Li Z, You H, Rodrigues R, Jump DB, Morgun A, Shulzhenko N. Role of gut microbiota in type 2 diabetes pathophysiology. EBioMedicine. 2020; 51:102590.
77. Russell JT, Roesch LFW, Ördberg M, Ilonen J, Atkinson MA, Schatz DA, Triplett EW, Ludvigsson J. Genetic risk for autoimmunity is associated with distinct changes in the human gut microbiome. Nat Commun. 2019; 10:3621.
78. Schéle E, Grahnemo L, Anesten F, Hallén A, Bäckhed F, Jansson JO. The gut microbiota reduces leptin sensitivity and the expression of the obesity-suppressing neuropeptides proglucagon (*Gcg*) and brain-derived neurotrophic factor (*Bdnf*) in the central nervous system. Endocrinology. 2013; 154:3643-3651.
79. Koliada A, Syzenko G, Moseiko V, Budovska L, Puchkov K, Perederiy V, Gavalko Y, Dorofeyev A, Romanenko M, Tkach S, Sineok L, Lushchak O, Vaiserman A. Association between body mass index and *Firmicutes*/*Bacteroidetes* ratio in an adult Ukrainian population. BMC Microbiol. 2017; 17:120.
80. Du Y, Chen L, Lin J, Zhu J, Zhang N, Qiu X, Li D, Wang L. Chromosomal karyotype in chorionic villi of recurrent spontaneous abortion patients. Biosci Trends. 2018; 12:32-39.
81. Tremellen K, Pearce K, Zander-Fox D. Increased miscarriage of euploid pregnancies in obese women undergoing cryopreserved embryo transfer. Reprod Biomed Online. 2017; 34:90-97.
82. Wang JH, Bose S, Shin NR, Chin YW, Choi YH, Kim H. Pharmaceutical impact of houttuynia cordata and metformin combination on high-fat-diet-induced metabolic disorders: Link to intestinal microbiota and metabolic endotoxemia. Front Endocrinol (Lausanne). 2018; 9:620.
83. Fei N, Zhao L. An opportunistic pathogen isolated from the gut of an obese human causes obesity in germfree mice. ISME J. 2013; 7:880-884.
84. Just S, Mondot S, Ecker J, *et al*. The gut microbiota drives the impact of bile acids and fat source in diet on mouse metabolism. Microbiome. 2018; 6:134.
85. Li S, Li J, Mao G, Yan L, Hu Y, Ye X, Tian D, Linhardt RJ, Chen S. Effect of the sulfation pattern of sea cucumber-derived fucoidan oligosaccharides on modulating metabolic syndromes and gut microbiota dysbiosis caused by HFD in mice. J Funct Foods. 2019; 55:193-210.
86. Cani PD, Amar J, Iglesias MA, *et al*. Metabolic endotoxemia initiates obesity and insulin resistance. Diabetes. 2007; 56:1761-1772.
87. Ryu JK, Kim SJ, Rah SH, Kang JI, Jung HE, Lee D, Lee HK, Lee JO, Park BS, Yoon TY, Kim HM. Reconstruction of LPS transfer cascade reveals structural determinants within LBP, CD14, and TLR4-MD2 for efficient LPS recognition and transfer. Immunity. 2017; 46:38-50.
88. Zheng X, Huang F, Zhao A, Lei S, Zhang Y, Xie G, Chen T, Qu C, Rajani C, Dong B, Li D, Jia W. Bile acid is a significant host factor shaping the gut microbiome of diet-induced obese mice. BMC Biol. 2017; 15:120.
89. Long X, Li R, Yang Y, Qiao J. Overexpression of IL-18 in the proliferative phase endometrium of patients with polycystic ovary syndrome. Reprod Sci. 2017; 24:252-257.
90. Sharma S, Morinaga H, Hwang V, Fan W, Fernandez MO, Varki N, Olefsky JM, Webster NJ. Free fatty acids induce Lhb mRNA but suppress Fshb mRNA in pituitary LβT2 gonadotropes and diet-induced obesity reduces FSH levels in male mice and disrupts the proestrous LH/FSH surge in female mice. Endocrinology. 2013; 154:2188-2199.
91. Parker VJ, Solano ME, Arck PC, Douglas AJ. Diet-induced obesity may affect the uterine immune environment in early-mid pregnancy, reducing NK-cell activity and potentially compromising uterine vascularization. Int J Obes (Lond). 2014; 38:766-774.
92. McGuire MJ, Ishii M. Leptin dysfunction and alzheimer's disease: Evidence from cellular, animal, and human studies. Cell Mol Neurobiol. 2016; 36:203-217.
93. Gupta A, Gupta V, Agrawal S, Natu SM, Agrawal CG, Negi MP, Tiwari S. Association between circulating leptin and insulin resistance, the lipid profile, and metabolic risk factors in North Indian adult women. Biosci Trends. 2010; 4:325-332.
94. Mullen KL, Pritchard J, Ritchie I, Snook LA, Chabowski A, Bonen A, Wright D, Dyck DJ. Adiponectin resistance precedes the accumulation of skeletal muscle lipids and

insulin resistance in high-fat-fed rats. Am J Physiol Regul Integr Comp Physiol. 2009; 296:243-251.
95. Taki K, Takayama F, Niwa T. Beneficial effects of *Bifidobacteria* in a gastroresistant seamless capsule on hyperhomocysteinemia in hemodialysis patients. J Ren Nutr. 2005; 15:77-80.
96. Salker MS, Nautiyal J, Steel JH, *et al*. Disordered IL-33/ST2 activation in decidualizing stromal cells prolongs uterine receptivity in women with recurrent pregnancy loss. PLoS One. 2012; 7:52252.
97. Rhee JS, Saben JL, Mayer AL, Schulte MB, Asghar Z, Stephens C, Chi MM, Moley KH. Diet-induced obesity impairs endometrial stromal cell decidualization: A potential role for impaired autophagy. Hum Reprod. 2016; 31:1315-1326.
98. Yu Y, Cao Y, Huang W, Liu Y, Lu Y, Zhao J. beta-Sitosterol ameliorates endometrium receptivity in PCOS-like mice: The mediation of gut microbiota. Front Nutr. 2021; 8:667130.
99. Samad F, Ruf W. Inflammation, obesity, and thrombosis. Blood. 2013; 122:3415-3422.

Received February 12, 2023; Revised June 6, 2023; Accepted June 22, 2023.

[§]These authors contributed equally to this work.

**Address correspondence to:*
Ling Wang, Laboratory for Reproductive Immunology, Obstetrics and Gynecology Hospital of Fudan University, 419 Fangxie Road, Shanghai 200011, China.
E-mail: Dr.wangling@fudan.edu.cn.

Released online in J-STAGE as advance publication June 25, 2023.

Mini-Review

DOI: 10.5582/ddt.2023.01008

Harmless and ecologically acceptable fabrication of long-acting injectable microspheres

Akihiro Matsumoto*, Masahiro Murakami

Laboratory of Pharmaceutics, Faculty of Pharmacy, Osaka Ohtani University, Osaka, Japan.

SUMMARY The use of harmful solvents during the preparation of pharmaceutical formulations is restricted to preserve environment and ensure safety of industrial operations. However, harmful solvents must be used to produce certain formulations. For instance, methylene chloride has been used in the fabrication of polylactic acid (PLA) and poly(lactic-co-glycolic) acid (PLGA) microspheres. This review highlights the latest advances in the strategy of PLA or PLGA microsphere production from non-halogenated solvents and describes advantages and limitations of these methods. The study also discusses the development of dry fabrication techniques for microsphere fabrication and the positioning of conventional and dry fabrication in the containment concept for workers' safety.

Keywords polylactic acid, poly(lactic-co-glycolic) acid, substitute solvents, containment, solventless fabrication

1. Introduction

Microsphere formulations play an important role in clinical drug therapy of various disorders. In drug delivery systems, microspheres are primarily used to control drug release. Most microsphere preparations for controlled drug release have particle sizes of several microns. The particle size determines the type of application. Microspheres with a size of 100-1,000 μm or more are mainly used as oral preparations, whereas microspheres with sizes ranging from several to tens of micrometers are used for injections. Long-acting injectable (LAI) microspheres are made of biodegradable polymers, including polylactic acid (PLA) and lactic acid-glycolic acid copolymer (PLGA).

The method for producing microspheres can be categorized based on the target particle size. For microspheres of 100 μm or more, a fabrication method by coating the core particles is mainly adopted, using a coating machine such as fluidized and tumbling fluidized bed coating machine. The conventional coating machine produces microspheres with sizes of several hundred micrometers. Because smaller microspheres tend to aggregate during the fabrication process, for their production, the coating machine needs to be equipped with specific functions. The Wurster method, utilized in one type of fluidized bed coating machines, can be used to produce microspheres of 100 μm (*1*) or smaller; however, it is difficult to obtain primary particles of 20-50 μm (*2*). In contrast, in the production of microspheres of 100 μm or smaller, spray drying and solvent evaporation from emulsion formation are generally performed (*3*). Figure 1 shows the scheme of particle production using an oil-in-water-type emulsion-solvent evaporation method. Low boiling point, water-insoluble solvents, such as methylene chloride, are used to dissolve the polymer and form the oil phase, in which the drug is then dissolved or dispersed. The oil is emulsified in an aqueous solution containing an emulsion stabilizer, such as polyvinyl alcohol, to form an oil-in-water emulsion. The emulsification process determines microsphere particle size, which can be regulated by adjusting the emulsification sheering speed and surfactant concentration, so that oil droplets reach the target size. After the emulsification process, the obtained emulsion is stirred to remove the solvent from the oil droplets, which are solidified as microspheres by heating and pressure reduction, if necessary. The collected microspheres are washed with water and dried by freeze-drying, typically used to ensure good dispersibility. If necessary, the freeze-dried microspheres can be filled into vials by a powder-filling machine.

Fabrication of microspheres using coating machines usually uses water and less harmful solvents, such as ethanol. Some methods require no solvent at all (*4*). In contrast, harmful solvents are commonly used in microsphere fabrication by solvent evaporation, which is a problem that needs to be resolved. In addition,

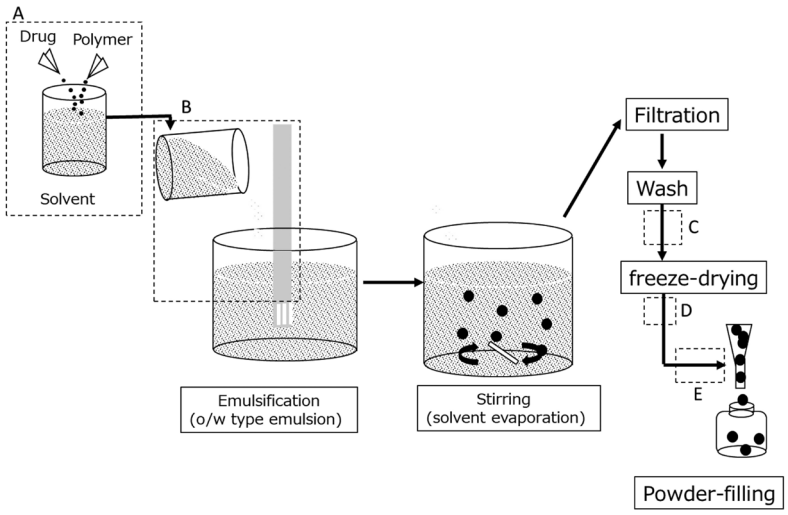

Figure 1. Solvent evaporation procedure for fabricating LAI microspheres. Dash line frame indicates the example of the risk points for workers' exposure to harmful ingredients or products; **(A)** charging ingredients in the oil phase preparation process, **(B)** charging oil phase in an emulsification process, **(C)** discharging the collected microspheres in a microspheres collection process, **(D)** charging and discharging the collected microspheres into a freeze dryer in the freeze-drying process, and **(E)** charging freeze-dried microspheres in a powder filling process.

workers' exposure to active pharmaceutical ingredients (API) can occur (Figure 1). This review mainly discusses the solutions proposed to solve the problems of the solvents used for the fabrication process of LAI microsphere formulations. The containment concept for workers' safety is explored in the microencapsulation of compounds with high pharmacological activity or toxicity. We hope that this review will promote further research into harmless and ecologically sound fabrication methods for LAI microsphere formulations.

2. Reduction of residual solvent content in PLGA microspheres

For the solvent evaporation method, it is instructed that a solvent should meet the following criteria: i) ability to dissolve the chosen polymer, ii) poor solubility in the continuous phase, iii) high volatility and low boiling point, and iv) low toxicity (*5*). In general, when PLGA microspheres are prepared by an oil-in-water-type emulsion-solvent evaporation method, it is common to use a halogen-based water-insoluble volatile organic solvent, such as methylene chloride, to dissolve PLGA because such solvents meet the criteria i), ii), and iii). However, halogen-containing organic solvents are highly toxic to the human body and have a significant impact on the environment. In the pharmaceutical industry, the use of such solvents is not prohibited, but the amount of the residual solvent in pharmaceuticals is regulated. For example, methylene chloride is categorized as a class 2 solvent, and its concentration limit was set at 600 ppm by ICH Q3C (R6) guideline of the International Conference on Harmonization of Technical Requirements for Registration of Pharmaceuticals for Human Use (ICH), organized by the regulatory authorities of Japan, Europe, and the United States, and the 18th edition of the Japanese Pharmacopoeia (*6*).

In the oil-in-water-type emulsion-solvent evaporation method, the solvent removal process includes solvent extraction from the oil phase into the water phase and solvent evaporation from the water phase into the vapor phase (*5*,*7*). Solvent extraction occurs at the beginning of the process to reach the saturated solubility of the solvent in the water phase immediately before solvent evaporation occur simultaneously (*8-11*). The state of the dispersed phase that includes PLGA changes from liquid to gel as the solvent extraction/evaporation process progresses (*7*). As the state of the oil phase changes from liquid to gel and solid, the diffusion coefficient of the solvent decreases in the dispersed phase. The speed of solvent extraction from the liquid state of the oil phase varies negligibly at the start of the emulsification process, despite the differences in oil phase sizes. In fact, it has been reported that the solvent was extracted in approximately 10 s during fabrication of microparticles with mode diameters of 2 μm and 20 μm (*7*). However, the speed of solvent extraction from the oil phase in gel state depends on the size of the oil phase and temperature. In our preliminary study, the residual methylene chloride in PLGA microspheres of approximately 10 and 40 μm, which were fabricated at 25°C for 3 h using the solvent evaporation method, was 500-700 and 2,000-3,000 ppm, respectively. For the encapsulation of water-insoluble drugs, reduction of the microsphere size is an effective approach to decrease the concentration of the residual solvent. Increasing the temperature during solvent evaporation is another effective approach. However, for the microencapsulation of water-soluble drugs, the reduction of particle size and solvent evaporation/extraction at higher temperatures are

not always possible in a proper approach. For smaller microspheres, extraction of a water-soluble drug into the water phase during the process increases, resulting in low encapsulation efficiency (*12*). In addition, the initial burst release was reported to increase during fabrication at higher temperature (*12-14*). The reduction in particle size and high-temperature fabrication can be a disadvantage for the properties of microspheres, although residual solvents can be reduced. Heating the dried (water removed) hardened microspheres with mannitol is an effective approach to solve the problem of residual solvents and improve other properties of microspheres, as this procedure guarantees the maintenance of encapsulation efficiency. Heating over the glass transition temperature of a base ingredient increases the diffusion coefficient in solidified microspheres, thereby reducing residual solvent. However, heating over the glass transition temperature can induce aggregation and deformation of the microspheres. Mannitol is a commonly used inactive ingredient in the lyophilization process that prevents aggregation. Co-heating with mannitol also suppresses aggregation. For example, co-heating microspheres with mannitol at a temperature 3-5°C higher than glass transition temperature for 24-120 h reduced the low level of residual methylene chloride (< 100 ppm) without microspheres aggregation or deformation and suppressed an initial burst release (*15*).

3. Development of a PLGA microsphere manufacturing method using low toxicity solvent

As we mentioned above, halogenated organic solvents have restricted industrial use owing to their toxicity and potential damage to the environment. Several less harmful solvents have been investigated as substitute solvents for the fabrication of PLGA microspheres. These solvents are classified as low toxicity solvents and are regulated by Good Manufacturing Practice or other quality standards described in guideline Q3C (R6) of the ICH and the 18th edition of the Japanese Pharmacopoeia. Ethyl acetate is a class 3, non-halogenated, low toxicity solvent, which is most used for the fabrication of PLGA microspheres as a substitute for halogenated solvents (*16-21*). Ethyl acetate has a boiling point of 77°C and a water solubility of 8.7 g/100 mL at 20°C, which are higher than those of methylene chloride. Therefore, in the case of ethyl acetate, solvent extraction rather than evaporation is the dominant mechanism of solidifying PLGA microspheres during fabrication. Although methylene chloride can contain very little water, ethyl acetate contains more, which leads to the immersion of water-in-oil phase of ethyl acetate during the emulsification process and formation of microspheres with a rough surface. PLGA microspheres prepared with the use of methylene chloride have high transparency, whereas those prepared using ethyl acetate often have low transparency during optical microscopic observation. The immersion of water in the oil phase causes the formation of micropores in the fabricated microspheres, which explains their low transparency. The porosity caused by the immersion of water also often decreases the efficiency of water-soluble drug encapsulation (*22*). Ethyl formate (*23*,*24*) and methyl propionate (*25*) have also been proposed as candidates to substitute methylene chloride for microsphere fabrication. A report shows that ethyl formate surpasses ethyl acetate in relation to volatility and water miscibility, which improves microsphere manufacturing process, helping to produce PLGA microspheres with better quality in terms of drug crystallization, drug encapsulation efficiency, microsphere size homogeneity, and residual solvent content (*23*,*24*).

Among other low toxicity solvents, acetone is another good option for PLGA and PLA microsphere production (*26-28*). Acetone is a popular solvent in industrial applications. Because acetone is miscible with water, it cannot form an emulsion, so the method of solvent evaporation from an oil-in-water emulsion is not applicable. However, phase separation occurs in the aqueous glycerin solution, when glycerin concentration is above a certain level (Figure 2A). Therefore, if a glycerin solution containing polyvinyl alcohol is used as the continuous phase, a polymer acetone solution can be emulsified as a dispersed phase. Microspheres can then be obtained by extracting the solvent from the dispersed phase by increasing the water content in the continuous phase. Figure 2B shows the dissolution of cyanocobalamin from PLGA microspheres. The dissolution was confirmed to be equivalent to that from conventional microspheres prepared using methylene chloride. Encapsulation efficiency of the resultant microspheres was also equivalent to that of the microspheres prepared with methylene chloride (*26*,*27*).

4. Development of a dry, solventless method for microsphere manufacturing

The manufacturing method introduced in the previous section uses a low toxicity organic solvent. In the fabrication of microspheres releasing controlled drugs, using an organic solvent is considered fundamental to PLGA microsphere fabrication because water-insoluble PLGA is required to dissolve in order to encapsulate the drug. However, because these organic solvents still have some negative effect on the environment despite their low toxicity, their use requires setting up the equipment for solvent recovery. Nonetheless, social demand for the development of fabrication methods that do not use organic solvents is increasing.

Mechanofusion is a dry manufacturing method used in fine particle design, whereby composite particles are obtained by attaching guest particles on the surface of core (host) particles for surface modification purposes (*29-31*). There are many commercially available

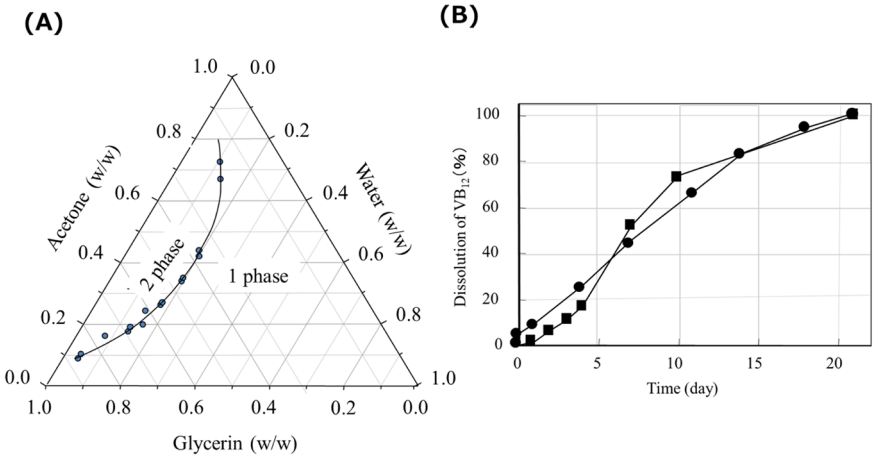

Figure 2. Microsphere fabrication using acetone as solvent in the oil phase. (A) Phase diagram of the acetone-glycerin-water ternary system (*26*). **(B)** Dissolution profiles of cyanocobalamin from poly(lactic-co-glycolic) acid microspheres fabricated using the acetone-glycerin-water ternary system: ●, microspheres fabrication using acetone; ■, microspheres fabrication using methylene chloride (conventional method) (*26*).

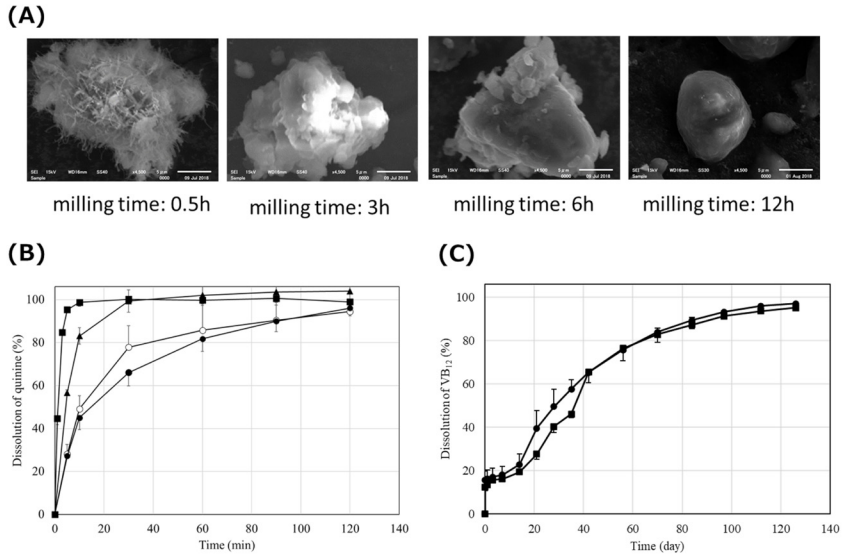

Figure 3. Method of solventless dry microsphere fabrication using a ball mill. (A) Influence of the milling time on the morphology of carnauba wax microspheres (*34*). **(B)** Influence of milling time on the duration of quinine release from carnauba wax microspheres: ■, pulverized quinine; ▲, milling time 0.5 h; ○, milling time 6 h; ●, milling time 12 h (*34*). **(C)** Cyanocobalamin release from poly(lactic-co-glycolic) acid microspheres: ●, solventless dry fabrication method; ■, conventional solvent evaporation method using methylene chloride (*35*).

formulation machines for mechanofusion technology. Following physical impact provided by these machines, van der Waals and electrostatic forces between particles as well as mechanochemical bonding forces are generated when particles collide. In general, the binding force between particles is relatively weak and considered unsuitable for the controlled release of water-soluble drugs. Furthermore, because the guest particles are usually smaller than the host particles, it is necessary to use nanoparticles as guest particles to fabricate particles of several to tens of micrometers using the mechanofusion method. In applying nanoparticles to the mechanofusion method, the preparation of soft-ordered nanocomposite particles with tens of micrometers for inhalation has been reported (*32,33*).

A dry manufacturing method can be introduced to fabricate sustained-release microspheres using a higher physical force than that of the mechanofusion machine (*34-36*). This method can use common manufacturing equipment such as a ball mill (*34*). A characteristic feature of this method is that milling is performed at a relatively low speed for a long time, so that the sample temperature does not become excessively high. An example of ball-milled pulverized quinine hydrochloride powder and carnauba wax is shown in Figures 3A and 3B. The obtained microspheres had an average particle size of approximately 10 μm, and their morphology changed from irregular to rounded particles as milling time increased (Figure 3A). In addition, the drug release time was also prolonged with milling time (Figure

3B). When particles smaller than 10 μm undergo dry pulverization with a ball mill, it is difficult to further decrease their sizes because agglomeration between particles rather than reduction in their size becomes a dominant process. As milling progresses, the coating materials with a large particle size become finer, but particle size of the pulverized drug powder is retained. The fine coating material particles generated during milling collide and become attached to the drug particles, forming agglomerates. When a coating material with a low melting point or a low softening point is used, melting occurs in the limited area at the collision point owing to the thermal energy generated by the collision between the particles and during prolonged processing, the melted part stochastically spreads over the entire particle and, as a result, fills the gaps in the composite particles.

This method also allows for the fabrication of PLGA microspheres (*35*). Figure 3C shows a profile of drug release from microspheres fabricated by ball milling finely ground cyanocobalamin powder and PLGA. Fabrication of conventional microspheres by the oil-in-water emulsion-solvent evaporation method using methylene chloride is accompanied by some drug loss, which was not observed during manufacturing of microspheres by ball milling. In addition, microspheres manufactured by the latter method showed drug release equivalent to microspheres fabricated by the solvent evaporation method. The morphology of the particles obtained by ball milling was irregular, whereas the conventional method generated spherical particles. Unlike carnauba, PLGA has a low plasticity to form a spherical shape. Ball milling is considered inefficient in providing enough energy generated by the collision between the PLGA particles to form a spherical shape.

Technologies using pulverizers other than ball mill were also used for the fabrication of microspheres. The preparation of protein-loaded microparticles using a jet mill has been reported (*36*). This technology produces spherical microparticles owing to the stronger force generated by the jet mill compared to that of the ball mill. The spherical shape allows better redispersion of the microparticles and easier passage through the needle during injection.

An additional feature of the dry fabrication method using a ball mill is its high airtightness owing to the excellent sealing performance of the ball mill. This property is advantageous for the aseptic preparation and containment fabrication of microspheres containing highly pharmacologically active substances.

5. Future prospective for harmless and ecologically acceptable LAI fabrication

To summarize and provide a prospective view, because some organic solvents used in manufacturing affect workers' health and the environment through exposure and leakage, respectively, there is an increasing social demand for harmless and ecologically acceptable fabrication technologies. Concerns are raised not only about solvents, but also about encapsulated drugs. Over the past decade, the impact of biotechnology on the global pharmaceutical industry has led to technological breakthroughs in new manufacturing and formulations. Biopharmaceutical formulations based on new drug delivery technologies are a significant value-added proposition. Although the dose of a drug encapsulated in LAI microspheres is limited, biological drugs with high pharmacological activity show efficacy in very low doses and are considered compatible with such microsphere formulations. Thus, the launch of LAI microsphere-encapsulated biopharmaceuticals is expected to increase. However, their manufacturing often inevitably includes a process that is harmful or environmentally unfriendly owing to their high pharmacological activity. Food and Drug Administration commented the following on workers' safety against exposure; "ICH Q7 does not define high pharmacological activity or toxicity; these characteristics are generally determined by evaluating relevant animal and human data collected during research and development. Important considerations in this evaluation of pharmacological activity or toxicity may include occupational exposure limit (OEL), permitted daily exposure (PDE), acceptable daily exposure (ADE), the threshold for toxicological concerns (TTC), no observed adverse effect level (NOAEL), and the consequences of cross-contamination" (*37*). Among these values, OELs, widely used for categorization, are regulatory values which indicate levels of exposure that are considered safe (health-based) for a chemical substance in the air of a workplace (*38*). Due to strict regulatory definitions, pharmaceutical companies set their own containment strategy by categorizing active pharmaceutical ingredients based on their individual OELs (*39*). The control approach is set using decision tools based on product OEL and exposure potential, such as substance allocated to dustiness or volatility band and a band for the scale of use (*40*). Moreover, the containment pyramid is commonly used as a decision tool (*41*). In general, rigid isolators, ventilated laminar flow cabinets, custom-designed glove bags, and bag-in/bag-out systems are used for the containment control approach (*42*). As the risk categorization increases, the system used to prevent exposure should become rigorous. For example, according to the Health and Safety Executive (HSE) of a United Kingdom government agency, as the categorization levels increase, the system should be selected in the order of general ventilation, local exhaust ventilation, full enclosures and containment, and expert advice (*40*). For LAI microspheres preparation, the containment level will not only be high if a high pharmacological activity drug is microencapsulated, but exposure potential will increase. LAI microsphere preparation by the conventional evaporation method

is inconvenient to these closed systems. In a closed system operation, the risk of breaking the closed system will increase when charging materials and solvents or discharging samples. LAI microspheres preparation includes lots of possible charging/discharging points due to its complicated procedure (Figure 1). The numbers of exposure risk points are considerably more than the ordinary injection formulations prepared by filling the API solution into vials. In addition, a solvent-recovering device for the evaporated solvents should be installed in/with the closed system. In contrast, the techniques that can guarantee containment, such as the dry fabrication method using a ball mill, can reduce the charging/discharging opportunities and the risk of workers' exposure to harmful ingredients or products.

6. Conclusion

In conclusion, harmless and ecologically acceptable fabrication technologies, such as containment and dry fabrication, enable safer and easier manufacturing of PLA or PLGA microspheres and facilitate the development of LAI formulations for biopharmaceuticals, which include microspheres as drug carriers.

Acknowledgements

We thank Dr. Murao for their useful advice. We are also grateful to Editage (www.editage.jp) for English language editing.

Funding: None.

Conflict of Interest: The authors have no conflicts of interest to disclose.

References

1. Nagane K, Kimura S, Ukai K, Takahashi C, Ogawa N, Yamamoto H. Application of spherical silicate to prepare solid dispersion dosage forms with aqueous polymers. Int J Pharm. 2015; 493:55-62.
2. Ichikawa H, Fukumori Y. Microagglomeration of pulverized pharmaceutical powders using the Wurster process I. Preparation of highly drug-incorporated, subsieve-sized core particles for subsequent microencapsulation by film-coating. Int J Pharm. 1999; 180:195-210.
3. Mishra M. Overview of encapsulation and controlled release. In: Handbook of Encapsulation and Controlled Release (Mishra M, eds.). CRC Press, Boca Raton, 2015: pp.12-13.
4. Bannow J, Koren L, Salar-Behzadi S, Löbmann K, Zimmer A, Rades T. Hot melt coating of amorphous carvedilol. Pharmaceutics. 2020; 12:519.
5. Li M, Rouaud O, Poncelet D. Microencapsulation by solvent evaporation: state of the art for process engineering approaches. Int J Pharm. 2008; 363:26-39.
6. Pharmaceuticals and Medical Devices Agency. Japanese Pharmacopoeia 18th Edition. *https://www.pmda.go.jp/english/rs-sb-std/standards-development/jp/0029.html* (accessed January 21, 2023).
7. Katou H, Wandrey AJ, Gander B. Kinetics of solvent extraction/evaporation process for PLGA microparticle fabrication. Int J Pharm. 2008; 364:45-53.
8. Li WI, Anderson KW, Deluca PP. Kinetic and thermodynamic modeling of the formation of polymeric microspheres using solvent extraction/evaporation method. J Control Rel. 1995; 37:187-198.
9. Kim JS, Lee KR. Prediction of mutual diffusion coefficients in polymer solution. Polymer. 2000; 41:8441-8448.
10. Doumec F, Guerrier B. Estimating polymer/solvent diffusion coefficient by optimization procedure. AIChE J. 2001; 47:984-993.
11. Hsu JP, Lin SH. Diffusivity of solvent in a polymer solution-expansive free volume effect. Eur Polym J. 2005; 41:1036-1042.
12. Fu X, Ping Q, Gao Y. Effects of formulation factors on encapsulation efficiency and release behaviour *in vitro* of huperzine A-PLGA microspheres. J Microencapsul. 2005; 22:57-66.
13. Yang YY, Chia HH, Chung TS. Effect of preparation temperature on the characteristics and release profiles of PLGA microspheres containing protein fabricated by double-emulsion solvent extraction/evaporation method. J Control Release. 2000; 69:81-96.
14. Zheng CH, Gao JQ, Liang WQ, Yu HY, Zhang YL. Effects of additives and processing parameters on the initial burst release of protein from poly(lactic-co-glycolic acid) microspheres. PDA J Pharm Sci Technol. 2006; 60:54-59.
15. Igari T, Takada S, Kosakai H. Production of sustained release pharmaceutical preparation. Japanese Patent No.3902272. 2007.
16. Sturesson C, Carlfors J. Incorporation of protein in PLG-microspheres with retention of bioactivity. J Control Release. 2000; 67:171-178.
17. Bahl Y, Sah H. Dynamic changes in size distribution of emulsion droplets during ethyl acetate-based microencapsulation process. AAPS PharmSciTech. 2000; 1:E5.
18. Wang FJ, Wang CH. Sustained release of etanidazole from spray dried microspheres prepared by non-halogenated solvents. J Control Release. 2002; 81:263-280.
19. Cho M, Sah H. Formulation and process parameters affecting protein encapsulation into PLGA microspheres during ethyl acetate-based microencapsulation process. J Microencapsul. 2005; 22:1-12.
20. Campbell CSJ, Delgado-Charro MB, Camus O, Perera S. Comparison of drug release from poly(lactide-co-glycolide) microspheres and novel fibre formulations. J Biomater Appl. 2016; 30:1142-1153.
21. Xiao CD, Shen XC, Tao L. Modified emulsion solvent evaporation method for fabricating core-shell microspheres. Int J Pharm. 2013; 452:227-232.
22. Herrmann, J, Bodmeier R. Somatostatin containing biodegradable microspheres prepared by a modified solvent evaporation method based on W/O/W-multiple emulsions. Int J Pharm. 1995; 126:129-138.
23. Sah H. Ethyl formate–alternative dispersed solvent useful in preparing PLGA microspheres. Int J Pharm. 2000; 195:103-113.
24. Shim H, Sah H. Qualification of non-halogenated organic solvents applied to microsphere manufacturing process. Pharmaceutics. 2020; 12:425.

25. Kang J, Sah E, Sah H. Applicability of non-halogenated methyl propionate to microencapsulation. J Microencapsul. 2014; 31:323-332.
26. Matsumoto A, Kitazawa T, Murata J, Horikiri Y, Yamahara H, A novel preparation method for PLGA microspheres using non-halogenated solvents. J Control Release. 2008; 129:223-227.
27. Suzuki T, Kitazawa T, Matsumoto A, Suzuki A. Process for the preparation of microspheres. Japanese Patent No. 3709808. 2005.
28. Murakami M, Matsumoto A, Watanabe C, Kurumado Y, Takama M. Fabrication of porous ethyl cellulose microspheres based on the acetone-glycerin-water ternary system: Controlling porosity *via* the solvent-removal mode. Drug Discov Ther. 2015; 9:303-309.
29. Chen W, Dave RN, Pfeffer R, Walton O. Numerical simulation of mechanofusion system. Powder Technol. 2004; 146:121-136.
30. Qu L, Zhou QT, Denman JA, Stewart PJ, Hapgood KP, Morton DAV. Influence of coating material on the flowability and dissolution of dry-coated fine ibuprofen powders. Eur J Pharm Sci. 2015; 78:264-272.
31. Hou D, Han J, Geng C, Xu Z, AlMarzooqi MM, Zhang J, Yang Z, Min J, Xiao X, Borkiewicz O, Wiaderek K, Liu Y, Zhao K, Lin F. Surface coating by mechanofusion modulates bulk charging pathways and battery performance of Ni-rich layered cathodes. Proc Natl Acad Sci U S A. 2022; 119:e2212802119.
32. Yang M, Yamamoto H, Kurashima H, Takeuchi H, Yokoyama T, Tsujimoto H, Kawashima Y. Design and evaluation of inhalable chitosan-modified poly (DL-lactic-co-glycolic acid) nanocomposite particles. Eur J Pharm Sci. 2012; 47:235-243.
33. Yang M, Yamamoto H, Kurashima H, Takeuchi H, Yokoyama T, Tsujimoto H, Kawashima Y. Design and evaluation of poly(DL-lactic-co-glycolic acid) nanocomposite particles containing salmon calcitonin for inhalation. Eur J Pharm Sci. 2012; 46:374-380.
34. Matsumoto A, Ono A, Murao S, Murakami M. Microparticles for sustained release of water-soluble drug based on a containment, dry coating technology. Drug Discov Ther. 2018; 12:347-354.
35. Matsumoto A, Murakami M. Dry fabrication of poly(dl-lactide-co-glycolide) microspheres incorporating a medium molecular drug by a ball mill method. Drug Discov Ther. 2021; 15:20-27.
36. Nykamp G, Carstensen U, Müller BW. Jet milling – a new technique for microparticle preparation. Int J Pharm. 2002; 242:79-86.
37. Food and Drug Administration. Q7 Good Manufacturing Practice Guidance for Active Pharmaceutical Ingredients: Questions and answers guidance for industry 2018. *https://www.fda.gov/media/112426/download* (accessed January 21, 2023).
38. European Chemicals Agency. Occupational exposure limits. *https://echa.europa.eu/oel#:~:text=Occupational%20exposure%20limits%20%28OELs%29%20are%20regulatory%20values%20which,chemical%20substance%20in%20the%20air%20of%20a%20workplace* (accessed January 22, 2023).
39. Dunny E, O'Connor I, Bones J. Containment challenges in HPAPI manufacture for ADC generation. Drug Discov Today. 2017; 22:947-951.
40. Health and Safety Executive. COSHH essentials: Controlling exposure to chemicals – a simple control banding approach. *https://www.hse.gov.uk/pubns/guidance/coshh-technical-basis.pdf* (accessed January 22, 2023).
41. International Society for Pharmaceutical Engineering D/A/CH. CoP Containment. *https://en.ispe-dach.org/membership-and-working-groups/containment-cop/?_ga=2.34200354.201344764.1674341598-696444732.1674341598&_gl=1*1txc72m*_ga*Njk2NDQ0NzMyLjE2NzQzNDE1OTg.*_ga_LD0MKRCC2N*MTY3NDM0MTU5Ny4xLjEuMTY3NDM0MTYwNC4wLjAuMA..&xdomain_data=dA3VAbk27Bld006e0r%2Fuaru4ip6x138ENodF7PYMIPOOzHNIbf4RlDPrV0gK%2F1tA*. (accessed January 21, 2023).
42. Haehl K. Choosing a CMO for your highly potent pharmaceutical. Looking beyond the isolator. Chem Today. 2013; 31:24-27.

Received February 6, 2023; Revised April 20, 2023; Accepted May 21, 2023.

Address correspondence to:
Akihiro Matsumoto, Laboratory of Pharmaceutics, Faculty of Pharmacy, Osaka Ohtani University, 3-11-1 Nishikori-kita, Tondabayashi, Osaka 584-0854, Japan.
E-mail: matumoaki@osaka-ohtani.ac.jp

Released online in J-STAGE as advance publication May 27, 2023.

Mini-Review

DOI: 10.5582/ddt.2023.01022

Autoimmune hepatitis following COVID-19 vaccination: Clinical characteristics of 35 reported cases

Meirong Wang[1,*], Juan Qi[1], Yujuan Liu[2,*]

[1] Qingdao Municipal Hospital, Qingdao, China;
[2] Qingdao Women and Children's Hospital, Qingdao, China.

SUMMARY The coronavirus disease 2019 (COVID-19) vaccines have been shown to be effective in protecting people from severe disease progression, hospitalisation and death. However, a wide range of side effects have been reported worldwide. New onset or flare-up of autoimmune hepatitis (AIH) is an extremely rare adverse event following COVID-19 vaccination, with the majority of cases presenting with mild symptoms. Unfortunately, there have been cases of fatal complications. In this mini-review, we have summarised the clinical characteristics of a total of 35 currently reported cases of AIH after COVID-19 vaccination and suggest that patients with autoimmune diseases may be at higher risk of developing AIH after vaccination.

Keywords COVID-19, vaccines, adverse events, autoimmune hepatitis

Coronavirus disease 2019 (COVID-19) vaccines are becoming an important means of reducing the likelihood of severe progression and death from infection, and may also act as a risk factor for the induction of autoimmune phenomena. Recently, there have been increasing reports of autoimmune disease flares or new onset after COVID-19 vaccination, ranging from mild to life-threatening. It is therefore necessary to develop effective strategies to identify and manage these adverse events in routine clinical practice. With more than 60% of the world's population having received at least one dose of the vaccine, there is an opportunity to further investigate the rare adverse events, particularly those not reported in the original trials.

Autoimmune hepatitis (AIH) after COVID-19 vaccination was first reported by Bril *et al.* (*1*). To the best of our knowledge, a total of 35 cases of AIH following COVID-19 vaccination have been reported worldwide, including two deaths (Table 1) (*1-26*). AIH after COVID-19 vaccination has been observed with mRNA vaccines (mRNA-1273; BNT162b2), recombinant adenovirus vaccines (ChAdOx1; Covishield) and inactivated vaccines (CoronaVac; Sinopharm). Patients range in age from 35 to 89 years with a female predominance (80%) and no cases have been reported in children or adolescents. Jaundice, pruritus, choluria and asthenia are the most common manifestations at onset, except in three cases which were asymptomatic and only hypertransaminasemia was found on routine liver function tests (*9,10,17*). Of these three cases, two developed obvious symptoms after a latency period of 5 weeks, while the other remained asymptomatic and liver enzymes returned to normal levels after steroid therapy (*9*).

The majority of cases occurred 1-3 weeks after the first dose of COVID-19 vaccine, but several cases showed rapid onset at 2-3 days, while one late case occurred 51 days after vaccination. Five cases showed significant symptoms 2 days to 3 weeks after the second dose of vaccine, and one case of AIH flare-up occurred after the third dose of vaccine (*26*). Usually, symptoms after the first dose were mild or non-specific and became more obvious or worse with the second dose. In general, physical and imaging examinations showed no obvious positive findings, except for occasional hepatomegaly. Levels of total/direct bilirubin, alanine aminotransferase (ALT), aspartate aminotransferase (AST), gamma glutamyl transferase (GGT), alkaline phosphatase (ALP) and international normalised ratio (INR) were elevated in the early phase of the disease in most cases, and no hepatophilic virus tests were positive, except in one case with a history of HCV treatment (*24*).

Anti-nuclear antibodies (ANA) were positive in the majority of AIH cases, mainly with a haemorrhagic or speckled pattern. The second most common autoantibody was anti-smooth muscle antibody (ASMA). Four cases were negative for autoantibodies (*2,4,5,18*). Total IgG was often elevated in most cases. Although the efficacy of these COVID-19 vaccines has not been fully reported, two cases had an extremely

Table 1. 35 cases of autoimmune hepatitis reported after COVID-19 vaccination

Study	Vaccine	Gender	Age (year)	Commodity, medical history	Time to onset	Antibody	Liver histology	Steroid response
Bril, *et al.* (*1*)	BNT162b2	Female	35	Post-partum, Hypertension	1 week post vaccination	ANA+homo Anti-dsDNA+	AIH, eosinophils score (Rev)=18	Response
Rela, *et al.* (*2*)	Covishield	Female	38	Hypothyroidism	20 days post vaccination	ANA+	AIH, eosinophils score (Simp)=6 score (Rev)=15	Response
Rela, *et al.* (*2*)	Covishield	Male	62	Diabetes, jaundice history	16 days post vaccination	Anti-HBV core+ ANA-,ANCA-, SMA-, LKM-1-	AIH, fibrosis (Ishak stage 2/6)	No,dead
Erard, *et al.* (*3*)	BNT162b2	Female	80	None	10 days post vaccination	ANA+	AIH	Response
Erard, *et al.* (*3*)	mRNA-1273	Female	73	None	21 days after vaccination	ANA+	AIH	Response
Erard, *et al.* (*3*)	ChAdOx1	Female	68	None	20 days after vaccination	ANA+	AIH	No, dead
Fimiano, *et al.* (*4*)	BNT162b2	Female	63	Hypothyroidism, familial autoimmunity	51 days post vaccination	ANA-,AMA-, LKM-1-,ANCA- Anti-SARS-CoV2 spike (high)	AIH	Response
Camacho-Domínguez, *et al.* (*5*)	ChAdOx1	Male	79	None	14 days after 1st dose, 15 days after 2nd dose exacerbation	ANA+gran, ASMA+ Anti-SARS-CoV2 spike (high)	AIH, ductular reaction, eosinophils	Response
Ghielmetti, *et al.* (*6*)	mRNA1273	Male	63	Diabetes, ischemic heart disease	1 week post vaccination	ANA+spec APCA+	AIH	Response
Vuille-Lessard,*et al.* (*7*)	mRNA1273	Female	76	Hashimoto, SARS-CoV-2, urothelial cancer	2-3 days after 1st dose	ANA+homo ASMA+, AAA+, ANCA+	AIH, score (Simp)=8	Response
Suzuki, *et al.* (*8*)	BNT162b2	Female	80	Gastroesophageal reflux disease	10 days after 2nd dose	ANA+Cent	AIH	Response
Suzuki, *et al.* (*8*)	BNT162b2	Female	75	Dyslipidemia	4 days after 2nd dose	ANA+spec/homo ANA+	AIH	Response
Suzuki, *et al.* (*8*)	BNT162b2	Female	78	Primary sclerosing cholangitis	7 days post vaccination	ANA+	AIH, eosinophils	Response
Palla, *et al.* (*9*)	BNT162b2	Female	40	Sarcoidosis	1 month post vaccination (asymptomatic)	ANA+	AIH, fibrosis	Response
Garrido, *et al.* (*10*)	mRNA1273	Female	65	Polycythemia vera (JAK2 V617F)	2 weeks post vaccination (asymptomatic), 5 weeks symptomatic	ANA+Spec	AIH	Response
Avci, *et al.* (*11*)	BNT162b2	Female	61	Hashimoto, SARS-CoV-2, hypertension	2 weeks post vaccination	ANA+ ASMA+	AIH, fibrosis	Response
Cao, *et al.* (*12*)	CoronaVac	Female	57	None	2 weeks post 1st vaccination exacerbation after 2 days post 2nd dose	ANA+hom ASS-A+ ACENP-B+ ASS-B+	AIH, fibrosis	Response
Lodato, *et al.* (*13*)	BNT162b1	Female	43	Dyslipidaemia with ALT increase	15 days post 1st vaccination, exacerbation after 2 days post 2nd dose	ANA-,ASMA-, LKM-1-,AMA-, ENA-	AIH, biliary injury and eosinophils	Response
Zhou, *et al.* (*14*)	mRNA-1273	Female	36	Primary sclerosing cholangitis	11 days post 1st vaccination, return of symptoms after 2nd dose	ANA+hom Anti-dsDNA+	AIH, ductular reaction, eosinophils	Response
Zin, *et al.* (*15*)	mRNA-1273	Male	47	None	3 days post vaccination	ANA+	AIH, fibrosis, eosinophils	Response
Rocco, *et al.* (*16*)		Female	80	Hashimoto, Glomerulonephritis	1 week after completing schedule	ANA+spec	AIH, Score (Rev)=19	Response
Clayton-Chubb,*et al.* (*17*)	BNT162b2	Male	36	Hypertension	26 days post vaccination (asymptomatic), 34 days symptomatic	ANA+	AIH, score (Rev)=15	Response

Notes: Antinuclear antibody (ANA) (hemo=hemogeneous pattern; spec=speckled pattern), anti-smooth muscle antibody (ASMA), Antimitochondrial antibodies (AMA), Anti-Extractable Nuclear Antigen (ENA), Anti-Sjögren syndrome antigen A (ASS-A), Anti-major centromere autoantigen B (ACENP-B), Anti-liver-kidney microsome-1(LMK-1), anti- soluble liver antigen/liver-pancreas (ASLA/LP).

Table 1. 35 cases of autoimmune hepatitis reported after COVID-19 vaccination (continued)

Study	Vaccine	Gender	Age (year)	Commodity, medical history	Time to onset	Antibody	Liver histology	Steroid response
McShane, *et al.* (*18*)	mRNA1273	Female	71	Cholecystectomy, hip replacement	4 days post vaccination	ASMA+	AIH, eosinophils	Response
Tan, *et al.* (*19*)	mRNA1273	Female	56		5 weeks post vaccination	ANA+, ASMA+	AIH, eosinophils, fibrosis	Response
Ghorbani, *et al.* (*20*)	Sinopharm	Male	62	None	3 days after 2nd dose	ANA-, ASMA-, LKM-1-	AIH, grading, staging Ishak modified HAI, 11/18, 1/6	Not use
Londoño,*et al.* (*21*)	mRNA1273	Female	41	Premature ovarian failure	no liver specific after 1st dose, significant after 1 week post 2nd dose	ANA+, ASMA+, SLA+, LC1+	AIH, fibrosis score (Simp)=8	Response
Mekritthikrai, *et al.* (*22*)	CoronaVac	Female	52	None	1 week after 2nd dose	ANA+Spec, ASMA+	AIH, fibrosis	Response
Izagirre, *et al.* (*23*)	ChAdOx1	Female	47	Hypothyroidism	24 days after 1nd dose	ANA+	AIH,score (Simp)=8	Response
Izagirre, *et al.* (*23*)	BioNTech	Male	72	Ischemic heart disease	46 days after 2nd dose	ANA+hom	AIH,score (Simp)=7 Eosinophils	Response
Izagirre, *et al.* (*23*)	ChAdOx1	Female	62	Celiac disease	4 days after 2nd dose	ANA+, ENA	AIH, score (Simp)=8 eosinophils	Response
Izagirre, *et al.* (*23*)	BioNTech	Female	72	None	14 days after 2nd dose	ANA+hom	AIH, score (Simp)=8	Response
Izagirre, *et al.* (*23*)	BioNTech	Female	59	Hypothyroidism	9 days after 1nd dose	ANA+Spec	None	Response
Hasegawa, *et al.* (*24*)	BioNTech	Female	82	HCV	4 day after 1nd dose	ANA+	AIH	Response
Brubaker, *et al.* (*25*)	BioNTech	Female	35	AIH, chronic sinusitis, insomnia	2 weeks after 2nd dose	ASMA+	AIH (onset)	Response
Mahalingham, *et al.* (*26*)	BioNTech	Female	32	AIH, liver transplantation	3 weeks after 3nd dose	ASLA/LP+	AIH	Response

Notes: Antinuclear antibody (ANA) (hemo=hemogeneous pattern; spec=speckled pattern), anti-smooth muscle antibody (ASMA), Antimitochondrial antibodies (AMA), Anti-Extractable Nuclear Antigen (ENA), Anti-Sjögren syndrome antigen A (ASS-A), Anti-major centromere autoantigen B (ACENP-B), Anti-liver-kidney microsome-1(LMK-1), anti- soluble liver antigen/liver-pancreas (ASLA/LP).

high vaccine antibody titre of 1,000 fold the upper normal level (*4,5*).

Histology of liver biopsies revealed typical AIH characterised by interface hepatitis, lymphoplasmacytic infiltrate and varying degrees of hepatocyte necrosis from scattered to widespread. Ten cases were classified as definite AIH according to simplified or revised systems. Eosinophilic infiltrate was found in 8 cases, and 4 cases showed ductal reaction, characterised by proliferation of reactive bile ducts induced by liver injury. In addition, significant hepatic fibrosis was observed in one fifth of the cases, suggesting the possibility of pre-existing subclinical liver disease in some patients.

Most patients with AIH had a good response to steroid treatment and no relapses were reported after drug-withdrawal. Two cases with poor steroid response died of liver failure (*2,3*). The deceased patients were not receiving concomitant life-threatening medications prior to COVID-19 vaccination. There was also no significant difference in the onset of clinical manifestations between the deceased and cured cases, except that one deceased case had two episodes of jaundice in the past decades (*2*).

There appears to be an association between the occurrence of AIH and the patients' pre-existing autoimmunity. At least 7 cases had an autoimmune disorder prior to COVID-19 vaccination, including Hashimoto's thyroiditis (3 cases) (*7,11,16*), primary sclerosing cholangitis (2 cases) (*8,14*), glomerulonephritis (1 case) (*16*), sarcoidosis (1 case) (*9*), and celiac disease (1 case) (*2,3*). Two patients with AIH had a history of symptomatic COVID-19 infection (*7,11*), both in the context of Hashimoto's thyroiditis.

More recently, Brubaker *et al*. (*25*) described a 35-year-old female AIH patient in remission who had a relapse two weeks after the second dose of mRNA vaccination. Mahalingham *et al.* (*26*) reported a stable post-transplant AIH patient who had a flare coinciding with mRNA vaccination. Therefore, COVID-19 vaccination may not only trigger the onset of AIH, but also promote immune reactivation. Although objective causality has not yet been established, the time course from vaccination to altered liver manifestations was significant in almost all reported cases. A significant percentage of patients had a history of liver-damaging drugs, suggesting that AIH following COVID-19 vaccination may be drug-induced rather than vaccine-induced. Liver histology in some cases also showed a marked eosinophilic infiltrate, characteristic of drug-induced autoimmune hepatitis (DIAIH). However, there are two lines of evidence against this possibility: firstly, DIAIH usually has a latency period of 2 to 24 weeks after drug treatment, and secondly, no recurrence has been observed after withdrawal of glucocorticoids in all reported cases. Therefore, it is now widely accepted that vaccines, which stimulate an abnormal immune response, are the main cause of AIH. Another important piece of evidence is that antibodies against the spike protein S1 of severe acute respiratory syndrome coronavirus 2 (SARS-CoV-2) had a high affinity for human liver proteins such as transglutaminase (*27*), suggesting that vaccination may directly induce spike-directed antibodies and thus autoimmune hepatocyte damage in predisposed individuals.

Although the underlying mechanisms have not been elucidated, various hypotheses have been suggested to establish a relationship between clinical manifestations of AIH and the active ingredients and adjuvants of vaccines (*28*). One of the major explanations for AIH following COVID-19 vaccines, particularly inactivated ones, is molecular mimicry, which is based on significant homology between amino acid sequences of vaccine determinants and prominent liver antigens (*22*). Moreover, the incorporation of lipid nanoparticle and adenovirus vectors in recently authorized vaccines could potentially enhance the inflammatory background, consequently resulting in an amplified immune response. Recent studies have also suggested that various types of vaccines may facilitate the promotion of autoimmunity through different mechanisms. mRNA vaccines may bind to pattern recognition receptors (PRRs) like Toll-like receptor 7 (TLR7), initiating multiple pro-inflammatory cascades, while adenovirus vaccines may activate innate immune responses by involving TLR9 to produce type 1 interferon secretion (*29*).

Another special group that requires our attention are vaccinated children. Clinical manifestations of AIH in children can be very variable, ranging from acute to chronic or even silent presentations (*30*). Although AIH after COVID-19 vaccination has not been reported in children and adolescents, several subclinical cases with hypertransaminasemia have been reported, suggesting that AIH may be a potential complication of vaccination in this population. Therefore, it is important to monitor vaccinated children for signs and symptoms of AIH, as it is possible that the cases identified now are just the tip of the iceberg, and as the vaccinated population expands to include children, asymptomatic or symptomatic paediatric AIH following COVID-19 vaccination may emerge in the near future. In children with abnormal liver function tests after COVID-19 vaccination, AIH should be considered and early diagnosis must be made to avoid progression to cirrhosis without treatment.

There is no doubt that vaccines have an important role to play in controlling the COVID-19 pandemic. As a large percentage of the world's population has been rapidly vaccinated, particularly with the introduction of mRNA vaccines in humans for the first time, in addition to the benefits of vaccination, some rare but serious adverse events are becoming more apparent. A number of autoimmune phenomena have been reported following COVID-19 vaccination, with different

clinical manifestations adding to the complexity of the existing human disease spectrum. As a life-threatening autoimmune adverse event, the risk assessment of AIH before and after COVID-19 vaccination should be of particular concern. Therefore, more efforts are needed to evaluate the predisposing autoimmune situation before and after COVID-19 vaccination. Furthermore, although a clear association between COVID-19 vaccination and AIH has been established, multicentre, prospective, longitudinal studies enrolling patients worldwide should be conducted in the future to clarify the clinical diversity, detailed pathological mechanisms, outcome prediction and management.

Funding: None.

Conflict of Interest: The authors have no conflicts of interest to disclose.

References

1. Bril F, Al Diffalha S, Dean M, Fettig DM. Autoimmune hepatitis developing after coronavirus disease 2019 (COVID-19) vaccine: Causality or casualty? J Hepatol. 2021; 75:222-224.
2. Rela M, Jothimani D, Vij M, Rajakumar A, Rammohan A. Auto-immune hepatitis following COVID vaccination. J Autoimmun. 2021; 123:102688.
3. Erard D, Villeret F, Lavrut PM, Dumortier J. Autoimmune hepatitis developing after COVID 19 vaccine: Presumed guilty? Clin Res Hepatol Gastroenterol. 2022; 46:101841.
4. Fimiano F, D'Amato D, Gambella A, Marzano A, Saracco GM, Morgando A. Autoimmune hepatitis or drug-induced autoimmune hepatitis following Covid-19 vaccination? Liver Int. 2022; 42:1204-1205.
5. Camacho-Domínguez L, Rodríguez Y, Polo F, Restrepo Gutierrez JC, Zapata E, Rojas M, Anaya JM. COVID-19 vaccine and autoimmunity. A new case of autoimmune hepatitis and review of the literature. J Transl Autoimmun. 2022; 5:100140.
6. Ghielmetti M, Schaufelberger HD, Mieli-Vergani G, Cerny A, Dayer E, Vergani D, Terziroli Beretta-Piccoli B. Acute autoimmune-like hepatitis with atypical anti-mitochondrial antibody after mRNA COVID-19 vaccination: A novel clinical entity? J Autoimmun. 2021; 123:102706.
7. Vuille-Lessard É, Montani M, Bosch J, Semmo N. Autoimmune hepatitis triggered by SARS-CoV-2 vaccination. J Autoimmun. 2021; 123:102710.
8. Suzuki Y, Kakisaka K, Takikawa Y. Letter to the editor: Autoimmune hepatitis after COVID-19 vaccination: Need for population-based epidemiological study. Hepatology. 2022; 75:759-760.
9. Palla P, Vergadis C, Sakellariou S, Androutsakos T. Letter to the editor: Autoimmune hepatitis after COVID-19 vaccination: A rare adverse effect? Hepatology. 2022; 75:489-490.
10. Garrido I, Lopes S, Simões MS, Liberal R, Lopes J, Carneiro F, Macedo G. Autoimmune hepatitis after COVID-19 vaccine - more than a coincidence. J Autoimmun. 2021; 125:102741.
11. Avci E, Abasiyanik F. Autoimmune hepatitis after SARS-CoV-2 vaccine: New-onset or flare-up? J Autoimmun. 2021; 125:102745.
12. Cao Z, Gui H, Sheng Z, Xin H, Xie Q. Letter to the editor: Exacerbation of autoimmune hepatitis after COVID-19 vaccination. Hepatology. 2022; 75:757-759.
13. Lodato F, Larocca A, D'Errico A, Cennamo V. An unusual case of acute cholestatic hepatitis after m-RNABNT162b2 (Comirnaty) SARS-CoV-2 vaccine: Coincidence, autoimmunity or drug-related liver injury. J Hepatol. 2021; 75:1254-1256.
14. Zhou T, Fronhoffs F, Dold L, Strassburg CP, Weismüller TJ. New-onset autoimmune hepatitis following mRNA COVID-19 vaccination in a 36-year-old woman with primary sclerosing cholangitis - should we be more vigilant? J Hepatol. 2022; 76:218-220.
15. Zin Tun GS, Gleeson D, Al-Joudeh A, Dube A. Immune-mediated hepatitis with the Moderna vaccine, no longer a coincidence but confirmed. J Hepatol. 2022; 76:747-749.
16. Rocco A, Sgamato C, Compare D, Nardone G. Autoimmune hepatitis following SARS-CoV-2 vaccine: May not be a casuality. J Hepatol. 2021; 75:728-729.
17. Clayton-Chubb D, Schneider D, Freeman E, Kemp W, Roberts SK. Autoimmune hepatitis developing after the ChAdOx1 nCoV-19 (Oxford-AstraZeneca) vaccine. J Hepatol. 2021; 75:1249-1250.
18. McShane C, Kiat C, Rigby J, Crosbie Ó. The mRNA COVID-19 vaccine - A rare trigger of autoimmune hepatitis? J Hepatol. 2021; 75:1252-1254.
19. Tan CK, Wong YJ, Wang LM, Ang TL, Kumar R. Autoimmune hepatitis following COVID-19 vaccination: True causality or mere association? J Hepatol. 2021; 75:1250-1252.
20. Ghorbani H, Rouhi T, Vosough Z, Shokri-Shirvani J. Drug-induced hepatitis after Sinopharm COVID-19 vaccination: A case study of a 62-year-old patient. Int J Surg Case Rep. 2022; 93:106926.
21. Londoño MC, Gratacós-Ginès J, Sáez-Peñataro J. Another case of autoimmune hepatitis after SARS-CoV-2 vaccination - still casualty? J Hepatol. 2021; 75:1248-1249.
22. Mekritthikrai K, Jaru-Ampornpan P, Komolmit P, Thanapirom K. Autoimmune hepatitis triggered by COVID-19 vaccine: The first case from inactivated vaccine. ACG Case Rep J. 2022; 9:e00811.
23. Izagirre A, Arzallus T, Garmendia M, Torrente S, Castiella A, Zapata EM. Autoimmune hepatitis following COVID-19 vaccination. J Autoimmun. 2022; 132:102874.
24. Hasegawa N, Matsuoka R, Ishikawa N, Endo M, Terasaki M, Seo E, Tsuchiya K. Autoimmune hepatitis with history of HCV treatment triggered by COVID-19 vaccination: Case report and literature review. Clin J Gastroenterol. 2022; 15:791-795.
25. Brubaker JED, Casaccio CL, Brazeau MJ. Recurrence of autoimmune hepatitis after COVID-19 vaccination. Cureus. 2022; 14:e25339.
26. Mahalingham A, Duckworth A, Griffiths WJH. First report of post-transplant autoimmune hepatitis recurrence following SARS-CoV-2 mRNA vaccination. Transpl Immunol. 2022; 72:101600.
27. Vojdani A, Kharrazian D. Potential antigenic cross-reactivity between SARS-CoV-2 and human tissue with a possible link to an increase in autoimmune diseases.

Clin Immunol. 2020; 217:108480.
28. Schinas G, Polyzou E, Dimakopoulou V, Tsoupra S, Gogos G, Akinosoglou K. Immune-mediated liver injury following COVID-19 vaccination. World J Virol. 2023; 25:100-108.
29. Teijaro JR, Farber DL. COVID-19 vaccines: Modes of immune activation and future challenges. Nat Rev Immunol. 2021; 21:195-197.
30. Pathak S, Kamat D. Autoimmune hepatitis in children. Pediatr Ann. 2018; 47:e81-86.

Received April 8, 2023; Revised May 28, 2023; Accepted May 31, 2023.

Address correspondence to:
Yujuan Liu, Qingdao Women and Children's Hospital, Qingdao, China.
E-mail: liuyujuan996@126.com

Meirong Wang, Qingdao Municipal Hospital, Qingdao, China.
E-mail: drwangmeirong@163.com

Released online in J-STAGE as advance publication June 16, 2023.

Original Article

DOI: 10.5582/ddt.2023.01007

Characteristics of adverse event reports among people living with human immunodeficiency virus (HIV) in Japan: Data mining of the Japanese Adverse Drug Event Report database

Hiroyuki Tanaka[1,*], Mitsutoshi Satoh[2], Masaki Takigawa[1,3], Toshihisa Onoda[1], Toshihiro Ishii[1]

[1] Department of Practical Pharmacy, Faculty of Pharmaceutical Sciences, Toho University, Chiba, Japan;
[2] Department of Toxicology and Pharmacology, Division of Pharmacy Practice, Meiji Pharmaceutical University, Tokyo, Japan;
[3] Department of Pharmacy, Tokyo Metropolitan Geriatric Hospital, Tokyo, Japan.

SUMMARY The development of new anti-HIV drugs and advances in antiretroviral therapy (ART) regimens have enabled longer and more effective treatments in people living with HIV (PLWH). However, the aging of PLWHs is another issue that needs to be addressed. In addition to ART, many PLWHs frequently receive medications for various comorbidities. However, real-world data on the occurrence of adverse events in PLWHs and their causative drugs are rare. Therefore, this study aimed to clarify the characteristics of adverse event reports among PLWHs in Japan. PLWH cases with adverse events were comprehensively searched and analyzed using the Japanese Adverse Drug Event Report database (JADER). Despite changes in guideline-recommended ART regimens, anti-HIV drugs were the main cause of adverse events in PLWHs throughout the study period. However, considerable variations have been observed in the reporting rate of anti-HIV drug classes registered as causative drugs in JADER, especially for anchor drugs. In other words, the reporting rate of integrase strand transfer inhibitors has increased in recent years, while that of protease inhibitors and non-nucleoside reverse transcriptase inhibitors has decreased. Immune reconstitution inflammatory syndrome was the most reported adverse event and was frequently noticed by healthcare providers managing patients with HIV infections. The trends in adverse event reports for female and older patients differed from those for the overall population. This study may provide insights that can help in the establishment of optimal management strategies for PLWHs.

Keywords People living with HIV, adverse events, anti-HIV drug, Japanese Adverse Drug Event Report database

1. Introduction

Current World Health Organization and most national guidelines recommend the initiation of antiretroviral therapy (ART) for all people living with human immunodeficiency virus (HIV) (PLWH) regardless of clinical or immune status (*1-3*). In Japan, combination antiretroviral therapy (cART) with three or more anti-HIV drugs has become available since 1997, and this has inhibited viral proliferation and restored immunity in PLWH (*4*). However, early ART regimens have many clinical limitations, such as various adverse events, interactions with concomitant drugs and food, and a high pill burden (*5*). The development of antiviral drugs, especially anti-HIV drugs, has been a remarkable feat (*6*). Furthermore, anti-HIV drugs developed in recent years have fewer problems than those developed earlier (*5*). Five classes of anti-HIV drugs, classified based on their mechanism of action, are used in Japan: nucleoside/nucleotide reverse transcriptase inhibitors (NRTIs), non-nucleoside reverse transcriptase inhibitors (NNRTIs), protease inhibitors (PIs), integrase strand transfer inhibitors (INSTIs), and C-C chemokine receptor type 5 antagonist (CCR5A) (*3*). HIV treatment guidelines generally recommend ART regimens that consist of two NRTIs as backbone drugs plus a third "anchor drug" from another drug class (INSTI, PI, or NNRTI) (*1-3*). However, with the advent of drugs with high anti-HIV activity in recent years, dual therapy regimens have become an option for eligible patients (*7*). All in all, the treatment modalities for HIV infection are frequently updated, and developing novel anti-HIV drugs and ART regimens has led to decreased HIV-related morbidity and mortality in PLWHs (*8*). However, HIV infection

is a chronic disease that cannot be cured by ART and thus needs lifelong treatment. In addition, an increasing lifetime risk of developing non-AIDS comorbidities owing to the increasing life expectancy and long-term use of ART among PLWHs has become a critical issue (*9-12*).

PLWHs are frequently prescribed drugs to prevent or treat opportunistic infections before or after cART initiation. In addition, with the increased life expectancy of PLWHs, new problems, such as the need for drug therapy for chronic complications associated with the aging of PLWH, have emerged (*9-12*). The proportion of older PLWHs (aged ≥ 50 years) with at least one chronic disease in addition to HIV exceeded 50% in a French study (*9*) and even reached 94% in a United States study (*10*). Regarding comorbidities among PLWHs in Japan, Naito *et al*. analyzed data from the National Database between 2009 and 2019 and found that 81.5% of the patients had chronic comorbidities (*11*). The most frequent comorbidities were diabetes, lipid disorders, psychiatric disorders, and hypertension. Therefore, the management of chronic diseases in PLWHs is becoming increasingly important. In addition, a previous study found that non-AIDS-defining cancers occurred more frequently in PLWHs aged ≥ 60 years, and this was attributed to an increase in older PLWHs (*13*). Therefore, cancer chemotherapy in PLWHs has also become an important consideration in the management of HIV infections.

Thus, PLWHs may frequently receive medications for various comorbidities in addition to ART. However, real-world data on the occurrence of adverse events in PLWHs and their causative drugs are rare. Therefore, this study aimed to comprehensively investigate and characterize the adverse event reports of PLWHs using the Japanese Adverse Drug Event Report database (JADER).

2. Materials and Methods

2.1. Data source

JADER is a large Japanese database that can be used to identify trends in the occurrence of adverse events; it is a spontaneously reporting database made publicly available by the Pharmaceuticals and Medical Devices Agency (*https://www.pmda.go.jp*). In this study, we downloaded and analyzed data registered in JADER in the period between April 2004 and March 2020. The database consists of four file types: "Demo" (patients' demographic information, such as sex and age), "Drug" (*e.g.*, drug name [generic and product names], causal relationship), "Reac" (*e.g.*, adverse events, clinical outcomes), and "Hist" (*e.g.*, medical history, primary disease). Based on their level of involvement in adverse events, drugs in the "Drug" file were assigned to one of three categories: "suspected drug," "interaction," and "concomitant drug."

2.2. PLWH cases

Cases that included anti-HIV drugs (Table S1, *http://www.ddtjournal.com/action/getSupplementalData.php?ID=148*) in the "Drug" file and/or those that included terms related to HIV infection (Table S2, *http://www.ddtjournal.com/action/getSupplementalData.php?ID=148*) in their "Hist" file were selected as PLWH cases. Given that lamivudine, tenofovir disoproxil fumarate, and tenofovir arafenamide fumarate are also used to treat hepatitis B virus infection, cases judged to have been treated for diseases other than HIV infection or unknown based on the product name, dose, and medical history were excluded from the analysis. In addition, cases treated with zidovudine in combination with interferon alpha for low-grade adult T-cell leukemia lymphoma were also excluded. Moreover, cases treated with lopinavir/ritonavir combination, an anti-HIV drug that was used for COVID-19 treatment, were excluded.

2.3. Causative drugs

Drugs registered as "suspected drug" or "interaction" in JADER were redefined as "causative drug" of adverse events, and all causative drugs reported in PLWHs were counted. The main ingredients of fixed-dose combinations of anti-HIV drugs were also evaluated. In addition, anti-HIV drugs were classified into five classes (NRTI, NNRTI, PI, INSTI, and CCR5A/fusion inhibitor [FI]) based on their mechanism of action. Given that some anti-HIV drugs belong to same class, drug classes appearing more than once in the same report were counted only once.

2.4. Adverse events

Adverse events were analyzed using the preferred term (PT) and system organ class (SOC) in the Medical Dictionary for Regulatory Activities (MedDRA). In general, adverse events in JADER are based on PTs. As the top level of the MedDRA hierarchy, the SOC provides the broadest concepts for data retrieval. There are a total of 27 SOCs in MedDRA, and the analysis of adverse events coded by PT assigned to the SOC may better reflect the impact on an organ or system of the human body. In this study, all individual PTs were mapped to SOC based on MedDRA. Considering that some PTs may belong to more than one SOC, we counted all SOCs for each. Although different PTs were assigned to the same SOC within the same report after mapping, the duplicated SOC was only counted once.

2.5. Statistical analysis

Demographic characteristics, causative drugs, and

adverse events were summarized descriptively based on the number of cases and their rates. All statistical analyses were performed using Microsoft® Excel® 2016 (Microsoft Corp, Redmond, WA, USA).

3. Results

3.1. PLWH characteristics

Among the 640,991 cases registered in JADER during the study period, 3,337 cases were included in the analysis. Table 1 shows the background data for the 3,337 PLWH cases with adverse events. Males accounted for 87.23%, and those in their 30s-40s accounted for 47.56% of the total population. Figure 1A shows the changes in the number of adverse event reports in PLWH over time. The highest number of reports was in fiscal year (FY) 2004, and the lowest was in FY 2011. The number of adverse event reports in PLWH showed a decreasing trend from FY 2004 to FY 2011. However, it had recently increased to the same level as that of FY 2004. Figures 1B and 1C show the longitudinal changes in the composition rate of sex and age in PLWH with adverse events, respectively. There were no considerable changes in the sex composition rate throughout the study period, whereas the composition of the 20-49 years age group declined in recent years. However, the interpretation of the results should consider the recent increase in the number of reports with incomplete data on sex and age.

3.2. Causative drugs

The causative drugs of some adverse events in more than 30 PLWHs are listed in Table 2. A total of 42 drugs were listed, of which 24 (57.1%) were anti-HIV drugs. Lamivudine was the most frequently reported causative drug, followed by ritonavir, tenofovir disoproxil fumarate, emtricitabine, and abacavir sulfate. When grouped into classes based on their mechanism of action, the reporting rate was higher for NRTIs (71.59%, 2389/3,337 cases), PIs (41.32%, 1379/3,337 cases), INSTIs (26.16%, 873/3,337 cases), NNRTIs (19.60%, 654/3,337 cases), and CCR5A/FI (1.68%, 56/3,337 cases). Furthermore, Figure 2 shows the time trends. In FY 2004, the reporting rate of NRTI, the backbone drag, was 88.05% (280/318 cases), but it has declined to approximately 60-70% since FY 2014. For anchor drugs, the reporting rate of INSTIs had increased in recent years, whereas that of PIs and NNRTIs had decreased.

For non-anti-HIV drugs, the sulfamethoxazole/trimethoprim combination, valganciclovir hydrochloride, doxorubicin hydrochloride, azithromycin hydrate, and atovaquone ranked high among causative drugs (Table 2). The reporting rates for drugs other than anti-HIV drugs

Table 1. Population characteristics

Characteristic	*n* (%)
Total	3337
Sex	
Male	2911 (87.23)
Female	329 (9.86)
Unknown	97 (2.91)
Age (years)	
<10	37 (1.11)
10-19	7 (0.21)
20-29	279 (8.36)
30-39	791 (23.70)
40-49	796 (23.85)
50-59	539 (16.15)
60-69	386 (11.57)
70-79	124 (3.72)
80-89	19 (0.57)
90-99	1 (0.03)
Unknown	358 (10.73)

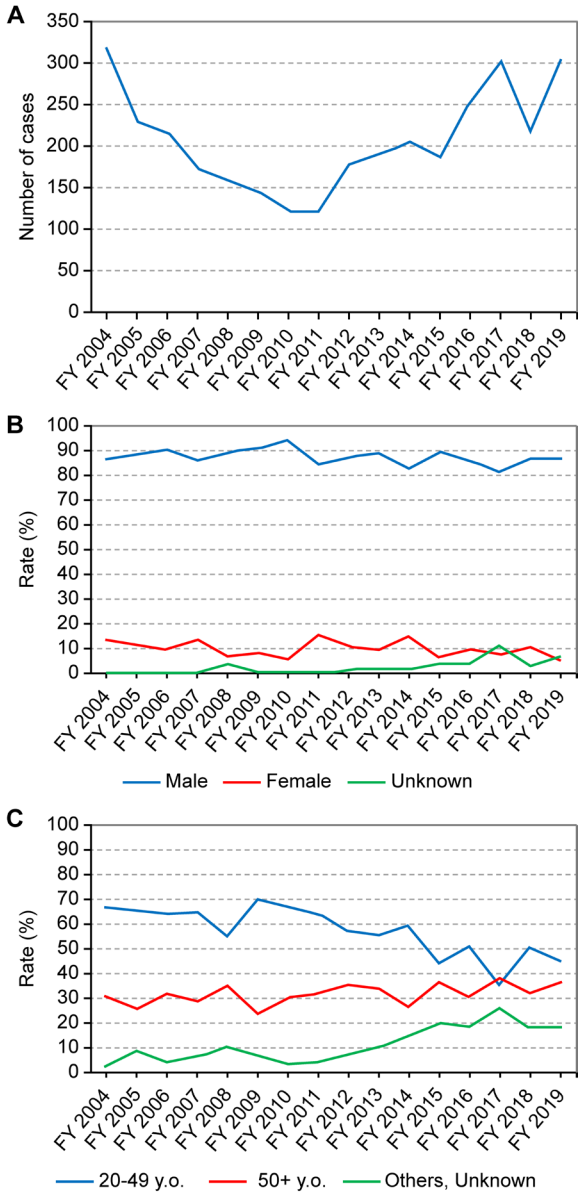

Figure 1. Time trends in the number of PLWH cases with reported adverse events and their sex and age structure. **(A)** Number of PLWH cases. **(B)** Composition rate of sex. **(C)** Composition rate of age groups

Table 2. Causative drugs of adverse events in more than 30 PLWH cases

Causative drugs	Reporting rate (*n*, %)
Lamivudine	1311 (39.29)
Ritonavir	1058 (31.71)
Tenofovir disoproxil fumarate	951 (28.50)
Emtricitabine	843 (25.26)
Abacavir sulfate	786 (23.55)
Efavirenz	498 (14.92)
Dolutegravir sodium	472 (14.14)
Lopinavir	455 (13.64)
Zidovudine	428 (12.83)
Sanilvudine	410 (12.29)
Raltegravir potassium	372 (11.15)
Darunavir ethanolate	358 (10.73)
Atazanavir sulfate	339 (10.16)
Tenofovir arafenamide fumarate	185 (5.54)
Sulfamethoxazole/Trimethoprim combination	178 (5.33)
Nelfinavir mesylate	153 (4.58)
Didanosine	132 (3.96)
Valganciclovir hydrochloride	122 (3.66)
Fosamprenavir calcium hydrate	110 (3.30)
Doxorubicin hydrochloride	85 (2.55)
Cobicistat	83 (2.49)
Azithromycin hydrate	81 (2.43)
Atovaquone	69 (2.07)
Prednisolone	66 (1.98)
Ethambutol hydrochloride	65 (1.95)
Rilpivirine hydrochloride	63 (1.89)
Elvitegravir	62 (1.86)
Nevirapine	60 (1.80)
Ribavirin	55 (1.65)
Indinavir sulfate ethanolate	55 (1.65)
Ganciclovir	54 (1.62)
Maraviroc	53 (1.59)
Clarithromycin	52 (1.56)
Rifabutin	46 (1.38)
Etravirine	46 (1.38)
Fluconazole	44 (1.32)
Peginterferon alfa-2b (Genetical Recombination)	43 (1.29)
Vincristine sulfate	43 (1.29)
Cyclophosphamide hydrate	39 (1.17)
Amphotericin B	33 (0.99)
Foscarnet sodium hydrate	30 (0.90)
Pentamidine isetionate	30 (0.90)

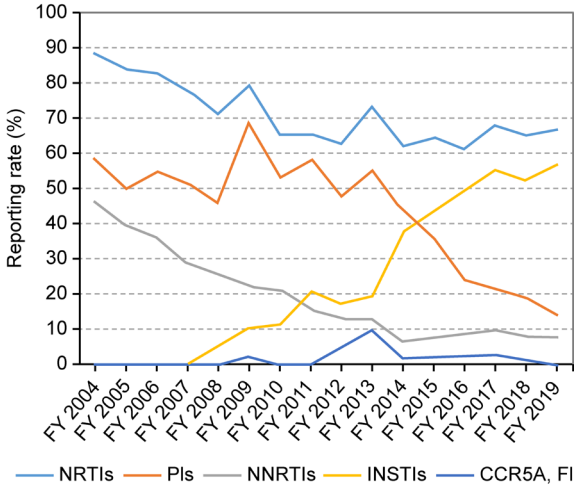

Figure 2. Time trends in reporting rates of anti-HIV drug-related adverse events by drug mechanism of action. NRTI, nucleoside/nucleotide reverse transcriptase inhibitor; PI, protease inhibitor; NNRTI, non-nucleoside reverse transcriptase inhibitor; INSTI, integrase strand transfer inhibitor; CCR5A, C-C chemokine receptor type 5 antagonist; FI, fusion inhibitor

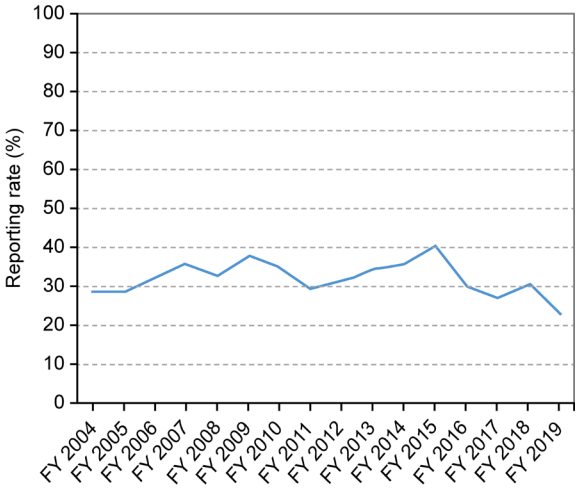

Figure 3. Time trends in reporting rates of non-anti-HIV drug-related adverse events.

ranged from 22.9% to 39.9% throughout the study period (Figure 3).

3.3. Adverse events

Table 3 summarizes the top 20 adverse events reported at the PT level. The most frequently reported adverse event was immune reconstitution inflammatory syndrome (IRIS) (346/3,337 cases, 10.37%), followed by renal impairment (178/3,337 cases, 5.33%), anaemia (122/3,337 cases, 3.66%), diabetes mellitus (99/3,337 cases, 2.97%), and hepatic function abnormal (88/3,337 cases, 2.64%). Table 4 summarizes the reported adverse events at the SOC level. "General disorders and administration site conditions" (649/3,337 cases, 19.45%) was the most frequently reported, followed by "immune system disorders" (625/3,337 cases, 18.73%), "infections and infestations" (605/3,337 cases, 18.13%), "metabolism and nutrition disorders" (552/3,337 cases, 16.54%), and "blood and lymphatic system disorders" (500/3,337 cases, 14.98%). The SOC-level adverse events according to sex and age are shown in Figure 4. The trends for females and those aged ≥ 50 years were different from those in the overall population. Among females, "immune system disorders" (68/329 cases, 20.67%) and "metabolism and nutrition disorders" (68/329 cases, 20.67%) were the most commonly reported, followed by "blood and lymphatic system disorders" (66/329 cases, 20.61%), "general disorders and administration site conditions" (51/329 cases, 15.50%), and "infections and infestations" (51/329 cases, 15.50%). In addition, "reproductive system and breast disorders" and "gestational and perinatal conditions" were mostly reported in females, probably because

Table 3. Top 20 adverse events at the PT level

PT	Reporting rate (*n*, %)
Immune reconstitution inflammatory syndrome	346 (10.37)
Renal impairment	178 (5.33)
Anaemia	122 (3.66)
Diabetes mellitus	99 (2.97)
Hepatic function abnormal	88 (2.64)
White blood cell count decreased	77 (2.31)
Liver disorder	70 (2.10)
Rash	65 (1.95)
Pyrexia	65 (1.95)
Acute kidney injury	63 (1.89)
Cytomegalovirus chorioretinitis	59 (1.77)
Pancytopenia	57 (1.71)
Platelet count decreased	56 (1.68)
Diarrhoea	54 (1.62)
Pneumocystis jirovecii pneumonia	47 (1.41)
Drug eruption	45 (1.35)
Nausea	45 (1.35)
Renal disorder	44 (1.32)
Vomiting	42 (1.26)
Myelosuppression	41 (1.23)

Table 4. Adverse events at the SOC level

SOC	Reporting rate (*n*, %)
General disorders and administration site conditions	649 (19.45)
Immune system disorders	625 (18.73)
Infections and infestations	605 (18.13)
Metabolism and nutrition disorders	552 (16.54)
Blood and lymphatic system disorders	500 (14.98)
Vascular disorders	451 (13.52)
Nervous system disorders	450 (13.49)
Renal and urinary disorders	444 (13.31)
Investigations	431 (12.92)
Hepatobiliary disorders	405 (12.14)
Gastrointestinal disorders	382 (11.45)
Skin and subcutaneous tissue disorders	352 (10.55)
Respiratory, thoracic and mediastinal disorders	269 (8.06)
Cardiac disorders	236 (7.07)
Endocrine disorders	231 (6.92)
Musculoskeletal and connective tissue disorders	212 (6.35)
Injury, poisoning and procedural complications	207 (6.20)
Psychiatric disorders	186 (5.57)
Neoplasms benign, malignant, and unspecified (incl cysts and polyps)	186 (5.57)
Eye disorders	122 (3.66)
Pregnancy, puerperium and perinatal conditions	63 (1.89)
Congenital, familial and genetic disorders	32 (0.96)
Reproductive system and breast disorders	31 (0.93)
Surgical and medical procedures	20 (0.60)
Ear and labyrinth disorders	13 (0.39)
Social circumstances	2 (0.06)
Product issues	1 (0.03)

of biological differences. In those aged ≥ 50 years, "metabolism and nutrition disorders" (202/1,069 cases, 18.90%) were the most commonly reported, followed by "renal and urinary disorders" (188/1,069 cases, 17.59%), "infections and infestations" (166/1,069 cases, 15.53%), "vascular disorders" (164/1,069 cases, 15.34%), and "nervous system disorders" (160/1,069 cases, 14.97%).

4. Discussion

The actual status of adverse event reports in PLWH remains unclear. In this study, anti-HIV drugs were the main causative drugs for adverse events in PLWHs throughout the study period. However, age composition and causative drugs also changed markedly during the study period. In addition, by analyzing the PT and SOC levels in the MedDRA hierarchy, it was possible to characterize the adverse events reported in PLWH cases. To our knowledge, this is the first study to identify trends in adverse event reports in PLWH in the real world using the JADER. Our study identifying the characteristics of adverse event reports among PLWHs in Japan has important implications for establishing optimal management strategies for this population.

Males accounted for 87.23% of the cases, consistent with findings that males account for more than 90% of PLWHs receiving cART in Japan (*14*). The annual number of reports differed to up to 196. Overall, the number of reports decreased until FY 2011 and then increased thereafter. This change in the number of reports may be related to the status of the development of an infrastructure for pharmacovigilance in Japan (*15*). It may also reflect adverse events associated with the long-term use of anti-HIV drugs and/or the "Weber effect" (*16*) on new drugs. In any case, future trends in the number of reports should be monitored. The time trends of the age structure of PLWHs with adverse events may reflect the aging of PLWHs in Japan. However, it should be noted that, in recent years, an increasing number of reports have provided unclear information on age. Nevertheless, it appears that the reporting rate for the 20-49 years age group has decreased, while that for the ≥ 50 years age group has increased.

A total of 42 drugs, 24 of which were anti-HIV drugs, were reported as causative drugs in more than 30 PLWHs. The top five causative drugs were lamivudine, ritonavir, tenofovir disoproxil fumarate, emtricitabine, and abacavir sulfate. Of these, lamivudine, tenofovir disoproxil fumarate, emtricitabine, and abacavir sulfate are NRTIs and are included in most standard ART regimens. Ritonavir inhibits intestinal and hepatic cytochrome P450 3A, and low-dose ritonavir is widely used as a booster for other PIs. This could explain these drugs being the top causative drugs of adverse events. The other causative drugs were efavirenz, an NNRTI; dolutegravir sodium, an INSTI; and lopinavir, a PI. Their reporting rates were similar (14.92%, 14.14%, and 13.64%, respectively). With respect to anti-HIV drug class, it varied markedly throughout the study period, which may have been influenced by the guideline recommendation of cART (*1-3*). In contrast, non-anti-HIV drugs accounted for only approximately 20-40% of adverse events cases throughout the study period.

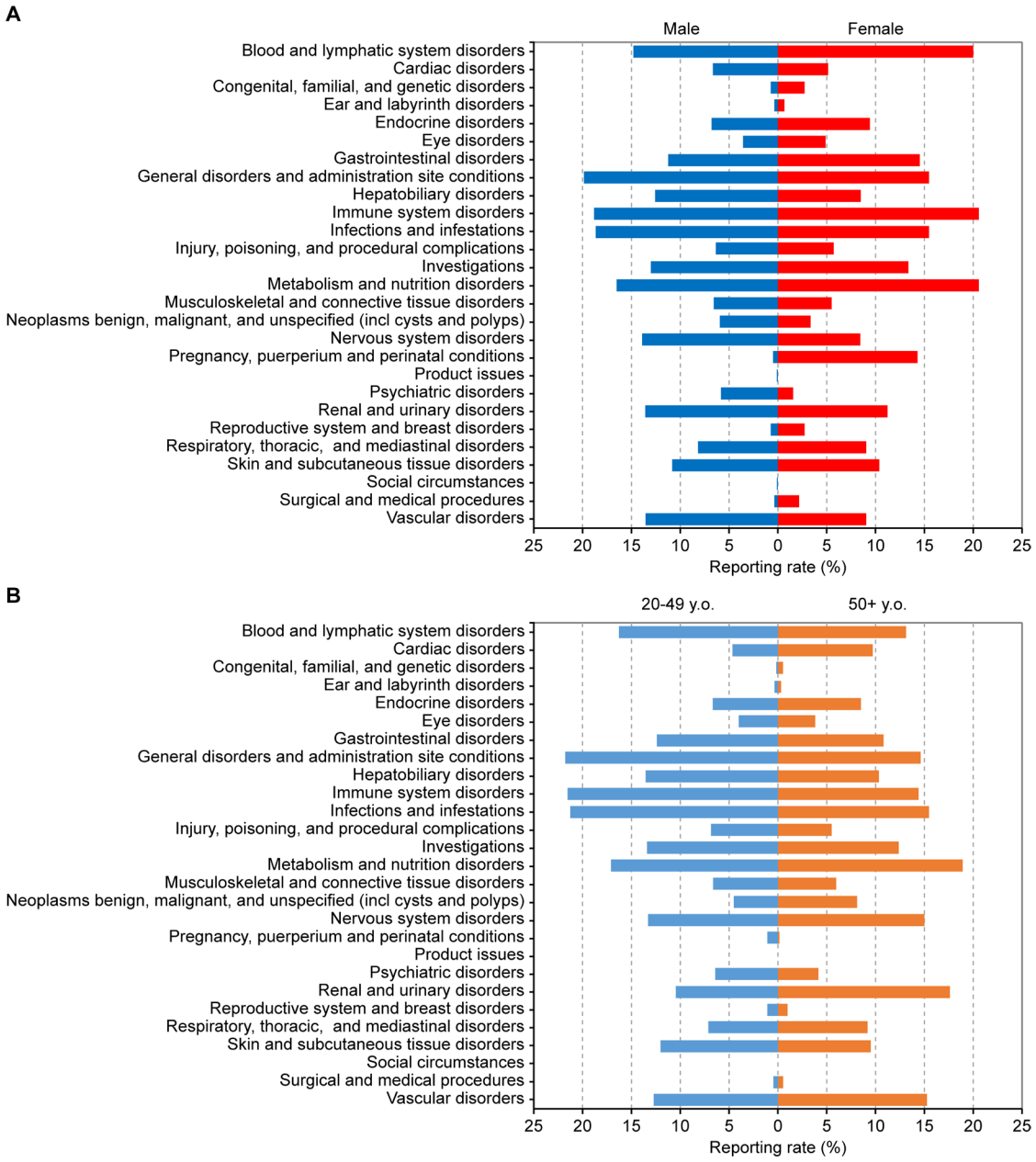

Figure 4. Comparison of adverse events at the SOC level by sex and age group. (A) Reporting rates by sex. **(B)** Reporting rates by age group.

Apparently, anti-HIV drugs were the primary causative drugs of adverse events in PLWHs. The most common non-anti-HIV drugs that caused adverse events were those used to prevent or treat AIDS-related diseases (opportunistic infections and AIDS-related cancers). Therefore, even if HIV infection can be controlled by cART, adverse events associated with these drugs must be carefully monitored. Using a large Japanese healthcare database, Ruzica *et al*. analyzed the 10 most common co-medications in PLWHs treated with cART. They found that all top 10 medications had higher rates of use in PLWHs than in the non-HIV-infected population (*17*). Therefore, healthcare providers involved in the treatment of HIV infection should also pay attention to the occurrence of adverse events associated with the use of these drugs.

In this study, IRIS was the most frequently reported adverse event at the PT level. IRIS is an undesirable disease- or pathogen-specific inflammatory reaction that may be triggered by the restoration of immune system function following cART initiation (*18*) and is a characteristic adverse event among PLWHs. This result is expected to some extent in studies of PLWH cases that use spontaneous reporting of adverse event databases, such as the current study. Common or high-incidence adverse events are not necessarily reported more frequently. The disadvantage of studies using spontaneous reporting adverse event databases is that it is not possible to calculate the incidence of adverse events owing to the lack of a denominator (*19*). However, if

the study is limited to a particular population, it may be possible to identify adverse events and the risk factors that are characteristic of that population. We focused on this feature and reported the results of our analysis of factors affecting the clinical outcomes of IRIS using the JADER (*20*). It may also be better to conduct an analysis at the SOC level rather than at the PT level to characterize adverse events occurring in a particular patient population. For example, "hepatic function abnormal" and "liver disorder" at the PT level (Table 2) may not be clinically distinct. These two PTs are classified as "hepatobiliary disorders" at the SOC level. The analysis of adverse events at the SOC level can better reflect their effects on human organs and systems. The top five SOC-level adverse events in this study were general disorders and administration site conditions, immune system disorders, infections and infestations, metabolism and nutrition disorders, and blood and lymphatic system disorders. However, it has been suggested that the occurrence of adverse events is influenced by sex and age, including in PLWHs (*21*). Thus, because 87.23% of the study population was male, the above results strongly reflect the status of adverse event reports in males. Therefore, when we analyzed SOC-level adverse events by sex and age, we found that the trends in females and in those aged ≥50 years were different from that in the overall group.

Recently, the life expectancy of properly treated PLWHs has approached that of non-HIV-infected individuals owing to the excellent efficacy of cART (*8*). However, the increasing number of PLWHs with comorbidities and the adverse events associated with long-term exposure to anti-HIV drugs have become a problem with the aging of PLWHs (*9-12*). Medications for comorbidities can cause problems related to polypharmacy and drug interactions (*22*). This problem is further complicated by an aging-related physiological decline (*23*).

Our study has some limitations. First, data from spontaneous reporting adverse event databases, such as JADER, has issues of over-reporting, under-reporting, missing data, lack of a denominator, and the presence of confounding factors (*19*). Second, adverse events are not always induced by treatment. Particularly, PLWHs are known to have higher rates of cardiovascular, renal, neurocognitive, oncology, and osteoporotic diseases than non-HIV-infected individuals (*12*). These factors may have affected the current analysis. Third, although trends in adverse event reports among PLWHs were examined in this study, the influence of the drug on the occurrence of each adverse event was not assessed.

In conclusion, despite the improved efficacy and safety of cART, anti-HIV drugs remain the leading cause of adverse events in PLWHs. In addition, the trends in adverse events differed according to sex and age, with females and those aged ≥ 50 years showing trends different from that in the overall population. Thus, the management of HIV infection and drug-related adverse events should consider age and sex. The findings of this study will be helpful for establishing optimal management strategies for PLWHs.

Funding: This research was partially funded by the Japan Society for the Promotion of Science (JSPS) KAKENHI [Grant No. 20K18892].

Conflict of Interest: The authors have no conflicts of interest to disclose.

References

1. World Health Organization. Guidelines for managing advanced HIV disease and rapid initiation of antiretroviral therapy July 2017. *https://www.who.int/publications/i/item/9789241550062* (accessed January 10, 2023).
2. Department of Health and Human Services. Panel on Antiretroviral Guidelines for Adults and Adolescents, Guidelines for the Use of Antiretroviral Agents in Adults and Adolescents with HIV. *https://clinicalinfo.hiv.gov/sites/default/files/guidelines/documents/adult-adolescent-arv/guidelines-adult-adolescent-arv.pdf* (accessed January 10, 2023).
3. Ministry of Health, Labour and Welfare. The Guidelines for the Treatment of HIV Infection, March 2022 Version. *https://hiv-guidelines.jp/pdf/guideline2022.pdf* (accessed January 10, 2023). (In Japanese).
4. Crum NF, Riffenburgh RH, Wegner S, Agan BK, Tasker SA, Spooner KM, Armstrong AW, Fraser S, Wallace MR. Triservice AIDS Clinical Consortium. Comparison of causes of death and mortality rates among HIV-infected persons: analysis of the pre-, early, and late HAART (highly active antiretroviral therapy) eras. J Acquir Immune Defic Syndr. 2006; 41:194-200.
5. Tanaka H, Wada T, Takayama Y, Matsumoto K, Atsuda K, Satoh M. Evaluation of the efficacy and safety of changes in antiretroviral regimens for HIV-infected patients. J Pharm Pharm Sci. 2014; 17:316-323.
6. De Clercq E, Li G. Approved antiviral drugs over the past 50 years. Clin Microbiol Rev. 2016; 29:695-747.
7. Pandit NS, Chastain DB, Pallotta AM, Badowski ME, Huesgen EC, Michienzi SM. Simplifying ARV therapy in the setting of resistance. Curr Infect Dis Rep. 2019; 21:38.
8. Antiretroviral Therapy Cohort Collaboration. Survival of HIV-positive patients starting antiretroviral therapy between 1996 and 2013: a collaborative analysis of cohort studies. Lancet HIV. 2017; 4:e349-e356.
9. Hentzien M, Dramé M, Allavena C, Jacomet C, Valantin MA, Cabié A, Cuzin L, Rey D, Pugliese P, Bani-Sadr F; Dat'AIDS Study Group. Impact of age-related comorbidities on five-year overall mortality among elderly HIV-infected patients in the late HAART era--role of chronic renal disease. J Nutr Health Aging. 2016; 20:408-414.
10. Balderson BH, Grothaus L, Harrison RG, McCoy K, Mahoney C, Catz S. Chronic illness burden and quality of life in an aging HIV population. AIDS Care. 2013; 25:451-458.
11. Naito T, Suzuki M, Fukushima S, Yuda M, Fukui N, Tsukamoto S, Fujibayashi K, Goto-Hirano K, Kuwatsuru R. Comorbidities and co-medications among 28089

people living with HIV: A nationwide cohort study from 2009 to 2019 in Japan. HIV Med. 2022; 23:485-493.
12. Wing EJ. HIV and aging. Int J Infect Dis. 2016; 53:61-68.
13. Ruzicka DJ, Imai K, Takahashi K, Naito T. Comorbidities and the use of comedications in people living with HIV on antiretroviral therapy in Japan: A cross-sectional study using a hospital claims database. BMJ Open. 2018; 8:e019985.
14. Tanaka H, Onoda T, Ishii T. Understanding the actual use of anti-HIV drugs in Japan from 2016 to 2019: Demonstrating epidemiological relevance of NDB Open Data Japan for understanding Japanese medical care. Int J Environ Res Public Health. 2022; 19:12130.
15. Kobayashi T, Noda A, Obara T, Tsuchiya M, Akasaka K, Yoshida M, Matsuura M, Sato M, Murai Y, Yamaguchi H, Tsuchiya F, Kihira K, Mano N. Knowledge, attitudes, and practice of hospital pharmacists regarding pharmacovigilance and adverse drug reaction reporting in Japan. Hosp Pharm. 2021; 56:7-16.
16. Wallenstein EJ, Fife D. Temporal patterns of NSAID spontaneous adverse event reports: the Weber effect revisited. Drug Saf. 2001; 24:233-237.
17. Ruzicka DJ, Imai K, Takahashi K, Naito T. Greater burden of chronic comorbidities and co-medications among people living with HIV versus people without HIV in Japan: A hospital claims database study. J Infect Chemother. 2019; 25:89-95.
18. French MA, Lenzo N, John M, Mallal SA, McKinnon EJ, James IR, Price P, Flexman JP, Tay-Kearney ML. Immune restoration disease after the treatment of immunodeficient HIV-infected patients with highly active antiretroviral therapy. HIV Med. 2000; 1:107-115.
19. Poluzzi E, Raschi E, Moretti U, De Ponti F. Drug-induced torsades de pointes: data mining of the public version of the FDA Adverse Event Reporting System (AERS). Pharmacoepidemiol Drug Saf. 2009; 18:512-518.
20. Tanaka H, Wada T, Ohyama K, Ishii T. Analysis of the time-to-onset and factors affecting clinical outcomes of immune reconstitution inflammatory syndrome in people living with HIV using data from the Japanese spontaneous reporting database. J Pharm Pharm Sci. 2021; 24:153-160.
21. Xiao J, Wang Y, Li Z, Zhang X, Feng K, Liu L. Assessing the gender differences of adverse effects in HIV infection treatment based on FDA AERS database. Curr Bioinform. 2013; 8:583-590.
22. Danjuma MI, Adegboye OA, Aboughalia A, Soliman N, Almishal R, Abdul H, Mohamed MFH, Elshafie MN, AlKhal A, Elzouki A, Al-Saud A, Chaponda M, Bidmos MA. Prevalence and global trends of polypharmacy among people living with HIV: A systematic review and meta-analysis. Ther Adv Drug Saf. 2022; 13:20420986221080795.
23. Demessine L, Peyro-Saint-Paul L, Gardner EM, Ghosn J, Parienti JJ. Risk and cost associated with drug-drug interactions among aging HIV patients receiving combined antiretroviral therapy in France. Open Forum Infect Dis. 2019; 6:ofz051.

Received February 2, 2023; Revised June 9, 2023; Accepted June 10, 2023.

Address correspondence to:
Hiroyuki Tanaka, Department of Practical Pharmacy, Faculty of Pharmaceutical Sciences, Toho University, 2-2-1 Miyama, Funabashi, Chiba 274-8510, Japan.
E-mail: hiroyuki.tanaka@phar.toho-u.ac.jp

Released online in J-STAGE as advance publication June 16, 2023.

Original Article

DOI: 10.5582/ddt.2022.01095

The role of APOBEC3A in cervical cancer development and progression: A retrospective study

Mo Zhang[1,2], Zhi Wei[1,2], Hongbo Zhao[1,2], Sai Zhang[1,2], Jing Wu[1,2], Jing Zhou[3,4,5], Yan Wang[3,4], Ling Wang[3,4,5,*], Yan Du[1,2,*]

[1] Clinical Research Unit, Obstetrics and Gynecology Hospital, Fudan University, Shanghai, China;
[2] Department of Obstetrics and Gynecology of Shanghai Medical School, Fudan University, Shanghai, China;
[3] Laboratory for Reproductive Immunology, Obstetrics and Gynecology Hospital of Fudan University, Shanghai, China;
[4] The Academy of Integrative Medicine of Fudan University, Shanghai, China;
[5] Shanghai Key Laboratory of Female Reproductive Endocrine-related Diseases, Shanghai, China.

SUMMARY The majority of cervical cancer cases are contributed to chronic infection with high-risk human papillomavirus (HPV), while only a fraction of infected women finally develop cancer. It is suggested that apolipoprotein B mRNA editing enzyme, catalytic polypeptide-like 3A (APOBEC3A), a type of mRNA editing enzyme, may be involved in the development and progression of HPV-related tumors. This study aimed to explore the role and potential mechanisms of APOBEC3A in cervical cancer. First, the expression levels, prognostic values and genetic alterations of *APOBEC3A* in cervical cancer were explored using various bioinformatics tools and databases. Then, functional enrichment analyses were performed. Finally, genetic polymorphisms (rs12157810 and rs12628403) of *APOBEC3A* were genotyped in our clinical sample of 91 cervical patients. The associations between *APOBEC3A* polymorphisms and clinical characteristics as well as patient overall survival were further evaluated. Compared with normal tissues, the expression level of APOBEC3A was significantly elevated in cervical cancer. High expression of APOBEC3A had better survival compared with the low expression group. The immunohistochemistry results showed that the expression of APOBEC3A protein was localized in the nucleus. APOBEC3A expression level in cervical and endocervical cancer (CESC) was negatively correlated with the infiltration level of cancer-associated fibroblasts, and positively correlated with the infiltration level of gamma delta T cells. No association was observed between *APOBEC3A* polymorphisms and patient survival. The expression of APOBEC3A was significantly higher in cervical cancer tissues, while high expression was associated with better prognosis in cervical cancer patients. APOBEC3A has the potential of being used in prognostic evaluation in cervical cancer patients.

Keywords APOBEC3A, expression, cervical cancer, bioinformatics, SNP, survival

1. Introduction

Worldwide, cervical cancer is the fourth most commonly diagnosed and the fourth leading cause of cancer death among women (*1*). There were an estimated 569,847 new cases of and 311,365 deaths caused by cervical cancer in 2018. The burden of cervical cancer is even higher in countries and regions with lower human development index (HDI) (*1*). Almost all cases of cervical cancer are attributed to persistent infection with high-risk human papillomavirus (HPV) genotypes (*2*). However, only a small fraction (about 10%) of infected women will develop viral persistence, and only some of those chronically infected with carcinogenic HPV types will eventually progress to neoplastic lesions (*3*). In addition, invasive cervical cancer is preventable through HPV vaccination (*4*). Furthermore, screening and removing precancerous cervical lesions can prevent its development into cervical cancer (*5*). Despite implementation of above public health intervention measures, health system barriers such as accessibility and affordability exist, especially in lower HDI countries and regions. Cervical cancer is and will continue to be a public health burden in China in the foreseeable future (*6*). It is important to have a better understanding of the molecular mechanisms so as to provide more opportunities for early diagnosis and prognosis assessment.

Apolipoprotein B mRNA editing enzyme, catalytic

polypeptide-like 3A (APOBEC3A) is a member of the APOBECs family, which plays an important role in the defense process of anti-viral infection (*7*). It is reported that APOBEC3A can enhance the ability of human immune system to recognize HPV infection (*8*). Research has shown that APOBEC3A has the function of genetic editing HPV DNA in the nucleus, thus playing an important role in combating and clearing HPV. Therefore, it is speculated that APOBEC3A may be involved in the inhibition of the occurrence and development of HPV-related tumors (*9*). However, some studies have shown that APOBEC3A may damage the DNA of its own cells, and the signature mutation of *APOBEC3A* increases in HPV-associated tumors, suggesting that APOBEC3A may also be closely related to tumorigenesis (*10-12*). Cancer is a complex disease resulting from interactions of various factors, and the same factor may also act differently at different stages of tumor development and progression. Furthermore, genetic variations may also affect an individual's susceptibility to cervical cancer and its prognosis. Therefore, it is important to conduct bioinformatics analysis of interested genes to assess its correlation with clinical prognosis and fully explore potential molecular mechanisms using publicly available database.

In this study, we first utilized various bioinformatics databases and tools to comprehensively analyze the relationship between APOBEC3A and the occurrence, development, and prognosis of cervical cancer. We further evaluated the effects of *APOBEC3A* genetic polymorphisms on the overall survival (OS) of cervical cancer in our own clinical samples.

2. Materials and Methods

2.1. Tumor Immune Estimation Resource (TIMER)

TIMER (version 2.0) (*http://timer.cistrome.org/*) is a resource for systematic analyses of immune cell infiltration across various cancer types based on The Cancer Genome Atlas (TCGA) database (*13*). In this study, "Exploration" module was used to display the differential gene expression of APOBEC3A in various tumor tissues (and corresponding normal tissues). The "Immune" module of the TIMER web server was used to explore the association between APOBEC3A expression and immune infiltrates of TCGA cervical and endocervical cancer (CESC). Purity-adjusted Spearman's rank correlation test was used to obtain *p*-values and partial correlation (rho) values. Algorithms of TIMER, EPIC, MCPCOUNTER, CIBERSORT, CIBERSORT-ABS, QUANTISEQ, XCELL, naïve_XCELL, and TIDE were used for immune infiltration estimations.

2.2. Oncomine database

Oncomine database (*http://www.oncomine.org*) is a web-based chip data-mining platform, including 715 tumor microarrays, and 86,733 cancer and normal tissue samples (*14*). Oncomine was used to analyze the mRNA expression of APOBEC3A in cervical cancer tissues and normal tissues, using the following parameters: Gene: *APOBEC3A*; Analysis Type: Cancer *vs.* Normal Analysis; Data Type: mRNA; threshold: *p* value < 0.05, Fold change > 2 and gene rank = top 10%.

2.3. Gene Expression Profiling Interactive Analysis (GEPIA) dataset analysis

GEPIA (version 2) (*http://gepia.cancer-pku.cn/*) is a database containing RNA sequencing expression data from TCGA and Genotype-tissue Expression dataset (GTEx) projects. It is a visual analysis website including information from 33 tumor types, 9736 tumor samples, and 8587 normal samples (*15*). In this study, GEPIA was applied to evaluate the differential expression of APOBEC3A in cervical squamous cell carcinoma and endocervical adenocarcinoma *vs.* normal cervical tissues. The criteria were: |Log2FC| Cutoff: 2; *p*-value Cutoff: 0.05. GEPIA was also used to evaluate the prognostic value of APOBEC3A expression in cervical cancer patients, with group cutoff set as Median.

2.4. TCGA data mining

The expression data of cervical squamous cell carcinoma tissues were downloaded from TCGA (https://cancergenome.nih.gov/) in TCGA-CESC dataset and utilized to analyze the expression of APOBEC3A. The TCGA-CESC dataset contains data of 308 cervical cancer cases; however, only 304 cases have expression data needed and hence were selected for relative expression analysis. Among them, 304 cervical cancer cases have detailed follow-up information of OS and 174 with recurrence-free survival (RFS) information, and were used for Kaplan-Meier analysis. These patients were divided into high and low APOBEC3A expression groups based on the RNA-Seq by Expectation-Maximization (RSEM) with an auto selected best cutoff value of 2.105.

2.5. Human Protein Atlas (HPA)

HPA (*https://www.proteinatlas.org/*) (Version: 20.0, updated date: 2020-11-19) is a free public platform that can be used for genome-wide exploration of individual proteins on clinical outcome in major human cancers (*16*). The database can provide the location, expression and prognosis of proteins in normal tissues, tumor tissues, cell lines and blood cells with immunology method. In this study, HPA database was used to analyze the immunohistochemical staining of APOBEC3A in cervical cancer tissues.

2.6. Tumor-Immune System Interactions (TISIDB) immune analysis

TISIDB database (*http://cis.hku.hk/TISIDB*) (*17*) integrates data related to immune-associated anti-tumor genes, high-throughput screening techniques, molecular profiles, and paracancerous multi-omics. In this study, TISIDB is used to explore the correlations of APOBEC3A expression with lymphocyte, immunomodulators, and major histocompatibility molecules (MHCs) in ovarian cancer.

2.7. Clinical samples and follow-up

The study patients were recruited at the Obstetrics and Gynecology Hospital of Fudan University in Shanghai. The study protocol was approved by the Institutional Review Board of the hospital, and all patients provided written informed consent. Cases were randomly selected newly diagnosed sporadic cervical cancer patients undergoing surgery at our hospital from November 2013 to September 2017. Pathological diagnosis was confirmed independently by two pathologists. Patients received any pre-operative therapies were not included. All patients were ethnic Han Chinese. Follow-up started after 6 months of the surgery. A dedicated unit in our hospital performed the follow-up every 3 months on an outpatient bases and/or by telephone calls according to standard protocol (*18*).

2.8. APOBEC3A SNP and genotyping

QIAquick PCR purification kits (QIAGEN, Hilden, Germany) were used to extract genomic DNA from blood samples. *APOBEC3A* single nucleotide polymorphism (SNP) rs12157810 (-535 A>C) was selected because it represented the haplotype block in the promoter region of APOBEC3A determined by Haploview 4.2. Intronic SNP rs12628403 (+4340 A>C) was selected for genotyping based on previous literatures and as the proxy tag of *APOBEC3B* deletion (*19,20*). Genotyping was conducted using fluorescent probe real-time quantitative PCR in a LightCyclerTM480 (Roche, Basel, Switzerland). Primers and probes (Minor Groove Binder [MGB]) were designed by GeneCore Bio Technologies Co. Ltd. (Shanghai, China). The primer and probe sequences were presented at Table S1 (*http://www.ddtjournal.com/action/getSupplementalData.php?ID=139*). Blind duplicates (5% of the samples) were included to assess laboratory reliability, and 100% concordance rate was achieved.

2.9. Statistical analysis

Categorical variables were summarized as number (percentage), and continuous variables were presented as median (range). Fisher's exact test was used to determine the differences of discrete variables between high- and low-expression subgroups. Kaplan-Meier survival analysis and log-rank test were used to assess the influence of *APOBEC3A* SNPs on cervical cancer prognosis. All significance tests were two sided; p value of < 0.05 was considered as statistically significant. Data analyses were performed by STATA version 15 (StataCorp LLC, College Station, TX, USA).

3. Results

3.1. Expression level of APOBEC3A mRNA in patients with various cancer types

The expression of APOBEC3A was evaluated in different tumor types and adjacent normal tissues using TIMER database. As shown in Figure 1A, the expression level of APOBEC3A was significantly higher than that in adjacent normal tissues in the following cancers: breast invasive carcinoma (BRCA), CESC, cholangiocarcinoma (CHOL), esophageal carcinoma (ESCA), head and neck cancer (HNSC), kidney renal clear cell carcinoma (KIRC), stomach adenocarcinoma (STAD), and uterine corpus endometrial carcinoma (UCEC).

We further detected the level of APOBEC3A mRNA in different cervical cancer types *vs.* normal tissues using Oncomine (Figure 1B and Table 1). In Pyeon Multi-cancer statistics, the level of APOBEC3A mRNA expression was significantly upregulated in cervical cancer compared with normal tissues (fold change = 2.010, $p = 0.026$). Although not meeting our screening criteria, in Biewenga Cervix statistics, the level of APOBEC3A mRNA expression was also elevated in cervical squamous cell carcinoma compared with normal tissues (fold change = 1.791, $p = 0.046$).

3.2. Differential expression level of APOBEC3A mRNA and protein in patients with cervical cancer

Cervical squamous cell carcinoma consists about 80% of cervical cancer cases and cervical adenocarcinomas accounts for 10%-20% of the cases (*7*). We then investigated APOBEC3A expression in cervical squamous cell carcinoma and endocervical adenocarcinoma *vs.* normal cervical tissues. GEPIA results showed that the expression level of APOBEC3A was significantly higher in cervical cancer tissues than that in normal tissues ($p < 0.05$) (Figure 1C), while there was no association between APOBEC3A mRNA level and Federation of Gynecologists and Obstetricians (FIGO) stage (Figure 1D).

We further explored the expression of APOBEC3A protein in cervical cancer tissues and normal tissues using immunohistochemistry with the HPA database. The immunohistochemistry staining results showed

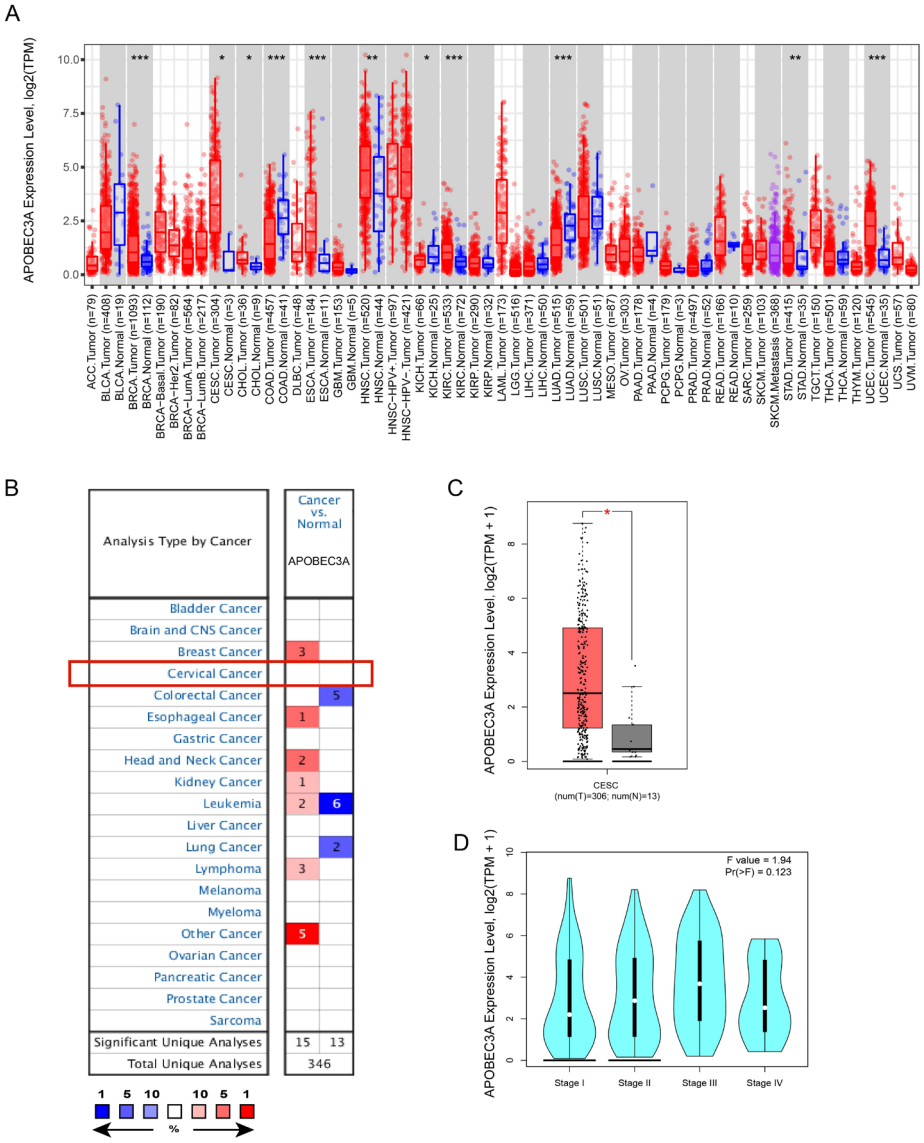

Figure 1. **Expression of APOBEC3A mRNA in different cancer types and correlation between APOBEC3A expression and tumor stages in cervical cancer (TIMER, Oncomine and GEPIA).** (**A**) Expression status of the *APOBEC3A* gene in different cancers or specific cancer subtypes was analyzed using TIMER. *$p < 0.05$; **$p < 0.01$; ***$p < 0.001$. (**B**) Expression of APOBEC3A in cervical cancer explored using Oncomine. The value represents the number of unique analyses. (**C**) APOBEC3A in cervical and normal tissues from GEPIA dataset. *$p < 0.05$ (**D**) APOBEC3A in different tumor stages in cervical cancer patients from GEPIA dataset. TPM: Transcripts Per Kilobase Million. T: tumor; N: normal.

that in both normal tissues and cervical squamous cell carcinoma tissues, the expression of APOBEC3A protein was localized in the nucleus. In normal cervix and uterine tissues, the intensity was moderate, and the staining was medium. While in cervical cancer tissues, the intensity was between moderate to strong, and the staining was between medium to high (Figure S1, *http://www.ddtjournal.com/action/getSupplementalData.php?ID=139*).

3.3. Prognostic value of APOBEC3A expression in cervical cancer patients

The prognostic value of APOBEC3A expression in cervical cancer was first explored by GEPIA, a total of 292 cases were selected. No association was found for APOBEC3A expression and OS [hazard ratio (HR) = 0.83, log-rank $p = 0.44$] (Figure 2A). At 200 months follow-up, the high APOBEC3A expression group had a significantly better disease-free survival (DFS) compared with the low APOBEC3A expression group (HR = 0.53, log-rank $p = 0.033$) (Figure 2B).

TCGA dataset analysis showed that the median survival time was 45.73 months and 21.4 months in the high expression group and low expression group, respectively. Kaplan-Meier analysis revealed that the high APOBEC3A expression group was associated with both better 10-year OS (HR = 0.62, 95% CI: 0.39-1, log-rank $p = 0.047$, Figure 2C) and RFS (HR = 0.3, 95% CI: 0.14-0.66, log-rank $p = 0.0015$, Figure 2D)

Table 1. APOBEC3A mRNA expression in different types of cervical cancer and normal cervical tissues (Oncomine).

Dataset	Tumor (cases)	Normal (cases)	Fold change	*t*-test	*p*-value
Zhai Cervix	Cervical Squamous Cell Carcinoma (21)	Cervix Squamous Epithelium (10)	1.631	1.035	0.160
	High Grade Cervical Squamous Intraepithelial Neoplasia (7)	Cervix Squamous Epithelium (10)	-2.019	-1.456	0.916
TCGA Cervix	Cervical Non-Keratinizing Squamous Cell Carcinoma (13)	Blood (93) + Cervix Uteri (3)	1.034	0.752	0.233
	Cervical Squamous Cell Carcinoma (82)	Blood (93) + Cervix Uteri (3)	-1.002	-0.107	0.543
	Cervical Keratinizing Squamous Cell Carcinoma (5)	Blood (93) + Cervix Uteri (3)	-1.033	-0.470	0.669
Scotto Cervix 2	Cervical Squamous Cell Carcinoma (32)	Cervix Squamous Epithelium (21) + Cervix Uteri (3)	-1.103	-0.291	0.614
Pyeon Multi-cancer	Cervical Cancer (20)	Cervix Uteri (8) + Oral Cavity (9) + Palate (1) + Tonsil (4)	2.010	2.002	0.026
Biewenga Cervix	Cervical Squamous Cell Carcinoma (40)	Cervix Uteri (5)	1.791	2.032	0.046
Scotto Cervix	Cervical Squamous Cell Carcinoma (79)	Cervix Squamous Epithelium (7)	1.035	1.663	0.067
	Cervical Adenocarcinoma (5)	Cervix Squamous Epithelium (7)	-1.004	-0.120	0.546

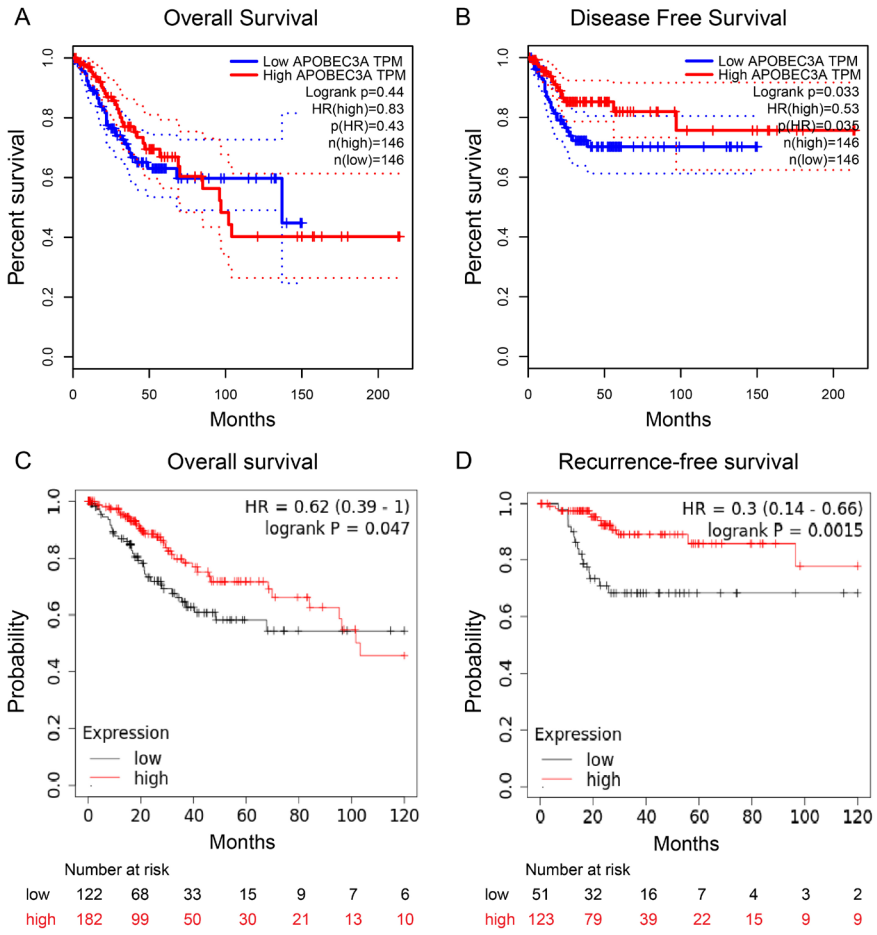

Figure 2. Prognostic value of APOBEC3A in cervical cancer (GEPIA and TCGA). (**A**) Relationship between the expression of APOBEC3A and overall survival in cervical cancer patients from GEPIA. (**B**) Relationship between the expression of APOBEC3A and disease-free survival in cervical cancer patients from GEPIA. (**C**) Relationship between the expression of APOBEC3A and overall survival in cervical cancer patients from TCGA. (**D**) Relationship between the expression of APOBEC3A and recurrence-free survival in cervical cancer patients from TCGA.

compared with the low APOBEC3A expression group.

3.4. Correlation between APOBEC3A expression and immune factors in cervical cancer

We evaluated the correlation of APOBEC3A expression and the estimated infiltration value of cancer-associated fibroblasts for the TCGA tumors of CESC (n = 306) using TIMER. The scatterplot data shows the correlation analysis of APOBEC3A expression with immune infiltration of cancer-associated fibroblasts. The APOBEC3A expression level in CESC was negatively

correlated with the infiltration level of cancer-associated fibroblasts based on EPIC, MCPCOUNTER, XCELL, and TIDE algorithms (Figure 3). The APOBEC3A expression level in CESC was positively correlated with the infiltration level of gamma delta T cells based on XCELL algorithm (rho = 0.395, p = 8.60e-12).

TISIDB database was utilized to analyze the correlations of APOBEC3A expression with tumor-infiltrating lymphocytes (TILs) and immunomodulators by Spearman correlation. Table S2 (*http://www.ddtjournal.com/action/getSupplementalData.php?ID=139*) presents detailed information of TILs, immunoinhibitors, immunostimulators, and MHCs that were significantly correlated with APOBEC3A expression in CESC.

3.5. Relationship of *APOBEC3A* SNPs with clinicopathological parameters and survival of cervical cancer patients

All patients were high-risk HPV associated cervical cancer. Table S3 (*http://www.ddtjournal.com/action/getSupplementalData.php?ID=139*) presents the clinicopathological characteristics of the 91 study patients. Briefly, most of the patients (71/91, 78%) were more than 39 years old, and about half (50/91, 54.9%) were before menopause. The majority of the patients were diagnosed as squamous cell carcinoma (82/91, 90.1%) and well differentiated (79/91, 86.8%). About 60% (n = 56) of the patients were diagnosed at the early FIGO stage (IA1-IB1), and a significant proportion of them received chemotherapy (61/91, 67%) and/or radiotherapy (56/91, 61.5%) after surgery.

In terms of associations between clinicopathological characteristics and *APOBEC3A* SNPs, only SNP rs12157810 was statistically significantly associated with FIGO stage (p = 0.02) (Table 2). Wide type of rs12157810 (AA genotype) was more prevalent in early stage (FIGO stage IA1-IB1) cervical cancer patients.

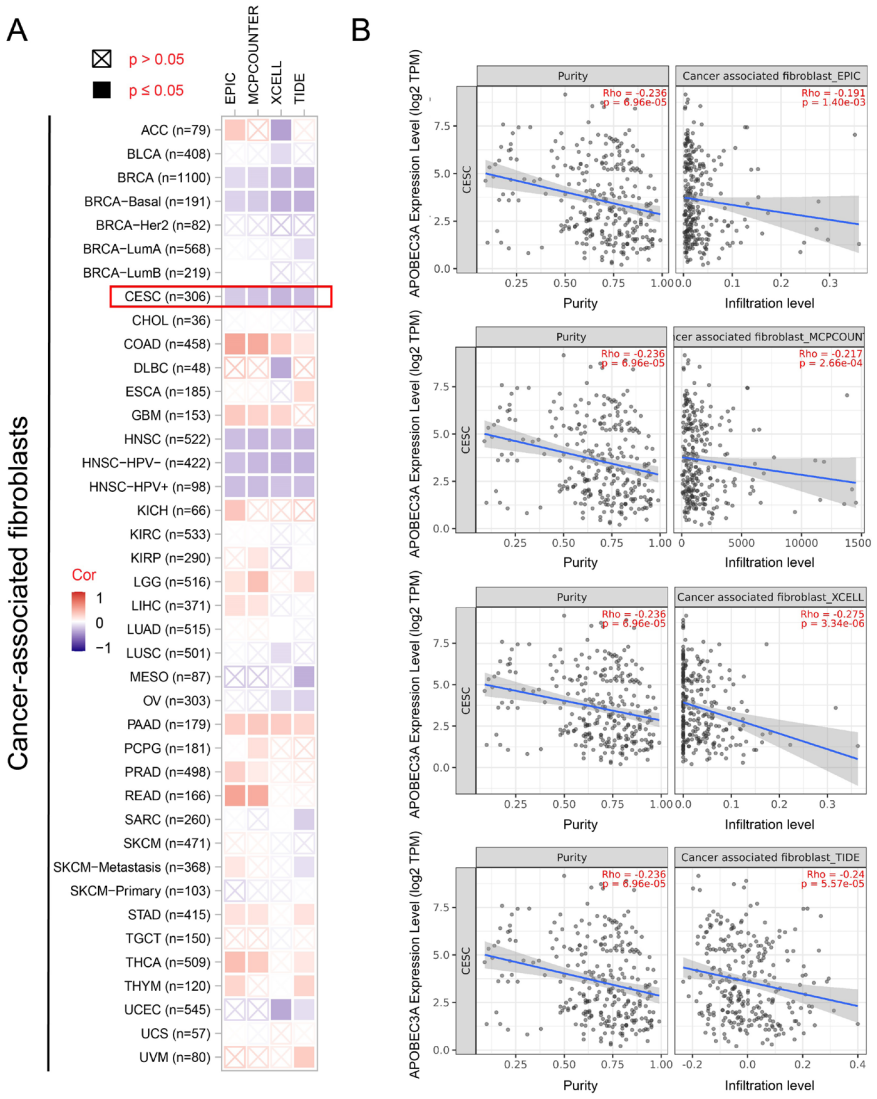

Figure 3. Correlation analysis between APOBEC3A expression and immune infiltration of cancer-associated fibroblasts (TISIDB). (A), Correlation between APOBEC3A expression and the infiltration level of cancer-associated fibroblasts based on EPIC, MCPCOUNTER, XCELL, and TIDE algorithms. **(B),** Negative correlation between APOBEC3A expression and cancer-associated fibroblasts.

After a median observation of 60 months (range 24.17-74.17 months), 3 patients had died. In general, no association was observed between *APOBEC3A* SNPs and OS in our cohort of cervical cancer patients (Figure 4).

4. Discussion

In this study, we used a series of public bioinformatics databases and tools to conduct analyses of APOBEC3A and cervical cancer. We explored a number of aspects, including gene expression, survival status, immune factors and immune infiltration, to investigate the probable mechanism of APOBEC3A in the occurrence and/or prognosis of cervical cancer. Furthermore, we tested the association of genetic polymorphisms of *APOBEC3A* with clinicophathological characteristics and survival of cervical cancer patients.

Our bioinformatics analyses showed that the expression of APOBEC3A was significantly higher in the cervical tumor tissues compared with normal tissues. *APOBEC3A*, located on chromosome 22q13.1, is a member of the cytidine deaminase gene family. It has two transcript variants encoding different isoforms. It is suggested that APOBEC3A may link immunity and viral infection during HPV-driven carcinogenesis. The protein encoded by *APOBEC3A* plays a role in immunity, by restricting viral infection (*21*). APOBEC3A protein can recognize HPV infection and restrict foreign DNA *via* catalyzing the deamination of cytosine bases in nucleic acids, causing the conversion of target cytosine (C) to uracil (U), which leads to DNA degradation. APOBEC3A may play a role in cancer development and progression through mediating the interactions between HPV and the host genome (*7*). Of the cancer types with high APOBEC3A expression

Table 2. Correlation of clinicopathological characteristics with APOBEC3A SNPs in cervical cancer patients. (*n* = 87)

Characteristics	rs12157810		*p* value*	rs12628403		*p* value*
	AA (*n* = 49)	AC+CC (*n* = 40)		AA (*n* = 13)	AC+CC (*n* = 75)	
Age			0.44			0.14
≤39	13	7		5	15	
>39	36	33		8	60	
Histology			0.55			1.00
Squamous cell carcinoma	45	35		12	67	
Adenocarcinoma	2	4		1	5	
Adenosquamous carcinoma	2	1		0	3	
Tumor size (cm)※ (*n* = 63)			0.22			0.62
≤5	30	21		6	46	
>5	5	8		2	9	
Differentiation			0.53			0.41
Well	43	35		11	65	
Moderate	1	3		0	4	
Poor	1	1		1	1	
Unknown	4	1		1	5	
FIGO stage			0.02			0.79
IA1-IB1	36	20		9	45	
IB2-IIA2	12	20		4	29	
IIB	1	0		0	1	

FIGO, Federation of Gynecologists and Obstetricians. *Fisher's exact test. ※ *n* = 64 for rs12157810 and *n* = 63 for rs12628403.

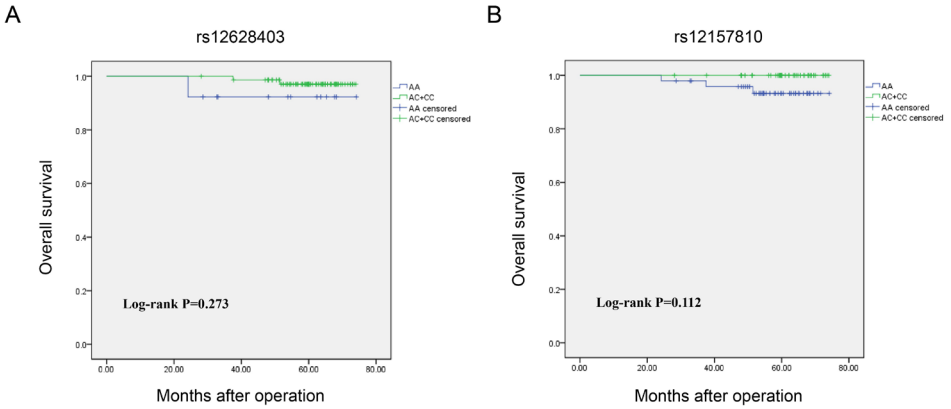

Figure 4. Association between *APOBEC3A* SNPs and overall survival in clinical samples. (**A**) Association between *APOBEC3A* rs12628403 and overall survival. (**B**) Association between *APOBEC3A* rs12157810 and overall survival.

discovered by TIMER database analyses, CESC, ESCA, and HNSC are HPV-related cancers. It is speculated that APOBEC3A may play a role in cancer occurrence *via* generating DNA mutations. Previous studies have found signature mutations of *APOBEC3A* in cervical cancer and other HPV-related tumor cancers (*22-24*). In addition, APOBEC3A was up-regulated in HPV-positive keratinocytes and cancer cells (*25,26*).

APOBEC family members are closely related to the occurrence and development of a variety of tumors. A recent meta-analysis of 20 eligible studies including 26,225 cases and 37,201 controls has reported that *APOBEC3* deletion was significantly associated with increased cancer risk in homozygous codominant inheritance model (*27*). After stratified by cancer type, the positive association was observed in breast cancer (10 studies including 14,757 cases and 17,930 controls) in heterozygous codominant, dominant, overdominant and allele inheritance models (*27*). *APOBEC3* may promote hepatocellular carcinoma (HCC) development through promoting the generation of high-risk hepatitis B virus mutations. A study by Liu *et al*. reported that *APOBEC3B* genetic polymorphisms (rs2267401-G allele) significantly increased HCC risk; and *APOBEC3B* rs2267401-GG genotype, higher APOBEC3B expression, and higher APOBEC3B/ uracil DNA glycosylase (UNG) expression ratio predicted poor prognosis of HCC patients (*19*). Our previous research has found that higher APOBEC3B expression independently predicted worse survival of ovarian cancer patients. Our cell line experiments suggested that APOBEC3B may play a role in ovarian cancer prognosis possibly *via* affecting viability of ovarian cancer (*28*).

Interestingly, our bioinformatics analyses showed that higher expression of APOBEC3A was associated with better OS and DFS/RFS. Cancer is a complex disease that results from gene-gene and gene-environment interactions. It is also very likely that the same factor may function differently at various stages of cancer development and progression. Furthermore, the favorable role of APOBEC3A expression in cervical cancer was supported by its negative association with the infiltration level of cancer-associated fibroblasts, and positive association with gamma delta T cell. As important elements constituting the tumor microenvironment, tumor-infiltrating immune cells are closely associated with cancer initiation, progression and/or metastasis (*29*). The functions of tumor-infiltrating immune cells are thought to be modulated by cancer-associated fibroblasts, which regulate cell-cell contact, release regulatory factors, and synthesize and remodel the extracellular matrix (*30*). Human gamma delta T cell is an important component of natural tumor surveillance and has the capacity for tumor cell killing. It has been a focus for the development of new cancer immunotherapy, especially for tumors lacking effective treatment (*31*). Moreover, a group of Chinese investigators studied the effect of APOBEC3A on the biological behaviors of cervical cancer using Hela cells. They found that transfection of APOBEC3A can suppress the migration ability and promote apoptosis of Hela cells, through inhibiting cell proliferation and growth (*32*). Therefore, high expression of APOBEC3A may facilitate better survival of cervical cancer patients, and may become a new therapeutic target for the treatment of cervical cancer.

Even though we detected a significant association between APOBEC3A expression and cervical cancer survival *via* bioinformatics analyses, we did not observe significant association between *APOBEC3A* polymorphisms and cervical cancer patient survival in our own clinical samples. One possible explanation is that the survival of early-stage cervical cancer is optimal, with a 4,5-year OS of about 90% for early-stage patients (*33*). We did not have enough follow-up time and enough events (only 3 deaths in our clinical samples) to detect a significant association between SNP and survival. Future prospective studies with a large sample size are needed to evaluate the associations. Functional studies are also required to further elucidate the underlying mechanisms.

5. Conclusion

To summarize, our bioinformatics analyses found that APOBEC3A expression was significantly higher in cervical cancer tissues compared with normal tissues, while high expression of APOBEC3A predicted better prognosis for cervical cancer patients. The APOBEC3A expression level in CESC was negatively correlated with the infiltration level of cancer-associated fibroblasts, and positively correlated with the infiltration level of gamma delta T cells. APOBEC3A has the potential of being used in prognostic evaluation in cervical cancer. Further studies are needed to investigate the mechanism and multilevel function of APOBEC3A in cervical cancer development and progression.

Acknowledgements

The results presented here are in part based upon data generated by the TCGA Research Network: https://www.cancer.gov/tcga.

Funding: This work was supported by the National Natural Science Foundation of China (grant no. 81973119 to Y Du), Shanghai Talent Development Fund (grant no. 2017090 to Y Du), a project under the Scientific and Technological Innovation Action Plan of the Shanghai Natural Science Fund (grant no. 20ZR1409100 to L Wang), a project of the Chinese Association of Integration of Traditional and Western

Medicine special foundation for Obstetrics and Gynecology-PuZheng Pharmaceutical Foundation (grant no. FCK-PZ-08 to L Wang), a project for hospital management of the Shanghai Hospital Association (grant no. X2021046 to L Wang), and a clinical trial project of the Special Foundation for Healthcare Research of the Shanghai Municipal Health Commission (grant no. 202150042 to L Wang). The funding agency played no role in the conduct of the research and preparation of the article.

Conflict of Interest: The authors have no conflicts of interest to disclose.

References

1. Bray F, Ferlay J, Soerjomataram I, Siegel RL, Torre LA, Jemal A. Global cancer statistics 2018: GLOBOCAN estimates of incidence and mortality worldwide for 36 cancers in 185 countries. CA Cancer J Clin. 2018; 68:394-424.
2. Schiffman M, Castle PE, Jeronimo J, Rodriguez AC, Wacholder S. Human papillomavirus and cervical cancer. Lancet. 2007; 370:890-907.
3. Guan P, Howell-Jones R, Li N, Bruni L, de Sanjosé S, Franceschi S, Clifford GM. Human papillomavirus types in 115,789 HPV-positive women: A meta-analysis from cervical infection to cancer. Int J Cancer. 2012; 131:2349-2359.
4. Lei J, Ploner A, Elfström KM, Wang J, Roth A, Fang F, Sundström K, Dillner J, Sparén P. HPV vaccination and the risk of invasive cervical cancer. N Engl J Med. 2020; 383:1340-1348.
5. US Preventive Services Task Force; Curry SJ, Krist AH, Krist AH, *et al*. Screening for cervical cancer: US preventive services task force recommendation statement. JAMA. 2018; 320:674-686.
6. Chen W, Zheng R, Baade PD, Zhang S, Zeng H, Bray F, Jemal A, Yu XQ, He J. Cancer statistics in China, 2015. CA Cancer J Clin. 2016; 66:115-132.
7. Chen L, Qiu X, Zhang N, Wang Y, Wang M, Li D, Wang L, Du Y. APOBEC-mediated genomic alterations link immunity and viral infection during human papillomavirus-driven cervical carcinogenesis. Biosci Trends. 2017; 11:383-388.
8. Ahasan MM, Wakae K, Wang Z, *et al*. APOBEC3A and 3C decrease human papillomavirus 16 pseudovirion infectivity. Biochem Biophys Res Commun. 2015; 457:295-299.
9. Vartanian JP, Guétard D, Henry M, Wain-Hobson S. Evidence for editing of human papillomavirus DNA by APOBEC3 in benign and precancerous lesions. Science. 2008; 320:230-233.
10. Green AM, Landry S, Budagyan K, Avgousti DC, Shalhout S, Bhagwat AS, Weitzman MD. APOBEC3A damages the cellular genome during DNA replication. Cell Cycle. 2016; 15:998-1008.
11. Nowarski R, Kotler M. APOBEC3 cytidine deaminases in double-strand DNA break repair and cancer promotion. Cancer Res. 2013; 73:3494-3498.
12. Alexandrov LB, Nik-Zainal S, Wedge DC, *et al*. Signatures of mutational processes in human cancer. Nature. 2013; 500:415-421.
13. Li T, Fu J, Zeng Z, Cohen D, Li J, Chen Q, Liu XS. TIMER2.0 for analysis of tumor-infiltrating immune cells. Nucleic Acids Res. 2020; 48:W509-W514.
14. Rhodes DR, Kalyana-Sundaram S, Mahavisno V, Varambally R, Yu J, Briggs BB, Barrette TR, Anstet MJ, Kincead-Beal C, Kulkarni P, Varambally S, Ghosh D, Chinnaiyan AM. Oncomine 3.0: Genes, pathways, and networks in a collection of 18,000 cancer gene expression profiles. Neoplasia. 2007; 9:166-180.
15. Tang Z, Kang B, Li C, Chen T, Zhang Z. GEPIA2: An enhanced web server for large-scale expression profiling and interactive analysis. Nucleic Acids Res. 2019; 47:W556-W560.
16. Uhlen M, Zhang C, Lee S, *et al*. A pathology atlas of the human cancer transcriptome. Science. 2017; 357:eaan2507.
17. Ru B, Wong CN, Tong Y, Zhong JY, Zhong SSW, Wu WC, Chu KC, Wong CY, Lau CY, Chen I, Chan NW, Zhang J. TISIDB: An integrated repository portal for tumor-immune system interactions. Bioinformatics. 2019; 35:4200-4202.
18. Zhou J, Du Y, Lu Y, Luan B, Xu C, Yu Y, Zhao H. CD44 expression predicts prognosis of ovarian cancer patients through promoting epithelial-mesenchymal transition (EMT) by regulating snail, ZEB1, and caveolin-1. Front Oncol. 2019; 9:802.
19. Liu W, Wu J, Yang F, *et al*. Genetic polymorphisms predisposing the interleukin 6-induced APOBEC3B-UNG imbalance increase HCC risk *via* promoting the generation of APOBEC-signature HBV mutations. Clin Cancer Res. 2019; 25:5525-5536.
20. Middlebrooks CD, Banday AR, Matsuda K, *et al*. Association of germline variants in the APOBEC3 region with cancer risk and enrichment with APOBEC-signature mutations in tumors. Nat Genet. 2016; 48:1330-1338.
21. Vartanian JP, Guetard D, Henry M, Wain-Hobson S. Evidence for editing of human papillomavirus DNA by APOBEC3 in benign and precancerous lesions. Science. 2008; 320:230-233.
22. Roberts SA, Lawrence MS, Klimczak LJ, Grimm SA, Fargo D, Stojanov P, Kiezun A, Kryukov GV, Carter SL, Saksena G, Harris S, Shah RR, Resnick MA, Getz G, Gordenin DA. An APOBEC cytidine deaminase mutagenesis pattern is widespread in human cancers. Nat Genet. 2013; 45:970-976.
23. Hoopes JI, Cortez LM, Mertz TM, Malc EP, Mieczkowski PA, Roberts SA. APOBEC3A and APOBEC3B preferentially deaminate the lagging strand template during DNA replication. Cell Rep. 2016; 14:1273-1282.
24. Burns MB, Temiz NA, Harris RS. Evidence for APOBEC3B mutagenesis in multiple human cancers. Nat Genet. 2013; 45:977-983.
25. Warren CJ, Xu T, Guo K, Griffin LM, Westrich JA, Lee D, Lambert PF, Santiago ML, Pyeon D. APOBEC3A functions as a restriction factor of human papillomavirus. J Virol. 2015; 89:688-702.
26. Vieira VC, Leonard B, White EA, Starrett GJ, Temiz NA, Lorenz LD, Lee D, Soares MA, Lambert PF, Howley PM, Harris RS. Human papillomavirus E6 triggers upregulation of the antiviral and cancer genomic DNA deaminase APOBEC3B. mBio. 2014; 5:e02234-14.
27. Hashemi M, Moazeni-Roodi A, Taheri M. Association of APOBEC3 deletion with cancer risk: A meta-analysis of 26 225 cases and 37 201 controls. Asia Pac J Clin Oncol.

2019; 15:275-287.
28. Du Y, Tao X, Wu J, Yu H, Yu Y, Zhao H. APOBEC3B up-regulation independently predicts ovarian cancer prognosis: A cohort study. Cancer Cell Int. 2018; 18:78.
29. Chen X, Song E. Turning foes to friends: Targeting cancer-associated fibroblasts. Nat Rev Drug Discov. 2019; 18:99-115.
30. Steven A, Seliger B. The role of immune escape and immune cell infiltration in breast cancer. Breast Care (Basel). 2018; 13:16-21.
31. Pauza CD, Liou ML, Lahusen T, Xiao L, Lapidus RG, Cairo C, Li H. Gamma delta T cell therapy for cancer: It is good to be local. Front Immunol. 2018; 9:1305.
32. Zheng T, Chen S, Zhang D. Effects of human APOBEC3A on biological behaviors of cervical cancer Hela cells. Zhong Shan Da Xue Xue Bao Yi Xue Ban. 2014; 35:371-377. [in Chinese]
33. Obermair A, Gebski V, Frumovitz M, Soliman PT, Schmeler KM, Levenback C, Ramirez PT. A phase III randomized clinical trial comparing laparoscopic or robotic radical hysterectomy with abdominal radical hysterectomy in patients with early stage cervical cancer. J Minim Invasive Gynecol. 2008; 15:584-588.

Received October 29, 2022; Revised January 19, 2023; Accepted March 3, 2023.

Address correspondence to:
Yan Du, Clinical Research Unit, Obstetrics and Gynecology Hospital of Fudan University, No. 128 Shenyang Road, Shanghai, China 200090.
E-mail: sophiedu_61@163.com

Ling Wang, Laboratory for Reproductive Immunology, Obstetrics and Gynecology Hospital of Fudan University, 419 Fangxie Road, Shanghai, China 200011.
E-mail: dr.wangling@fudan.edu.cn

Released online in J-STAGE as advance publication March 9, 2023.

Original Article

DOI: 10.5582/ddt.2022.01119

Skin properties of itching without symptoms and associated factors among older adults in long-term care facilities

Dianis Wulan Sari[1,2,*], Takeo Minematsu[3,4,5], Mikako Yoshida[6], Aya Kitamura[1,4], Sanai Tomida[1], Masatoshi Abe[7], Uswatun Khasanah[8], Hiromi Sanada[1,4,5,*]

[1] Department of Gerontological Nursing/Wound Care Management, the University of Tokyo, Tokyo, Japan;
[2] Faculty of Nursing, Universitas Airlangga, Surabaya, Indonesia;
[3] Department of Skincare Science, the University of Tokyo, Tokyo, Japan;
[4] Global Nursing Research Center, Graduate School of Medicine, The University of Tokyo, Tokyo, Japan;
[5] Ishikawa Prefectural Nursing University, Ishikawa, Japan;
[6] Department of Women's Health Nursing & Midwifery, Tohoku University Graduate School of Medicine, Miyagi, Japan;
[7] Sapporo Skin Clinic, Sapporo, Hokkaido, Japan;
[8] Faculty of Health Science, Universitas Islam Negeri Syarif Hidayatullah Jakarta, Tangerang selatan, Indonesia

SUMMARY Since itching without rash frequently among older adults' population, study about skin properties of itching without rash is important to develop prevention methods. Therefore, this study explored the skin properties related to itching without rash and the factors associated with them. A correlation, predictive designs study was conducted at Indonesian Long-term Care (LTC) facilities. Skin properties including skin barrier function and skin inflammation were examined by photographs (macroscopic and microscopic), stratum corneum (SC) hydration, skin Potential of Hydrogen (pH), and skin blotting. Itching experience and skincare behavior were obtained by questionnaire. The itching-related skin properties and associated factors were analyzed. A total of 405 residents participated in this study, with mean age was 74 years. The prevalence of itching on the whole body was 69.1%, and 50.3% of those manifesting itching on the left forearm involved itching without macroscopic abnormalities (itching without rash). SC hydration, skin pH, albumin and nerve growth factor β (NGFβ) were associated with itching without rash (p = 0.007, 0.012, < 0.001, and < 0.001, respectively). Additionally, factors associated with skin properties were age, sex, sun exposure experience, skincare, and hygiene care in the linear regression analysis. Measurement of skin biomarkers using skin blotting was a possible objective measurement of itching skin properties without rash regardless of the environmental condition.

Keywords Health service, hygiene care, health care quality, itching, long-term care, prevalence

1. Introduction

Itching is a predominant skin symptom in older adults (*1-3*). While these adults who suffer from itching can express the need for treatment and skincare, those with cognitive impairment have difficulty expressing their discomfort. Health workers in long-term care (LTC) must detect itching from the skin appearance in such cases. Itching can be due to dermatological diseases (*4*) but may also occur without macroscopic skin abnormalities, making them difficult to be assessed in bedridden patients.

Appropriate treatment requires valid skin examination (*5*). There is an objective skin assessment technique to measure skin properties (*6*). A study on the validity of skin blotting to test for the presence of itchy skin found that albumin, nerve growth factor β (NGFβ), and thymic stromal lymphopoietin (TSLP) are associated with itching (*7*). However, the association of these skin blotting biomarkers with itchy skin without rash needs to be examined.

Early detection of skin conditions will help health workers to cure and prevent severe itching (*8*). Knowledge of the factors associated with the skin properties of itchy skin without rash is also important for planning preventative measures. Therefore, we conducted a dermato-epidemiological study of itchy skin to determine measures to prevent itching.

As the triggers of itching differ among inflammation types, we planned to separately assess itching without rash-associated factors of each inflammation type and skin barrier functionality to identify intervention targets

for preventing itching without rash. Previous studies have reported an association between itching and factors such as age, sweat, sun exposure, season, and systemic disease (*9-12*). However, existing studies have focused on the general population and general itching but did not examine the factors associated with the properties of itchy skin.

This study aims to examine the properties and associated factors of itchy skin without rash, including skin barrier function and inflammation status, in older adults at LTC facilities in Indonesia.

2. Materials and Methods

2.1. Study design and setting

This study used a correlative, predictive design. It clarified itching without rash among the older adult population (prevalence, skin properties, and factors related to those skin properties). The participant was older adults who stayed at three LTCs in Indonesia between January and September 2016. The current study was analyzed and reported after we confirmed the validity of skin blotting examination to detect itching on the skin of older adults (*7*). These facilities provide accommodation for physically and cognitively relative normal older adults and are funded by the government.

2.2. Study participants

All residents of the three LTCs constituted the study population. For sample size, we performed a power analysis based on the effect size of itchy skin in the preliminary study (alpha = 0.05, power = 0.80), along with the number of study variables. We recruited all older adults at the three LTCs to account for attrition. The inclusion criterion was age ≥ 65 years. The exclusion criteria were difficulty in communicating; clinically inappropriate (*e.g.*, severe illness, total paralysis); memory difficulties; and participation in the preliminary study. A preliminary study was conducted among 35 older adults to confirm the research protocols, tools, and skin examinations.

All participants received an explanation of the study. Participants were told not to bathe or perform ablution 30 minutes before the skin examination and not to use skincare/ointment products on that day. Residents in the LTC receive equal daily care, while residents who need medical treatment are transferred to the hospital.

2.3. Measurements

Measurement was conducted using the cross-sectional method. Data collection was performed by certified wound, ostomy, and continence nurse researchers. The nurse researcher was trained to perform skin blotting and other skin examinations.

The study protocol was approved by the Research Ethics Committee of the Graduate School of Medicine, the University of Tokyo (11076). All procedures followed the Declaration of Helsinki. The presence of adverse events of skin examination was confirmed the day after. The principal investigator conducted the interviews and skin measurements. The researcher explained the study protocol and obtained written informed consent from all participants.

2.4. Investigation of itching

Information regarding itching was collected through a questionnaire based on the guidelines of the International Forum for the Study of Itch (*13*). We defined itching as the sensation of needing to scratch the skin. The questionnaire included the body parts affected (forearm, back, thighs, chest, legs, abdomen, instep, fingers, palm, groin), frequency of itching (daily, weekly, monthly), length/duration of daily itching (< 6, 6-12, and > 12 h/day), intensity (mild, moderate, and severe), sensation of itching (pure itching, stinging, burning, mixed sensation), and scratch response to itching (rubbing, squeezing, skin pinching).

2.5. Classification of itching

The dermatologist diagnosed the skin disease based on the interview data and skin photographs (macroscopic and microscopic). In patients with itching, clinical signs such as scaly areas, inflammation, swelling, rash, leathery patches, crusting, visible sweat ducts, and dark colored patches of skin were assessed. The dermatologist defined normal skin, itching without rash, or other skin diseases such as xerosis, prurigo, miliaria, or eczema. The term "itching without rash" was used when participants who complained of itchy skin but had no skin signs while the term "normal skin" was used when the participants had no clinical signs or itching symptoms.

2.6. Skin properties

Skin property examinations, including macroscopic and microscopic examination, stratum corneum (SC) hydration and skin Potential of Hydrogen (pH) measurement, and skin blotting, were performed to evaluate skin inflammation and barrier function. We examined the skin on the outer side of the left forearm between the elbow and wrist. The selection of skin examination site was based on the skin blotting reliability and validity in a previous studies (*7*,*14*).

Details of the skin examination procedure have been described elsewhere (*7*). Briefly, macroscopic examination using a digital camera (Samsung, Seoul, KOR) and microscopic examination (3R Systems, Fukuoka, JP) were performed. Photographs were taken three times for each forearm and included color charts.

From the photos and participants' itch symptoms, a dermatologist and certified wound, ostomy, and continence nurse researcher made the diagnoses. The participant data were blinded to the skin blotting results, without names. We diagnosed the skin for itch without abnormal skin appearance or with abnormalities such as dry skin, eczema, miliaria, or prurigo.

After skin photography, we measured SC hydration and skin pH, SC hydration was measured using mobile skin moisture (Courage+Khazaka Electronic GmbH, Cologne, DE) and skin pH using Skincheck1 (Hanna Instruments, Woonsocket, RI). These measurements were performed three times, and the mean of those examinations was used. The mobile skin moisture was attached to the measurement site until a value appeared on the screen. Higher SC hydration levels indicated good skin moisture and skin barrier function (*15*). To measure skin pH, the Skincheck^{TM}1 was attached to the measurement site after dipping in a neutral solution. The skin pH value is displayed on the screen. A natural skin surface was indicated by lower skin pH (4.7-< 5) (*16*).

For skin blotting, the biomarkers were albumin for skin barrier function (*17*), nerve growth factor β (NGFβ) for epidermal inflammation (*18*), interleukin (IL) 2 for Th1 inflammation (*19*) and TSLP for Th2 inflammation (*20*). The presence of those biomarkers on the blotting membrane has been validated previously (*7,14,17,21,22*). We confirmed the validity of skin blotting for measuring albumin and NGFβ to detect itching of the skin in older adults (*7*).

Skin blotting was developed as an objective skin assessment technique to measure skin biomarkers (*6*). To prepare the skin blotting kit, a piece of 1-cm square nitrocellulose membrane (Bio-Rad Inc., Hercules, CA) was attached with filter paper, gentle medical adhesive tape (Nitoms, Inc., Tokyo, JP), and adhesive tape. To attach the skin blot to the skin, a skin blotting kit pre-wetted with 50 µL of normal saline was attached with medical tape to the measurement site for 10 min. Participants were asked to limit movement of the measurement site. Thereafter, the blot was removed from the skin with a minimal stimulus. Then skin blotting kit was attached to filter paper. The collected membranes were kept dry and stored at 4°C until staining (*6*).

For skin blotting analysis, we analyzed biomarkers for albumin, NGFβ, IL2, and TSLP. Skin blotting membrane was divided into two pieces, and each piece was subjected to immunological double staining according the host of antibodies. Therefore, we performed double staining for albumin (American Qualex Inc., San Clemente, CA) and NGFβ (Abcam Plc., Cambridge, UK) or TSLP (R&D Systems, Minneapolis, MN) and IL2 (Cell Signaling Technology, Inc., Danvers, MA) after blocking using Blocking One (Nacalai Tesque, Kyoto, JP).

Before staining, we confirmed the antibody reaction's reactivity, specificity, and linearity using dot blot and western blot samples. We used different amounts (0.2-200 ng) of full-length recombinant proteins for dot blot examination and cell lysate or tissue homogenate, including the target proteins, for western blot examination. We used only those antibodies whose specificity and dose-dependent immunoreactivity was confirmed in these examinations. Direct method using appropriate secondary antibodies labelled with peroxidase was used to detect albumin, while NGFβ, IL2, and TSLP using indirect method.

We used SNAP i.d. 2.0 Protein Detection System (Merck Millipore, Billerica, MA) for immunostaining procedures. Then, immunoreactivity was visualized using chemiluminescent substrates for alkaline phosphatase (BioFX Laboratories, Owings Mills, MD) and peroxidase (Merck Millipore, Billerica, MA). Thereafter, a chemiluminescence imaging system (Liponics Inc., Tokyo, JP) was used to capture the signal. All process of immunostaining was conducted by a professional laboratory staff.

Biomarker levels on the skin blot were quantified using ImageJ image analysis software (National Institutes of Health, Bethesda, MD). ImageJ separated the pictures into red, green, blue (RGB) color images. Then, the overlaying of corresponding bright field images by GNU Image Manipulation Program 2.6.5 was used to measure the area. The level of biomarker protein secretion was identified based on the signal intensity level on the skin blotting membrane using ImageJ. Skin blotting pictures were normalized with that of the positive control.

2.7. Participant characteristics and skincare behaviors

These were obtained through the questionnaires and medical records. Participant characteristics included age, sex, body mass index (BMI), literacy, cumulative lifetime sun exposure at work, and activities of daily living (ADL) using the Barthel Index (*23*,*24*). The cumulative lifetime sun exposure at work was calculated from the average daily sun exposure (hours) across 365 days for the total years of work (*25*).

Skincare behavior (current and past) included bathing frequency and duration, body washing while bathing, clothing change frequency, and clothing type and material. Data on prevalence and experience of itching were collected using a questionnaire based on the International Forum for the Study of Itching guideline (*13*).

2.8. Statistical analysis

The prevalence of itching was described using frequency distributions and measures of central tendency. To confirm the skin properties of itchy skin without rash, we classified participants into 'itching without rash' and 'normal skin' groups. The Mann-Whitney *U* test was

used to compare skin properties between the groups. The Kruskal-Wallis and Mann-Whitney *U* tests were used to measure the association between participant characteristics and skin properties for categorical and continuous variables, respectively.

To predict the associated factors of skin properties of itching without rash, multiple linear regression analyses were performed using skin properties as the dependent variable. Variables were simultaneously entered in the models based on the literature review; variables with $p \leq 0.05$ in univariate analysis were considered significant. A multicollinearity test was conducted before the variables were entered in the models, and the variance inflation factor was calculated. All analyses were performed using SPSS ver. 26 for Windows (IBM corp., Armonk, USA), and $p < 0.05$ was considered statistically significant.

3. Results

3.1. Participant characteristics and skincare behaviors

A total of 469 eligible residents were available in LTCs. We excluded 64 older adults because of severe psychological conditions, hospitalization, communication disorders, an inability to speak Indonesian or Java, and participation in a preliminary study. Of the remaining 405 residents (response rate = 96.5%), 14 declined to participate, so 391 participants were included.

As shown in Table 1, the mean age was 74 years and 61.6% were female. The proportion of independent older adults was 66.8%. For skincare behavior, 30.2% of participants had a skincare routine before moving into the LTC, with only 10.2% continuing thereafter. Overall, 49.9% bathed ≥ 2 times/day, while 63.9% changed their clothes ≤ 1 time/day, implying that they wore the same clothing during the day and night.

For the prevalence of itching, 69.1% had itching symptoms, which occurred mainly on the forearms (43.7%), back (40.7%), and thighs (34.8%). Older adults who reported forearm itching (n = 171) experienced it daily (95.9%).

Table 1. Participant characteristics (n = 391)

Items	Mean ± SD or n (%)
Demographic factors	
Age (years)	74.3 ± 7.3
Sex (male)	241 (61.6)
BMI (kg/m^2)	21.2 ± 3.3
Barthel Index, (independent)	261 (66.8)
Literate (yes)	172 (44.0)
Cumulative lifetime sun exposure at work (hours)	79.210.1 ± 28.072.4
Skincare behaviors	
Past skincare regimen (yes)	118 (30.2)
Current skincare regimen (yes)	40 (10.2)
Bathing frequency (≥ 2 times/day)	195 (49.9)
Bathing duration (≥ 5 minutes)	299 (76.5)
Wash body while bathing (yes)	308 (78.7)
Clothing change frequency (≤ 1 time/day)	250 (63.9)
Clothing type (short sleeves)	344 (88.0)
Clothing material (cotton)	377 (96.4)
Itching experience*	
Itching perception on any part of body (yes)[†]:	270 (69.1)
Forearm	171 (43.7)
Back	159 (40.7)
Thighs	136 (34.8)
Chest	126 (32.2)
Legs	114 (29.2)
Abdomen	110 (28.1)
Instep	102 (26.1)
Fingers	99 (25.3)
Palm	101 (25.8)
Groin	85 (21.7)
Experience of left forearm itch [‡] (n = 171)	
Frequency (daily)	164 (95.9)
Duration of symptoms (> 12 h/day)	69 (40.4)
Intensity (moderate)	87 (50.9)
Sensory (pure itching)	155 (90.6)
Scratch response (rubbing)	169 (98.8)

BMI, Body Mass Index; SD, Standard deviation. * One participant had more than one itchy skin area. [†]Prevalence of itching in older adults. [‡]The complete skin examination was conducted on the left forearm: Frequency (daily, weekly, monthly), Duration of symptoms (< 6 h/d, 6-12 h/d, > 12 h/d), Intensity (mild, moderate, severe), Sensory (pure itching, stinging, burning, mixed sensation), Scratch response (rubbing, squeezing, pinching the skin).

Table 2. Skin diagnosis on left forearm by a dermatologist*

Items	Itching symptoms n (%)	
	No (n = 226)	Yes (n = 165)
Normal skin	193 (85.4)	0 (0)
Itching without rash	0 (0)	83 (50.3)
Xerosis	17 (7.5)	30 (18.2)
Eczema	4 (1.8)	44 (26.7)
Others[†]	12 (5.3)	8 (4.8)

* The dermatologist diagnosed the skin on the left forearm based on skin photographs (macroscopic and microscopic) and itching symptoms. For example, a participant had itching on their left forearm without skin signs. A dermatologist then diagnosed 'itching without rash'. [†]Other skin diseases: prurigo, miliaria, dry skin.

3.2. Skin diagnosis and itching symptoms

Table 2 shows the left forearm diagnosis by a dermatologist. There were 193 participants who did not report itching and were diagnosed as having normal skin on forearm (Figure 1a). Of the 165 participants who reported left forearm itching, 50.3% were diagnosed with itching without rash on forearm (Figure 1b) and 49.7% with other skin diseases because itching was accompanied by clinical signs on forearm (Figure 1c).

3.3. Itching-related skin properties

To identify the specific skin properties associated with itching without rash, we compared the properties between participants who had itching without rash and those with normal skin (Table 3). We excluded skin with other diseases (n = 115). Participants with itching without rash had significantly higher skin pH, albumin,

and NGFβ (p = 0.012, < 0.001, < 0.001, respectively), and significantly lower SC hydration (p = 0.007) than those with normal skin.

3.4. Factors associated with skin properties of itching without rash

Differences in SC hydration, skin pH, and skin blotting findings based on the participants' characteristics were analyzed using univariate analysis (data not shown). The following associations were observed: SC hydration with past skin care (p = 0.001), bathing frequency (p = 0.002), bathing duration (p = 0.035), clothing change frequency (p = 0.038), and clothing type (p = 0.011); skin pH with past skin care (p = 0.018), bathing frequency (p = 0.004), and clothing change frequency (p = 0.031); albumin level with cumulative lifetime sun exposure at work (p = 0.046), past skin care (p < 0.001), bathing frequency (p < 0.001), and clothing type (p = 0.002); and NGFβ level with cumulative lifetime sun exposure at work (p = 0.002), past skin care (p < 0.001), bathing frequency (p = 0.012), and bathing duration (p = 0.016).

In the multiple linear regression model (Table 4), the following associations were observed: SC hydration with clothing change frequency (β = 0.135, p = 0.029) and clothing type (β = − 0.139, p = 0.021); skin pH with clothing change frequency (β = − 0.137, p = 0.029); albumin level with age (β = − 0.130, p=0.044); and NGFβ with cumulative lifetime sun exposure at work (β = 0.145, p = 0.026) and bathing duration (β = − 0.151, p = 0.022).

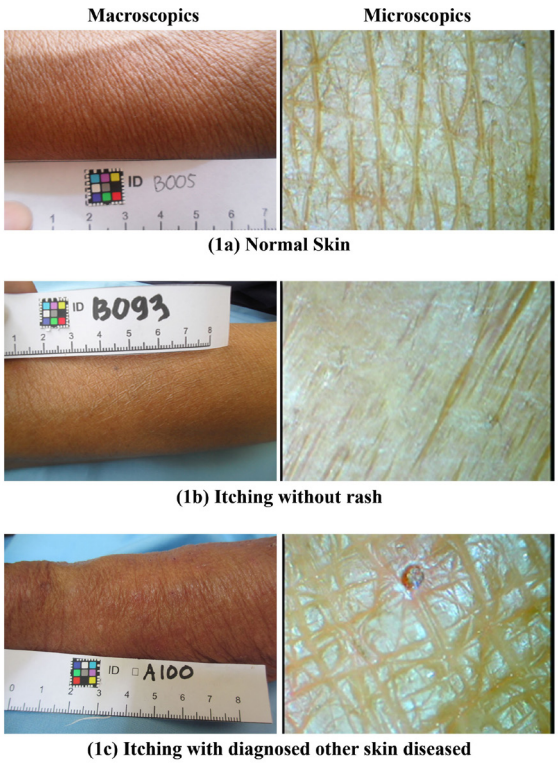

Figure 1. Macroscopic and microscopic photographs of forearm. (**a**). Normal skin: macroscopic photograph sample from participants without itching symptoms and skin disease signs. The microscopic photograph shows good skin structure, *i.e.*, skin with hair and sweat glands, clear skin triangle line, and no scales. (**b**). Itching without rash: macroscopic photograph sample from participants with itching symptoms but no skin disease signs, *i.e.*, no rash. The microscopic photograph shows bad skin structure, *i.e.*, skin without hair and sweat glands, and no skin triangle line, but no scales. (**c**). Itching with other skin diseases: microscopic photograph sample from participants with itching symptoms and skin disease signs. In this case, a dermatologist diagnosed eczema. The microscopic photograph shows bad skin structure, *i.e.*, skin without hair and sweat glands, unstructured skin triangle line, and with scales.

4. Discussion

This study evaluated albumin and NGFβ levels using skin blotting as a novel method of assessing itching without rash. This contributes to understanding the pathophysiology of itching in older adults. High albumin and NGFβ levels indicated disrupted skin barrier function and epidermal inflammation associated with itching without rash. Furthermore, the association of albumin and NGFβ with bathing emphasized the importance of skincare and hygiene in keeping the skin healthy and preventing itching in older adults.

The prevalence of itching in this study was 69.1%. The prevalence of itching in older adults was reported to be 6-42% in western countries (*1*). The relatively higher prevalence in this study was probably due to environmental conditions and racial skin property differences between western and Asian people (*26*). This study was conducted in a tropical region on the equator, with high temperatures and long sun exposure

Table 3. Comparison of skin properties between the itching without rash and normal skin groups (n = 276)

Items	Median (Range)		p-value
	Itching without rash (n = 83)	Normal skin (n = 193)	
SC hydration	66.0 (47.7-86.3)	76.3 (59.8-89.8)	0.007
Skin pH	5.0 (4.6-5.7)	4.8 (4.4-5.2)	0.012
Albumin (ng), n = 257	284.1 (206.2-536.4)	201.6 (145.8-265.3)	< 0.001
IL2 (pg)	337.8 (261.8-401.5)	334.2 (263.6-425.1)	0.654
NGFβ (ng)	276.0 (207.7-393.0)	209.1 (161.9-332.2)	< 0.001
TSLP (ng), n = 257	2.1 (1.7-2.4)	2.0 (1.8-2.3)	0.900

SC, Stratum corneum; IL2, Interleukin 2; NGFβ, Nerve growth factor β; TSLP, Thymic stromal lymphopoietin. Differences were compared using the Mann–Whitney U test.

Table 4. Multiple linear regression analysis predicting associated factors of skin properties of itching without rash

Items	SC hydration (n = 276)		Skin pH (n = 276)		Albumin (n = 257)		NGFβ (n = 276)	
	β	*p*	*β*	*p*	*β*	*p*	*β*	*p*
Age (years)	0.020	0.746	0.106	0.087	-0.130	0.044	-0.055	0.378
Sex	0.075	0.220	-0.084	0.177	0.061	0.341	0.031	0.620
Body mass index (kg/m^2)	0.077	0.193	-0.049	0.411	0.057	0.358	0.014	0.823
Barthel Index	-0.028	0.668	0.061	0.353	0.081	0.237	-0.024	0.716
Cumulative lifetime sun exposure at work (hours)	0.045	0.479	-0.013	0.837	0.118	0.076	0.145	0.026
Current skincare regimen	0.026	0.678	-0.067	0.282	-0.023	0.727	-0.039	0.533
Bathing frequency	0.109	0.094	-0.059	0.368	-0.134	0.051	-0.040	0.546
Bathing duration	0.098	0.129	-0.038	0.557	-0.054	0.423	-0.151	0.022
Clothing change frequency	0.135	0.029	-0.137	0.029	0.116	0.072	-0.003	0.958
Clothing type	-0.139	0.021	0.092	0.130	0.056	0.370	0.015	0.806
R^2	0.092		0.077		0.082		0.058	
Adjusted R^2	0.058		0.042		0.045		0.023	
P	0.004		0.017		0.018		0.095	

SC, Stratum corneum; NGFβ, Nerve growth factor β. Sex: 0 = Male, 1 = Female, Cumulative lifetime sun exposure at work (hours): 0 = ≤100,000 h, 1 = ≥ 100,001, Bathing frequency: 0 = ≤ 1 time/day, 1 = ≥ 2 times/day, Bathing duration: 0 = ≤ 5 minutes, 1 = > 5 minutes, Clothing change frequency: 0 = ≤ 1 time/day, 1 = ≥ 2 times/day, Clothing type: 0 = Long sleeves, 1 = Short sleeves. β: standardized partial regression coefficients; R2: coefficients of determination.

throughout the year. The residents have therefore experienced relatively long sun exposure, resulting in photoaging. Skin stimulated by sunlight releases histamine in epidermal cells (*10*), which may contribute significantly to skin inflammation and itching (*27*). More than half the cases of itchy skin in this study were diagnosed as itching without rash. Itching without rash shows no macroscopic abnormalities; therefore, caregivers overlook itching symptoms in older adults, especially if the affected individuals cannot report it themselves. Thus, these results emphasize the importance of an objective assessment tool for itching without rash in older adults.

Skin pH, SC hydration, and albumin levels in skin blot are indicators of skin barrier functionality (*17,28*). As they were all associated with itching without rash, they are candidate tools for its objective assessment. The skin barrier consists of sebum, a corneocyte lipid envelope, and tight junctions of the stratum granulosum. Sebum, the lipid-rich substance secreted from the sebaceous glands, forms a hydrophobic thin layer on the skin's surface. Skin commensal bacteria hydrolyze sebum and release free fatty acids. As a result, the skin surface is kept in an acidic state to prevent the growth of pathogenic microbes (*29*). The corneocyte lipid envelope consists of ceramide and fatty acids and forms a lamellar structure overlying the water and lipid layers to restrict water and electrolyte leakage and prevent irritant invasion (*30*). The tight junction in the stratum granulosum plays an important role in the selective permeability of substances, including albumin (*31*).

However, in this study, skin pH and SC hydration findings did not indicate impaired skin barrier function. These results were similar to those previously reported in healthy skin, although the results in the itching without rash group were significantly different from those in the normal skin group in this study (*28,32*). Lower SC hydration and higher skin pH significantly correlated with a low clothing change frequency and use of short sleeves. Skin with hair, scales, and sweat glands was significantly correlated with low cumulative lifetime sun exposure, doing skin care, low bathing frequency, and low clothing change frequency. These correlations suggested that stimulation with sweat, water, and sun exposure induced itching without rash (*33*). In contrast, skin blotting showed higher albumin levels in the itching without rash group than in the normal skin group, suggesting that this method could evaluate skin barrier function appropriately regardless of environmental conditions.

Invisible skin inflammatory status was evaluated by skin blotting using NGFβ, IL2, and TSLP levels. NGFβ is a marker for epidermal inflammation, while IL2 and TSLP are markers of Th1-type and Th2-type inflammation, respectively. A higher NGFβ level was significantly related to the presence of itching without rash, whereas no significant difference was found between itchy skin without rash and normal skin in IL2 and TSLP. NGFβ upregulates neuropeptides, especially substance P (SP) and calcitonin-gene-related peptide, in adult rat primary sensory neurons (*34*). Neuropeptides are involved in hypersensitivity itch sensation, and neurogenic inflammation also causes skin scratching (*35*). Furthermore, factors associated with a higher NGFβ level were bathing duration and cumulative lifetime sun exposure at work. These results suggest that itching without rash is induced by water exposure during hygiene care (aquagenic pruritus) (*36*) and sun exposure induces cutaneous inflammation (*35*). Hypo-osmotic shock by water exposure leads to cellular damage in the epidermis, and keratinocytes release NGFβ, inducing the elongation of C nerve fibers in the epidermis and resulting in hypersensitive itching (*18*,*37*). Our findings showed that the skin blotting examination of NGFβ is a

possible assessment tool for itching without rash.

In this study, the multiple linear regression model analysis revealed the association of skin properties of itching without rash with sun exposure, bathing frequency, bathing duration, and clothing change frequency. These findings implied the importance of skincare and hygiene care for preventing itching without rash. Future studies should be based on longitudinal designs to test the association direction and further potential presence of itching without rash.

Certain limitations of this study should be mentioned. First, this study was conducted in LTCs in a city without randomizing selection. Nevertheless, we assumed that public LTCs have the same standard of care, thereby reducing bias due to non-randomization. Second, for participants without itching on their forearm, we performed skin examinations only on the left forearm. In the previous study, we confirmed that normal skin on both forearms have similar skin properties (*7*,*14*).

In conclusion, the prevalence of itching was 69.1%, and approximately half these cases were diagnosed as itching without rash. Albumin and NGFβ in skin blotting, SC hydration, and skin pH were significantly correlated with itching without rash. The skin properties of pruritic skin were significantly correlated with skincare; hygiene care practices, including bathing and changing clothes; and aging and sun exposure. However, further studies are needed to reveal which skincare regimes and maximum duration of water exposure are compatible with hygiene care for older adults' skin. Measurement of albumin and NGFβ levels using skin blotting was identified as an objective and non-invasive assessment method. Thus, albumin and NGFβ are appropriate biomarkers for itching without rash.

Acknowledgements

We are grateful to Indonesian government for giving permission us in data collection at LTC. The author also expresses gratitude to all of participants who took part in this study.

Funding: This work was supported by Japan Society for the Promotion of Science KAKENHI Grant Numbers 15H05066; and the Indonesia Endowment Fund for Education (LPDP). Grant do not have involvement in study design, data collection, analysis, interpretation, and writing of this paper.

Conflict of Interest: Prof. Takeo Minematsu belong to a department that receives financial support from Saraya Corporation, however, this company did not have any concern in this study.

References

1. Weisshaar E, Dalgard F. Epidemiology of itch: adding to the burden of skin morbidity. Acta Derm Venereol. 2009; 89:339-350.
2. Cowdell F, Dyson J, Long J, Macleod U. Self-reported skin concerns: An epidemiological study of community-dwelling older people. Int J Older People Nurs. 2018; 13:e12195.
3. Hahnel E, Lichterfeld A, Blume-Peytavi U, Kottner J. The epidemiology of skin conditions in the aged: A systematic review. J Tissue Viability. 2017; 26:20-28.
4. Weisshaar E, Kallen U, Weiß M. "The itching hand" – important differential diagnoses and treatment. J Dtsch Dermatol Ges. 2013; 11:31-42.
5. National Clinical Guideline Centre (UK). The prevention and management of pressure ulcers in primary and secondary care. London; 2014.
6. Minematsu T, Horii M, Oe M, Sugama J, Mugita Y, Huang L, Nakagami G, Sanada H. Skin blotting: A noninvasive technique for evaluating physiological skin status. Adv Skin Wound Care. 2014; 27:272-279.
7. Sari DW, Minematsu T, Yoshida M, Noguchi-Watanabe M, Tomida S, Kitamura A, Abe M, Sanada H. Validity of skin blot examination for albumin and nerve growth factor β to detect itching of the skin in Indonesian older adults. J Tissue Viability. 2021; 30:42-50.
8. Golińska J, Sar-Pomian M, Rudnicka L. Haemorrhagic dots as a dermoscopic marker of itch severity in psoriasis. Australas J Dermatol. 2021; 62:e559-e562.
9. Murota H, Katayama I. Exacerbating factors of itch in atopic dermatitis. Allergol Int. 2017; 66:8-13.
10. Malaviya R, Morrison AR, Pentland AP. Histamine in human epidermal cells is induced by ultraviolet light injury. J Invest Dermatol. 1996; 106:785-789.
11. Garibyan L, Chiou AS, Elmariah SB. Advanced aging skin and itch: Addressing an unmet need. Dermatol Ther. 2013; 26:92-103.
12. Dickison P, Swain G, Peek J, Smith S. Itching for answers: Prevalence and severity of pruritus in psoriasis. Australas J Dermatol. 2017; 79:AB172.
13. Elke W, Uwe G, Jörg K, Masutaka F, Hidehisa S, Gil Y. Questionnaires to assess chronic itch: a consensus paper of the special interest group of the international forum on the study of itch. Acta Derm Venereol. 2012; 92:493-496.
14. Koyano Y, Nakagami G, Minematsu T, Sanada H. Reliability of the skin blotting method when used on the elderly. Int Wound J. 2018:807-813.
15. Ya-Xian Z, Suetake T, Tagami H. Number of cell layers of the stratum corneum in normal skin - relationship on the anatomical location an the body, age, sex and physical parameters. Arch Dermatol Res. 1999; 291:555-559.
16. Lambers H, Piessens S, Bloem A, Pronk H, Finkel P. Natural skin surface pH is on average below 5, which is beneficial for its resident flora. Int J Cosmet Sci. 2006; 28:359-370.
17. Tamai N, Minematsu T, Tsunokuni S, Aso K, Higashimura S, Nakagami G. Detection of albumin using skin blotting as a measure of skin barrier function. J Nurs Sci Eng. 2017; 4:116-120.
18. Kishi C, Minematsu T, Huang L, Mugita Y, Kitamura A, Nakagami G, Yamane T, Yoshida M, Noguchi H, Funakubo M, Mori T, Sanada H. Hypo-osmotic shock-induced subclinical inflammation of skin in a rat model of disrupted skin barrier function. Biol Res Nurs. 2015; 17:135-141.
19. Romagnani S. T-cell subsets (Th1 versus Th2). Ann Allergy Asthma Immunol. 2000; 85:9-18.

20. Ziegler SF, Roan F, Bell BD, Stoklasek TA, Kitajima M, Han H. The biology of thymic stromal lymphopoietin (TSLP). Adv Pharmacol. 2013; 66:129-155.
21. Nakai A, Minematsu T, Tamai N, Sugama J, Urai T, Sanada H. Prediction of healing in Category I pressure ulcers by skin blotting with plasminogen activator inhibitor 1, interleukin-1α, vascular endothelial growth factor C, and heat shock protein 90α: A pilot study. J Tissue Viability. 2019; S0965-206X:30051-2.
22. Minematsu T, Dai M, Tamai N, *et al*. Risk scoring tool for forearm skin tears in Japanese older adults: a prospective cohort study. J Tissue Viability. 2021; 30:155-160.
23. Karsten K. Geriatric depression scale in Indonesian version. *https://web.stanford.edu/~yesavage/GDS.html*.
24. Yesavage JA, Brink TL, Rose TL, Lum O, Huang V, Adey M, Leirer VO. Development and validation of a geriatric depression screening scale: A preliminary report. J Psychiatr Res. 1982; 17:37-49.
25. Yu CL, Li Y, Freedman DM, Fears TR, Kwok R, Chodick G, Alexander B, Kimlin MG, Kricker A, Armstrong BK, Linet MS. Assessment of lifetime cumulative sun exposure using a self- administered questionnaire: reliability of two approaches. Cancer Epidemiol Biomarkers Prev. 2009; 18:464-471.
26. Wesley NO, Maibach HI. Racial (ethnic) differences in skin properties: The objective data. Am J Clin Dermatol. 2003; 4:843-860.
27. Shim WS, Oh U. Histamine-induced itch and its relationship with pain. Mol Pain. 2008; 4:1-6.
28. Zaniboni M, Samorano L, Orfali R, Aoki V. Skin barrier in atopic dermatitis: Beyond filaggrin. An Bras Dermatol. 2016; 19:265-278.
29. du Plessis J, Stefaniak A, Eloff F, John S, Agner T, Chou TC, Nixon R, Steiner M, Franken A, Kudla I, Holness L. International guidelines for the *in vivo* assessment of skin properties in non-clinical settings: part 2. transepidermal water loss and skin hydration. Skin Res Technol. 2013; 19:265-278.
30. Grice EA, Segre JA. The skin microbiome. Nat Rev Microbiol. 2013; 9:244-253.
31. Elias PM, Gruber R, Crumrine D, Menon G, Williams ML, Wakefield JS, Holleran WM, Uchida Y. Formation and functions of the corneocyte lipid envelope (CLE). Biochim Biophys Acta. 2014; 1841:314-318.
32. Lizaka S, Takehara K, Sanada H. Validation of a portable device for measuring stratum corneum hydration. J Jpn Wound Ostomy Continence Manag. 2015; 19:33-39.
33. Rittie L, Fisher GJ. Natural and sun-induced aging of human skin. Cold Spring Harb Perspect Med. 2015; 5:1-14.
34. Verge VMK, Richardson PM, Wiesenfeld-Hallin Z, Hokfelt T. Differential influence of nerve growth-factor on neuropeptide expression *in vivo*: A novel role in peptide suppression in adult sensory neurons. J Neurosci. 1995; 15:2081-96.
35. Eschenfelder CC, Benrath J, Zimmermann M, Gillardon F. Involvement of substance-P in ultraviolet irradiation-induced inflammation in rat skin. Eur J Neurosci. 1995; 7:1520-1526.
36. Bircher AJ, Meier-Ruge W. Aquagenic pruritus: Water-induced activation of acetylcholinesterase. Arch Dermatol. 1988; 124:84-89.
37. Yamamoto H, Ikeda M, Okajima Y, Okajima M. Electrolytic-reduction ion water induces ceramide synthesis in human skin keratinocytes. Drug Discov Ther. 2021; 15:248-253.

Received December 14, 2022; Revised April 23, 2023; Accepted April 27, 2023.

**Address correspondence to:*
Hiromi Sanada, Department of Gerontological Nursing/ Wound Care Management, the University of Tokyo, 7-3-1 Hongo, Bunkyo-ku, Tokyo 113-0033, Japan.
E-mail: hsanada@g.ecc.u-tokyo.ac.jp

Dianis Wulan Sari, Faculty of Nursing, Universitas Airlangga, Campus C, Mulyorejo, Surabaya 60115, Indonesia.
E-mail: dianis.wulan.sari@fkp.unair.ac.id

Released online in J-STAGE as advance publication May 11, 2023.

Brief Report

DOI: 10.5582/ddt.2023.01003

Docosahexaenoic acid contributes to increased CaMKII protein expression and a tendency to increase nNOS protein expression in differentiated NG108-15 cells

Daisuke Miyazawa*, Kinari Suzuki, Hikari Sato, Natsumi Katsurayama, Tomoko Tahira, Hideki Mizutani, Naoki Ohara

College of Pharmacy, Kinjo Gakuin University, Nagoya, Japan.

SUMMARY Docosahexaenoic acid (DHA; 22:6*n*-3), an *n*-3 polyunsaturated fatty acid, has various important roles in brain functions. Nitric oxide (NO) produced by neuronal NO synthase (nNOS) and Ca^{2+}/calmodulin-dependent protein kinase II (CaMKII) is also involved in brain functions. We investigated the influence of DHA on nNOS and CaMKII protein expression in differentiated NG108-15 cells. NG108-15 cells were seeded in 12-well plates, and after 24 h, the medium was replaced with Dulbecco's modified Eagle's medium containing 1% fetal bovine serum, 0.2 mM dibutyryl cyclic adenosine monophosphate and 100 nM dexamethasone as differentiation-inducing medium. When cells were cultured in differentiation-inducing medium, neurite-like outgrowths were observed on days 5 and 6. However, no significant difference in morphology was observed in cells with or without DHA treatment. With or without DHA addition, nNOS protein expression was increased on days 5 and 6 compared with day 0. This increase tended to be enhanced by DHA. CaMKII protein expression did not change after differentiation without DHA, but was significantly increased on day 6 compared with day 0 with DHA addition. These data indicate that DHA is involved in brain functions by regulating CaMKII and nNOS protein expression.

Keywords DHA, *n*-3 polyunsaturated fatty acids, neuronal cell, nNOS, CaMKII

1. Introduction

In the brain, nitric oxide (NO) plays important roles in neural development, neuroprotection, synaptic plasticity, long-term potentiation, learning, and memory (*1-4*). NO is synthesized from L-arginine by NO synthases (NOSs). Three NOS isoforms have been characterized, namely neuronal NOS (nNOS), endothelial NOS, and inducible NOS (*5,6*). In particular, nNOS has been found in neuronal tissue (*7,8*). The activity of this enzyme requires Ca^{2+} and calmodulin (*8*). Ca^{2+}/calmodulin-dependent protein kinase II (CaMKII) is highly expressed in the brain (*9-11*). Neuronal activation induces CaMKII to translocate from the cytoplasm to the active zone at presynaptic membranes and the postsynaptic density (*12,13*). Presynaptic CaMKII regulates neurotransmitter synthesis and release (*14*). CaMKII is an important protein of synaptic plasticity (*15*).

Polyunsaturated fatty acids are essential components of membrane lipids in the mammalian brain. Docosahexaenoic acid (DHA), an *n*-3 polyunsaturated fatty acid, is a phospholipid component of the cell membrane, which is particularly abundant in neuronal tissues and essential for neuronal functions including neurite outgrowth, synaptic plasticity, behavior, mood regulation, learning, and memory (*11,16-20*).

In this study, we examined the effect of DHA addition to differentiation-inducing medium on nNOS and CaMKII protein expression in the neuroblastoma - glioma hybrid cell line NG108-15.

2. Materials and Methods

2.1. Materials

NG108-15 cells were purchased from the American Type Culture Collection (Manassas, VA, USA). Cell culture medium and dexamethasone (DEX) were purchased from Fujifilm Wako (Osaka, Japan). Fetal bovine serum (FBS) was purchased from Gibco (Grand Island, NY, USA). Penicillin and streptomycin were purchased from Nacalai Tesque (Kyoto, Japan). HAT supplement (hypoxanthine, aminopterin, and thymidine, 50×) was purchased from MP biomedicals (Santa

Ana, CA, USA). DHA was purchased from Cayman (Ann Arbor, MI, USA). Dibutyryl cyclic adenosine monophosphate (dbcAMP) was purchased from Sigma (St. Louis, MO, USA).

2.2. Cell culture and microscopy

NG108-15 cells were grown and maintained in high-glucose Dulbecco's modified Eagle's medium (DMEM) containing 10% FBS, HAT (0.1 mM hypoxanthine, 0.4 µM aminopterin, and 16 µM thymidine), 100 U/mL penicillin, and 100 µg/mL streptomycin at 37°C with 5% CO_2. Figure 1 shows the study design. Cells were seeded in 12-well plates 5000 cells/cm^2. After 24 h, the medium was replaced with DMEM supplemented with 1% FBS, 1% HAT, 100 U/mL penicillin, 100 µg/mL streptomycin, 10 µM α-tocopherol, 0.2 mM dbcAMP, and 100 nM DEX, which was added to induce differentiation (*21,22*). DHA (2 µM) bound to 0.05% fatty acid-free bovine serum albumin was added to the appropriate treatment groups. Then, the cells were cultured for 5 or 6 days. Microscopy performed under an Axiovert200 (Carl Zeiss, Oberkochen, Germany).

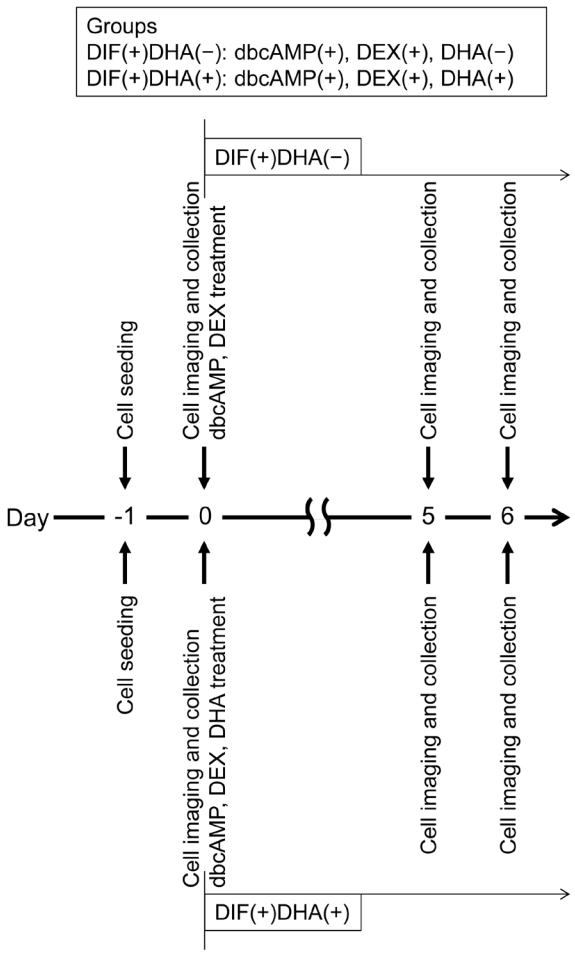

Figure 1. Cell culture and treatment. The day after seeding cells (day 0), differentiation medium and/or docosahexaenoic acid were added. At day 6, cells were observed by microscopy and collected. DIF, differentiation medium; DHA, docosahexaenoic acid; DEX, dexamethasone; dbcAMP, dibutyryl cyclic AMP.

2.3. Preparation of samples for western blotting

Cells were harvested in ice-cold lysis buffer (20 mM Tris-HCl, pH 7.5, 150 mM NaCl, 1 mM Na_2EDTA, 1 mM EGTA, 1% Triton X-100, 2.5 mM sodium pyrophosphate, 1 mM β-glycerophosphate, 1 mM Na_3VO_4, 1 µg/mL leupeptin, and 1 mM PMSF), and the samples were sonicated. The protein concentration was determined with a BCA protein assay kit (Pierce, Rockford, IL, USA) using bovine serum albumin as the standard (*23*).

Aliquots were mixed with concentrated sodium dodecyl sulfate polyacrylamide gel electrophoresis (SDS-PAGE) sample buffer (final concentrations: 62.5 mM Tris-HCl, pH 6.8, 2% 2-mercaptoethanol, 10% glycerol, 2% SDS, and 10% bromophenol blue).

2.4. Western blotting

For SDS-PAGE, samples containing equal amounts of protein were loaded onto 10% SDS-polyacrylamide gels and subsequently transferred to polyvinylidene fluoride (PVDF) membranes. The membranes were blocked with PVDF blocking reagent (Toyobo, Osaka, Japan) and then incubated overnight at 4°C with primary antibodies [nNOS (#4236, Cell Signaling Technology, Danvers, MA, USA), CaMKII (#3362, Cell Signaling Technology), and β-actin (Sigma)]. The membranes were then incubated with horseradish peroxidase-conjugated secondary antibodies (Dako, Glostrup, Denmark) and developed with SuperSignal West Pico (Thermo Fisher, Waltham, MA, USA) or ImmunoStar LD reagents (Fujifilm Wako). Signal detection and quantification of the band intensity were performed using an Amersham Imager 680 (Cytiva, Marlborough, MA, USA).

2.5. Statistical analysis

Significant differences among day 0, 5, and 6 values within each group were evaluated by Fisher's test and between the DIF(+)DHA(−) and DIF(+)DHA(+) groups within each day were evaluated by Student's t test. $p < 0.05$ was considered significant. Excel-Toukei software (2012, Social Survey Research Information Co., Ltd., Tokyo, Japan) was used for the statistical analysis.

3. Results and Discussion

To determine the effects of DHA on differentiated NG108-15 cells, we investigated nNOS and CaMKII protein expression on day 0 (undifferentiated) and days 5 and 6 (differentiated). This cell line is known to differentiate on days 4-6 of induced differentiation,

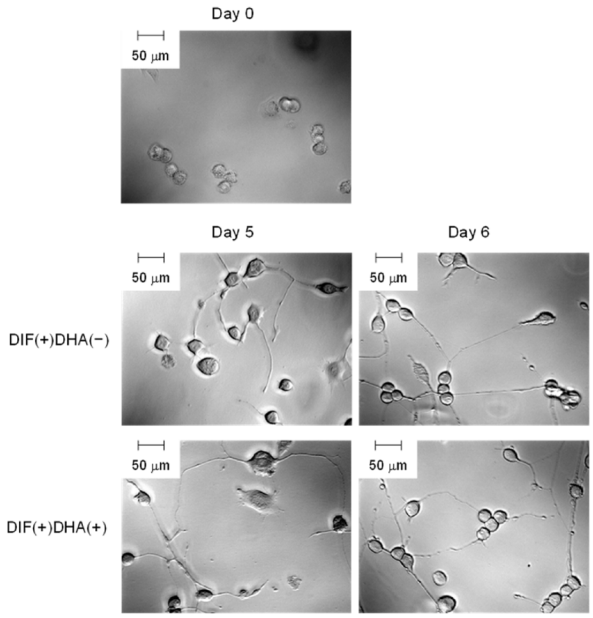

Figure 2. Microscopy observation of NG108-15 cells. The upper micrograph shows the day 0 (undifferentiated), the middle micrograph shows the DIF(+)DHA(−) group, and the lower micrograph shows the DIF(+)DHA(+) group.

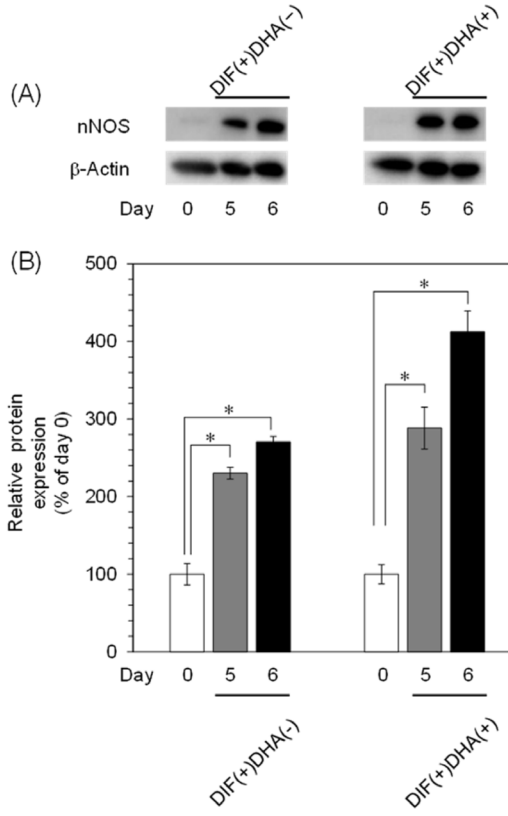

Figure 3. Western blot analysis of nNOS expression in NG108-15 cells on days 0 (undifferentiated), 5, and 6 of differentiation. (**A**) Representative western blots of nNOS and β-actin. (**B**) Semiquantitative analysis of nNOS/β-actin. Each column and bar represents the mean and SEM of four individual experiments. (* $p < 0.05$) nNOS, neuronal NO synthase; DIF, differentiation medium; DHA, docosahexaenoic acid; DEX, dexamethasone; dbcAMP, dibutyryl cyclic AMP.

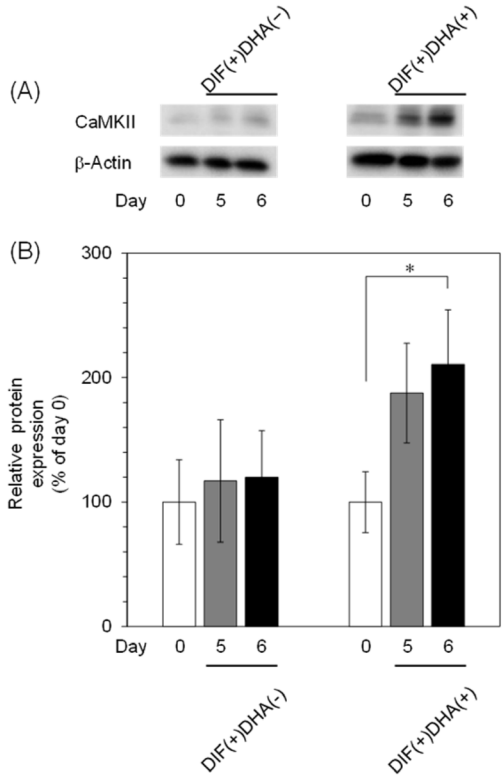

Figure 4. Western blot analysis of CaMKII expression in NG108-15 cells on days 0 (undifferentiated), 5, and 6 of differentiation. (**A**) Representative western blots of CaMKII and β-actin. (**B**) Semiquantitative analysis of CaMKII/β-actin. Each column and bar represents the mean and SEM of four individual experiments (* $p < 0.05$). CaMKII Ca^{2+}/calmodulin-dependent protein kinase II; DIF, differentiation medium; DHA, docosahexaenoic acid; DEX, dexamethasone; dbcAMP, dibutyryl cyclic AMP.

and the changes on days 0, 5, and 6 were confirmed to assess time dependency.

Figure 2 shows micrographs of the cell morphology. Neurite outgrowth occurred on days 5 and 6 of differentiation. However, no significant morphological changes due to DHA addition were observed on days 5 or 6.

Figure 3 shows nNOS protein expression in NG108-15 cells after incubation for 5 or 6 days in differentiation-inducing medium. In the DIF(+)DHA(−) group, nNOS protein expression was increased on days 5 and 6 compared with day 0. Additionally, in the DIF(+)DHA(+) group, nNOS protein expression was increased on days 5 and 6 compared with day 0. These increases tended to be enhanced by DHA addition.

Figure 4 shows CaMKII protein expression in NG108-15 cells. No significant difference was observed in the DIF(+)DHA(−) group even on days 5 and 6 after treatment. However, in the DIF(+)DHA(+) group, a significant increase was observed on day 6 compared with day 0, and a non-significant tendency to increase was observed on day 5 compared with day 0. However. the expressions of nNOS and CaMKII were not significantly different between DIF(+)DHA(-) and

DIF(+)DHA(+) groups on day 5 and 6.

nNOS protein expression was increased on days 5 and 6 compared with day 0 by differentiation without DHA. These increases tended to be enhanced by DHA (Figure 3). CaMKII protein expression was increased on day 6 compared with day 0 by differentiation with DHA, but its expression in the DHA(−) group did not change from day 0 to days 5 and 6. (Figure 4). Therefore, nNOS and CaMKII protein expression in NG108-15 cells was simultaneously affected by DHA.

It has been reported that DHA regulates the expression of several transcription factors. For example, it has been reported that DHA increases the expression of NeuroD, a transcription factor, which is involved in neural differentiation (*24*). It has also been reported that DHA increases the expression of several proteins *via* the tyrosine kinase receptor B (trkB) – extracellular signal-regulated kinase (ERK)1/2 – cAMP-response element binding protein (CREB) pathway (*25*). In this study, it may be that the protein levels of CaMKII and nNOS were changed by being involved in these pathways and/or other transcriptional regulation.

Long-term potentiation (LTP) of hippocampal synaptic transmission plays a role in the mechanism of learning memory. Glutamate receptors are involved in LTP induction. Glutamate receptors are ionotropic or G protein-coupled receptors, and the ionotropic NMDA receptor and its downstream CaMKII pathway play an important role in LTP induction (*26*), learning, and memory (*27*). Additionally, nNOS/endothelial NOS double mutations reduce hippocampal LTP in mice (*4*). It has also been reported that the NMDA receptor-nNOS pathway acts in the induction of presynaptic plasticity (*28*). Several studies have reported that CaMKII and nNOS act in concert with each other (*29,30*), and colocalization of CaMKII, nNOS, and postsynaptic density 95 is important for acting together in a coordinated manner (*31*). nNOS activity is suppressed by phosphorylation of Ser845 by CaMKII (*29*). NO overproduced during ischemia suppresses CaMKII activity *via* S-nitrosylation of Cys6 (*30*). It has been reported that nNOS and CaMKII may perform appropriate functions by coordinating their activities with each other (*32*).

Several studies have reported that DHA is involved in neuroplasticity, LTP, learning, and memory (*11,19,20*). Although our experiments were performed in cells, addition of DHA caused a significant increase in CaMKII protein expression and a tendency to increase nNOS protein expression. Our findings and those in other reports (*11,19,20*) suggest that recovery of synaptic plasticity and learning memory by *n*-3 fatty acids is affected by regulation of nNOS and/or CaMKII expression by *n*-3 fatty acids. We believe that further research, including gene expression, phosphorylation, and intracellular localization of nNOS and CaMKII *in vitro* and *in vivo*, may reveal the mechanisms by which DHA plays several roles in brain functions.

Acknowledgements

We thank Mitchell Arico from Edanz (https://jp.edanz.com/ac) for editing a draft of this manuscript.

Funding: This work was supported by JSPS KAKENHI Grant Number JP16K00876.

Conflict of Interest: The authors have no conflicts of interest to disclose.

References

1. Garthwaite J. NO as a multimodal transmitter in the brain: Discovery and current status. Br J Pharmacol. 2019; 176:197-211.
2. Garthwaite J, Boulton CL. Nitric oxide signaling in the central nervous system. Annu Rev Physiol. 1995; 57:683-706.
3. Hawkins RD. NO honey, I don't remember. Neuron. 1996; 16:465-467.
4. Son H, Hawkins RD, Martin K, Kiebler M, Huang PL, Fishman MC, Kandel ER. Long-term potentiation is reduced in mice that are doubly mutant in endothelial and neuronal nitric oxide synthase. Cell. 1996; 87:1015-1023.
5. Knowles RG, Moncada S. Nitric oxide synthases in mammals. Biochem J. 1994; 298 (Pt 2):249-258.
6. Moncada S, Bolaños JP. Nitric oxide, cell bioenergetics and neurodegeneration. J Neurochem. 2006; 97:1676-1689.
7. Bredt DS, Hwang PM, Glatt CE, Lowenstein C, Reed RR, Snyder SH. Cloned and expressed nitric oxide synthase structurally resembles cytochrome P-450 reductase. Nature. 1991; 351:714-718.
8. Bredt DS, Snyder SH. Isolation of nitric oxide synthetase, a calmodulin-requiring enzyme. Proc Natl Acad Sci U S A. 1990; 87:682-685.
9. Erondu NE, Kennedy MB. Regional distribution of type II Ca^{2+}/calmodulin-dependent protein kinase in rat brain. J Neurosci. 1985; 5:3270-3277.
10. Peng J, Kim MJ, Cheng D, Duong DM, Gygi SP, Sheng M. Semiquantitative proteomic analysis of rat forebrain postsynaptic density fractions by mass spectrometry. J Biol Chem. 2004; 279:21003-21011.
11. Fedorova I, Salem N, Jr. Omega-3 fatty acids and rodent behavior. Prostaglandins Leukot Essent Fatty Acids. 2006; 75:271-289.
12. Tao-Cheng JH, Dosemeci A, Winters CA, Reese TS. Changes in the distribution of calcium calmodulin-dependent protein kinase II at the presynaptic bouton after depolarization. Brain Cell Biol. 2006; 35:117-124.
13. Strack S, Choi S, Lovinger DM, Colbran RJ. Translocation of autophosphorylated calcium/calmodulin-dependent protein kinase II to the postsynaptic density. J Biol Chem. 1997; 272:13467-13470.
14. Liu Q, Chen B, Ge Q, Wang ZW. Presynaptic Ca^{2+}/calmodulin-dependent protein kinase II modulates neurotransmitter release by activating BK channels at Caenorhabditis elegans neuromuscular junction. J Neurosci. 2007; 27:10404-10413.
15. Lisman J. Criteria for identifying the molecular basis of

the engram (CaMKII, PKMzeta). Mol Brain. 2017; 10:55.
16. Harauma A, Sagisaka T, Horii T, Watanabe Y, Moriguchi T. The influence of *n*-3 fatty acids on maternal behavior and brain monoamines in the perinatal period. Prostaglandins Leukot Essent Fatty Acids. 2016; 107:1-7.
17. Ikemoto A, Kobayashi T, Emoto K, Umeda M, Watanabe S, Okuyama H. Effects of docosahexaenoic and arachidonic acids on the synthesis and distribution of aminophospholipids during neuronal differentiation of PC12 cells. Arch Biochem Biophys. 1999; 364:67-74.
18. Ikemoto A, Kobayashi T, Watanabe S, Okuyama H. Membrane fatty acid modifications of PC12 cells by arachidonate or docosahexaenoate affect neurite outgrowth but not norepinephrine release. Neurochem Res. 1997; 22:671-678.
19. Ikemoto A, Ohishi M, Sato Y, Hata N, Misawa Y, Fujii Y, Okuyama H. Reversibility of *n*-3 fatty acid deficiency-induced alterations of learning behavior in the rat: level of *n*-6 fatty acids as another critical factor. J Lipid Res. 2001; 42:1655-1663.
20. Fujita S, Ikegaya Y, Nishikawa M, Nishiyama N, Matsuki N. Docosahexaenoic acid improves long-term potentiation attenuated by phospholipase A(2) inhibitor in rat hippocampal slices. Br J Pharmacol. 2001; 132:1417-1422.
21. Machová E, Málková B, Lisá V, Nováková J, Dolezal V. The increase of choline acetyltransferase activity by docosahexaenoic acid in NG108-15 cells grown in serum-free medium is independent of its effect on cell growth. Neurochem Res. 2006; 31:1239-1246.
22. Machová E, Nováková J, Lisá V, Dolezal V. Docosahexaenoic acid supports cell growth and expression of choline acetyltransferase and muscarinic receptors in NG108-15 cell line. J Mol Neurosci. 2006; 30:25-26.
23. Smith PK, Krohn RI, Hermanson GT, Mallia AK, Gartner FH, Provenzano MD, Fujimoto EK, Goeke NM, Olson BJ, Klenk DC. Measurement of protein using bicinchoninic acid. Anal Biochem. 1985; 150:76-85.
24. Katakura M, Hashimoto M, Shahdat HM, Gamoh S, Okui T, Matsuzaki K, Shido O. Docosahexaenoic acid promotes neuronal differentiation by regulating basic helix-loop-helix transcription factors and cell cycle in neural stem cells. Neuroscience. 2009; 160:651-660.
25. Bie N, Feng X, Li C, Meng M, Wang C. The protective effect of docosahexaenoic acid on PC12 cells in oxidative stress induced by H_2O_2 through the TrkB-Erk1/2-CREB Pathway. ACS Chem Neurosci. 2021; 12:3433-3444.
26. Silva AJ, Stevens CF, Tonegawa S, Wang Y. Deficient hippocampal long-term potentiation in alpha-calcium-calmodulin kinase II mutant mice. Science. 1992; 257:201-206.
27. Silva AJ, Paylor R, Wehner JM, Tonegawa S. Impaired spatial learning in alpha-calcium-calmodulin kinase II mutant mice. Science. 1992; 257:206-211.
28. Hardingham N, Dachtler J, Fox K. The role of nitric oxide in pre-synaptic plasticity and homeostasis. Front Cell Neurosci. 2013; 7:190.
29. Komeima K, Hayashi Y, Naito Y, Watanabe Y. Inhibition of neuronal nitric-oxide synthase by calcium/ calmodulin-dependent protein kinase IIalpha through Ser847 phosphorylation in NG108-15 neuronal cells. J Biol Chem. 2000; 275:28139-28143.
30. Song T, Hatano N, Kambe T, Miyamoto Y, Ihara H, Yamamoto H, Sugimoto K, Kume K, Yamaguchi F, Tokuda M, Watanabe Y. Nitric oxide-mediated modulation of calcium/calmodulin-dependent protein kinase II. Biochem J. 2008; 412:223-231.
31. Watanabe Y, Song T, Sugimoto K, Horii M, Araki N, Tokumitsu H, Tezuka T, Yamamoto T, Tokuda M. Post-synaptic density-95 promotes calcium/calmodulin-dependent protein kinase II-mediated Ser847 phosphorylation of neuronal nitric oxide synthase. Biochem J. 2003; 372:465-471.
32. Araki S, Osuka K, Takata T, Tsuchiya Y, Watanabe Y. Coordination between calcium/calmodulin-dependent protein kinase II and neuronal nitric oxide synthase in neurons. Int J Mol Sci. 2020; 21:7997.

Received January 16, 2023; Revised May 2, 2023; Accepted May 21, 2023.

**Address correspondence to:*
Daisuke Miyazawa, College of Pharmacy, Kinjo Gakuin University, 2-1723 Omori, Moriyama-ku, Nagoya 463-8521, Japan.
E-mail: miyazawa@kinjo-u.ac.jp

Released online in J-STAGE as advance publication May 27, 2023.

Correspondence

DOI: 10.5582/ddt.2022.01121

Factors contributing to carboplatin blockade and interruption in its route of administration in paclitaxel-carboplatin therapy

Motoki Inoue[1], Kazuhiko Nakadate[1], Mami Oosaki[2], Mikio Shirota[2], Takeo Yasu[1,2,3,*]

[1] Meiji Pharmaceutical University, Tokyo, Japan;
[2] Department of Pharmacy, Tokyo Metropolitan Bokutoh Hospital, Tokyo, Japan;
[3] Bokutoh Hospital-Meiji Pharmaceutical University Joint Research Center, Tokyo, Japan.

SUMMARY The interruption of anticancer infusion processes in patients undergoing chemotherapy may affect their quality of life and the efficacy and safety of the therapy. We experienced several interruptions of carboplatin infusion in multiple patients receiving paclitaxel-carboplatin combination therapy. Therefore, we investigated the causes of these interruptions. The filter and catheter surfaces were evaluated by scanning electron microscopy. Moreover, using a texture analyzer, the mechanical strengths of catheter-attached syringes were compared pre- and post-administration. We observed that the syringe pushing force requirement was higher following dripping failure. However, precipitates were not evident on the filter surfaces, regardless of the dripping failure route. In this case, some of the drug adhered to the catheters' surfaces and interrupted the carboplatin titration. Consequently, in patients receiving combination therapy with paclitaxel and carboplatin, and experiencing interruptions in carboplatin infusion, attention should be paid to the catheter.

Keywords adsorption, catheters, scanning electron microscopy, syringe pushing force

The incidence of cancer is increasing with the aging population and mirrored by the rising number of patients undergoing cancer chemotherapy. Recently, several cancer chemotherapies have become available on an outpatient basis, allowing recipients access to treatment daily. Multiple medical devices are employed for administering anticancer drugs, including intravenous catheters, in-line filters, and closed-system drug transfer devices (*1*). In clinical practice, antiemetic agents, including serotonin (5HT3) receptor antagonists, dexamethasone, and fosaprepitant are used for preventing chemotherapy-induced nausea and vomiting. In addition, histamine H1 and H2 receptor antagonists act as prophylactic measures against allergies to anticancer drugs, such as paclitaxel, which are administered intravenously before initiating chemotherapy. Therefore, it is essential to appropriately assess anticancer drug compatibility with other drugs administered *via* the same route. Additionally, medical devices made of non-polyvinyl chloride materials should be utilized to avoid exposure to diethylhexyl phthalate during the administration of intravenous anticancer drugs, such as etoposide (*2*). Data on the interactions between anticancer drugs and medical devices during intravenous administration are currently limited.

We encountered several patients with ovarian cancer who were treated with paclitaxel and carboplatin (TC) therapy (*3*) and who could not receive the full dose of carboplatin owing to failure of carboplatin titration post paclitaxel administration. All patients had plastic peripheral intravenous catheters placed in their arms and had received fosaprepitant, meglumine, palonosetron, dexamethasone, chlorpheniramine, and famotidine from the same peripheral route before paclitaxel administration. If carboplatin could not be titrated, the infusion was improved slightly by administering saline before restarting carboplatin. However, despite frequent notifications by the infusion monitor alarm, saline and carboplatin were often administered alternately. The eventual outcome in these cases would be the complete removal of the peripheral intravenous catheter and replacement of all peripheral routes, which is a heavy burden on patients and nurses. While anticancer drugs are routinely administered *via* a plastic indwelling peripheral intravenous catheter placed in a vein in the arm or another body part, there is little information available on the interactions between the catheter material and the drugs. We identified the cause of blockage on the inner surface of these devices and compared the pushing force of blocked and unblocked catheters.

We investigated the cause of blockage using

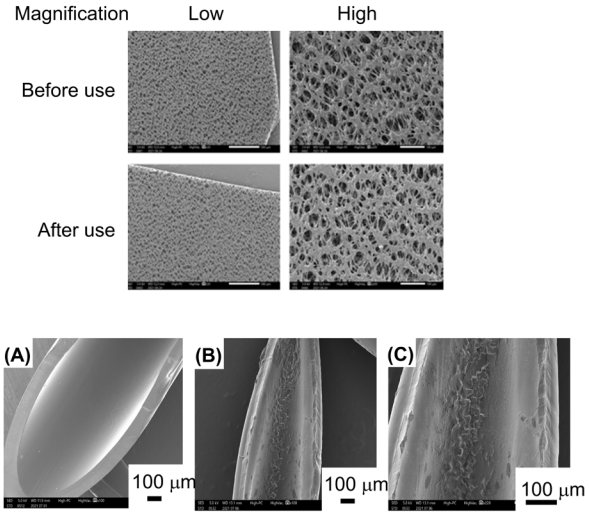

Figure 1. (Top): Visual and SEM images of the filter along the infusion route post administration of a TC regimen. (Bottom): SEM images of the catheter surface (A) saline immersion (B) low and (C) high magnification of catheter cross-section post administration of TC regimens.

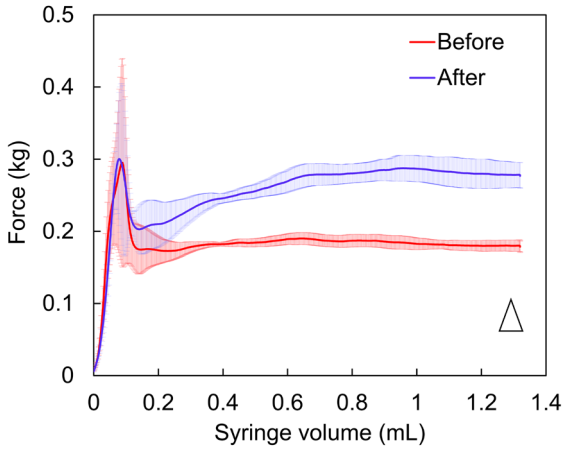

Figure 2. Comparison of catheter extrusion force before and after paclitaxel and carboplatin administration. Triangle indicates the value used for evaluation. Error bars represent standard deviations (n = 5).

an infusion set filter membrane and catheter used by a patient who could not titrate carboplatin after receiving paclitaxel with a TC regimen. The absence of precipitates in the bottle containing the solution to be infused was confirmed before detailed observation. The microstructures of the surfaces of the infusion set filter membranes and the catheter, obtained after the TC regimen, were assessed using JCM-7000 scanning electron microscopy (SEM) (JEOL Ltd. Tokyo, Japan). The disassembled in-line filter and catheters were immersed in distilled water for desalination. Post drying, they were coated with osmium tetroxide (OsO_4) and observed by SEM. Additionally, we evaluated the catheter extrusion force before and after paclitaxel and carboplatin administration. A syringe was filled with 5 mL water to prevent the entry of air, followed by placing a catheter at the tip, which was subsequently set in a TX-TA Plus texture analyzer (Stable Micro Systems, UK). The experimental conditions were compression at 2 mm/s, and measurements were stopped after the syringe had been pushed out and moved by 10 mm. The passage of a total amount of 1.32 mL water through the catheters was evaluated and force–distance plot for 5 s was recorded. Paclitaxel IV Infusion Hospira (Pfizer Japan Inc., Tokyo, Japan) and carboplatin NK injection (Mylan Inc., Tokyo, Japan) were utilized. Terufusion™ (Terumo Co. Tokyo, Japan) and Surshield SURFLO 2 (Terumo Co.) were used as the route and catheter, respectively. Post administration, the catheter was rinsed with deionized water, dried *in vacuo* at room temperature, and used for further examination. Blockade after drug administration was evaluated by assessing the extrusion force of the syringe, which was connected by a tube. Statistical significance was set at a $p < 0.05$, and data were analyzed using Microsoft Excel.

Visual and SEM images of the filter along the infusion route post administration of the TC regimen were identical in all aspects to an unused sample with no evidence of adsorption on the filter surface (Figure 1). Figure 1 (top) shows the SEM images of the catheter cross-sectional surface. As shown in Figure 1 (bottom), the surface of the control catheter, immersed in saline for 3 h was smooth, without any evidence of precipitates. By contrast, precipitates were observed on the catheter surface post paclitaxel and carboplatin administration (Figure 1, bottom, B and C). Figure 2 compares catheter extrusion force before and after paclitaxel and carboplatin administration. The extrusion force of five catheters at the end of the extrusion in the unused product (1.32 mL; open circle) was 0.179 ± 0.008 kg. The pushing force determined after five experimental procedures that involved duplicate or triplicate readings using two catheters was 0.277 ± 0.018 kg. There was a significant difference in the catheter extrusion force before and after paclitaxel and carboplatin administration ($p < 0.01$).

We investigated the cause of carboplatin infusion interruption in a patient receiving a TC regimen. The surfaces of filters and catheters were evaluated using SEM. A texture analyzer was used to compare the mechanical strength of syringes and catheters before and after administration. There was no sediment on the filter surface; however, there was sediment on the catheter surface, resulting in higher syringe push force requirements. We found that adsorption to the catheter surface causes interference and interruption of carboplatin.

Following paclitaxel and carboplatin administration, a higher force of approximately 0.5 kg was required for catheter extrusion force compared to that required by an unused one. Furthermore, since the observation

was made in the dry state, the perceived thickness may have been less than that of the actual precipitate. When patients receiving combination therapy with paclitaxel and carboplatin experience interruptions in carboplatin infusion, attention should be paid to the catheter as well as the filter.

Catheter blockages pose two significant issues. First, there is the risk of a puncture during catheter replacement. While none of our patients complained of vascular pain while flushing with saline, there are reports of its occurrence in carboplatin-containing regimens (*4*). Second, prolonged carboplatin infusion time may adversely affect its efficacy or augment associated side effects. Adverse events, including increased myelosuppression, have not yet been reported in the context of carboplatin treatment. However, increased myelosuppression has been reported with prolonged infusion of gemcitabine (*5*). Evidence-based medicine mandates that healthcare professionals strictly adhere to the recommended dosages and administration rates during anticancer treatments, which have been confirmed to be effective and safe in clinical trials. Furthermore, doctors and nurses are well-familiarized with the usage of devices, such as catheters and filters, during drug administration. However, in the context of interactions between devices and therapeutic agents, pharmacists play a central role in scientifically establishing the physical properties of the materials used in devices and drugs. Thus, appropriate awareness of interactions between devices and drugs is essential to ensure effective and safe chemotherapy. This report will aid pharmacists in avoiding dose discontinuation scenarios caused by interactions between devices and therapeutic agents.

Funding: None.

Conflict of Interest: The authors have no conflicts of interest to disclose.

References

1. American Society of Health-System Pharmacists. ASHP guidelines on handling hazardous drugs. Am J Health Syst Pharm. 2006; 63: 1172-1193.
2. de Lemos ML, Hamata L, Vu T. Leaching of diethylhexyl phthalate from polyvinyl chloride materials into etoposide intravenous solutions. J Oncol Pharm Pract. 2005; 11:155-157.
3. Parmar MK Ledermann JA, Colombo N, *et al*. Paclitaxel plus platinum-based chemotherapy versus conventional platinum-based chemotherapy in women with relapsed ovarian cancer: The ICON4/AGO-OVAR-2.2 trial. Lancet. 2003; 361:2099-2106.
4. Nagase S, Fukazawa T, Uehara N, Fujimori R, Watanabe T, Shimizu K, Aizawa Y, Kanno H. The effectiveness of a glucose solution for vascular pain in patients who received line flushing after administration of carboplatin based regimens. Jpn J Pharm Palliat Care Sci. 2017; 10: 35-40. (in Japanese)
5. Grunewald R, Abbruzzese JL, Tarassoff P, Plunkett W. Saturation of 2′,2′-difluorodeoxycytidine 5′-triphosphate accumulation by mononuclear cells during a phase I trial of gemcitabine. Cancer Chemother Pharmacol. 1991; 27:258-262.

Received December 16, 2022; Revised April 18, 2023; Accepted May 20, 2023.

**Address correspondence to:*
Takeo Yasu, Department of Medicinal Therapy Research, Pharmaceutical Education and Research Center, Meiji Pharmaceutical University; 2-522-1, Noshio, Kiyose, Tokyo 204-8588, Japan.
E-mail: yasutakeo-tky@umin.ac.jp

Released online in J-STAGE as advance publication May 23, 2023.

Letter to the Editor

DOI: 10.5582/ddt.2023.01009

Laparoscopic-assisted treatment for diospyrobezoar-induced intestinal obstruction after distal gastrectomy and cholecystectomy

Yuki Ohya[1,*], Shintaro Hayashida[1], Akira Yoneda[2], Akira Tsuji[1], Taihei Inoue[3], Suguru Chiyonaga[2], Kunitaka Kuramoto[1], Kotaro Oda[4], Masayoshi Iizaka[1], Osamu Nakahara[1], Yukihiro Inomata[1]

[1] Department of Surgery, Kumamoto Rosai Hospital, Kumamoto, Japan;
[2] Department of Gastroenterology, Kumamoto Rosai Hospital, Kumamoto, Japan;
[3] Department of Radiology, Kumamoto Rosai Hospital, Kumamoto, Japan;
[4] Oda Medical Clinic, Kumamoto, Japan.

SUMMARY Diospyrobezoar is a relatively uncommon cause of small bowel obstruction. Here we report successful treatment in a patient with small bowel obstruction due to diospyrobezoar by laparoscopic-assisted surgery. A 93-year-old woman who had undergone distal gastrectomy and laparoscopic cholecystectomy presented with nausea and anorexia. An intestinal obstruction and an intestinal intraluminal mass were discovered on abdominal enhanced computed tomography. Following a transnasal ileus tube placement, the patient underwent laparoscopic surgery to remove the diospyrobezoar from the small intestine. The postoperative course of the patient was uneventful. Laparoscopic-assisted surgery following the transnasal ileus tube was beneficial for the patient's small bowel obstruction caused by diospyrobezoar.

Keywords diospyrobezoar, small bowel obstruction, laparoscopic-assisted surgery

Letter to the Editor,

Bezoars are the most common gastrointestinal foreign bodies. Bezoars are classified into phytobezoar, trichobezoars, lactobezoars, mixed medication bezoars, and food bolus bezoars based on their compensation (*1-5*). A diospyrobezoar is a type of phytobezoar caused by an excess of persimmons consumption that is difficult to treat due to its hard consistency (*1-5*). Small intestinal obstruction caused by a primary bezoar is uncommon and is usually caused by the migration of a gastric bezoar (*2-5*). Dissolution with Coca-Cola® removal with endoscopic devices, laparotomy, and laparoscopic surgery are currently available treatment options for an intestinal bezoar (*3-5*). Our report describes the successful laparoscopic-assisted treatment of a diospyrobezoar in the ileum following the placement of a transnasal ileus tube. It was thought that the diospyrobezoar migrated from the stomach.

In October, a 93-year-old woman with dementia presented to a clinic with nausea and anorexia. She had advanced dementia and was living with family members, but they were unable to fully manage her eating. She had been admitted to the local hospital and treated with conservative therapy for 10 days because she was suspected of having enteritis and subileus. She was referred to our hospital because her symptom persisted. She had severe dementia and it was difficult to obtain sufficient information about her recent daily activities, including eating habits. According to her medical records, she had a Billroth I distal gastrectomy at the age of 74 and laparoscopic cholecystectomy at the age of 89. An intestinal obstruction and an intestinal intraluminal mass were discovered on abdominal enhanced computed tomography (Figures 1A, 1B, and 1C). As a result, she was suspected of having small bowel obstruction caused by a foreign body, such as food.

She had a transnasal ileus tube placed for proximal intestine drainage. Although the placement reduced intestinal dilatation, the bowel obstruction was not relieved. Three days after the ileus tube was placed, a contrast examination with Gastrografin® revealed a foreign body obstructing the intestinal tract to the ileus tube (Figure 1D). The body removal of the foreign body required surgery. The laparoscopic examination was attempted through two ports, one in the umbilicus and the other in the left abdomen. There was enough peritoneal space for laparoscopic movement because the ileus tube had previously decompressed the intestine (Figure 2A). The foreign body was easily identified in the distal ileum (Figure 2A), using the moving tip of

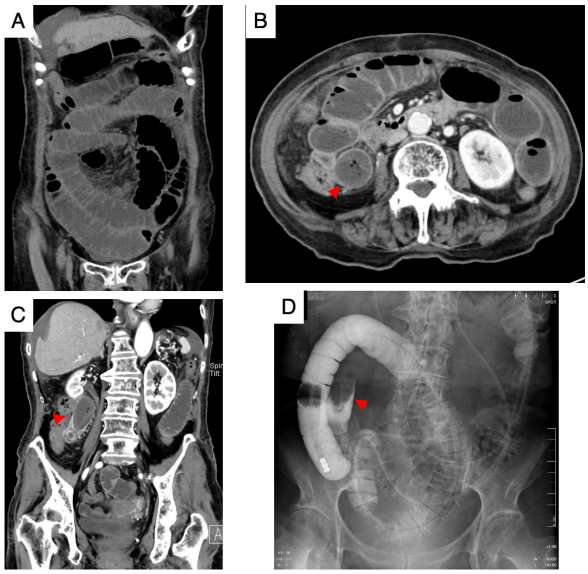

Figure 1. Findings from an imaging study. (A) Computed tomography scan reveals a small bowel obstruction. **(B, C)** Enhanced computed tomography reveals a foreign body obstructing the small bowel (red allow head). **(D)** Contrast examination revealed a foreign body obstructing the intestinal tract at the ileus tube's end (red allow head).

the transnasal ileus tube as a guide. The umbilical port site was then extended to a 4 cm incision to allow for the removal of the foreign body via an extracorporeal incision of the pulled-up ileum (Figures 2B, 2C, and 2D). The postoperative course went smoothly, and the patient was able to eat on the third postoperative day.

Bezoar extracted had a hard and fibrotic content (Figures 2E and 2F). Because component analysis revealed that this bezoar contained more than 98% tannin, the foreign body was classified as a diospyrobezoar.

Diospyrobezoar is an uncommon but occasionally reported cause of small bowel obstruction (*2-5*). Although the cause of the ileus was unknown before surgery in our case, the hybrid procedure combining laparoscopic examination after intestinal decompression and open surgery with a small incision was effective in removing the intraluminal foreign body.

Diospyrobezoar is an unknown cause of small bowel obstruction (*2-5*). Based on imaging studies alone, it is extremely difficult to determine that the cause of the small bowel obstruction is a diospyrobezoar (*6,7*). A diospyrobezoar in the small intestine cannot be removed using standard upper gastrointestinal endoscopy and must be removed using a double-balloon endoscopy. It is difficult to try the dissolution by Coca-Cola® without a confirmed diagnosis. Although small bowel obstruction limits the working space for laparoscopic surgery and makes findings foreign bodies difficult, the laparoscopic approach to small bowel obstruction is becoming more popular (*8,9*). We had enough working space because we performed the laparoscopic procedure after intestinal decompression with a transnasal ileus tube, and the foreign body was easily identified.

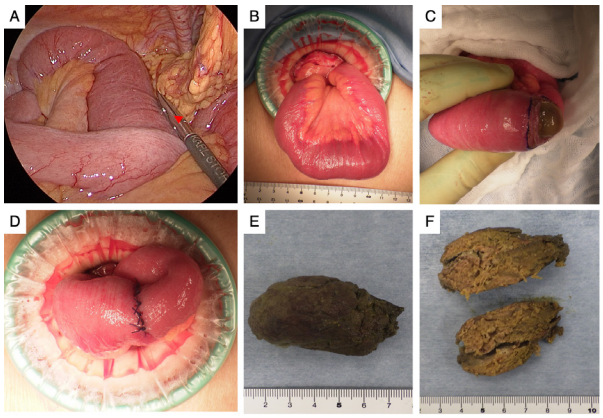

Figure 2. Findings from operations. The foreign body in the intestine was easily identified and extracted from the abdominal cavity **(A, B)** (red allow head). The foreign body was removed from the small intestine **(C, D). (E, F)** The appearance of the foreign body was removed.

Previous gastric surgery, persimmon consumption, and diabetes mellitus, among other things, are known risk factors for diospyrobezoar (*1,3-5*). She had previously had a distal gastrectomy. It was later revealed that she had harvested and eaten many persimmons from her garden before the outbreak. However, due to her advanced dementia, this critical information for the preoperative diagnosis could not be obtained. The post-gastrectomy state, possibly uncontrolled persimmon intake due to senile dementia, and the season with abundant persimmon in the rural area should all be considered for the diagnosis.

In conclusion, laparoscopic-assisted surgery of an intestinal diospyrobezoar with intentional decompression using a transnasal ileus tube is useful and can be applied to other intraluminal foreign bodies.

Funding: None.

Conflict of interest: The authors have no conflicts of interest to disclose.

*Informed consen*t: Written informed consent was taken from the patient for the publication of case details and photographs.

References

1. Morey DAJ, Means RL, Hirsley EL. Diospyrobezoar in the postgastrectomy stomach. AMA Arch Surg. 1955; 71:946-948.
2. Andrus CH, Ponsky JL. Bezoars: Classification, pathophysiology, and treatment. Am J Gastroenterol. 1988; 83:476-478.
3. Erzurumlu K, Malazgirt Z, Bektas A, Dervisoglu A, Polat C, Senyurek G, Yetim I, Ozkan K. Gastrointestinal bezoars: A retrospective analysis of 34 cases. World J Gastroenterol. 2005; 11:1813-1817.
4. Iwamuro M, Okada H, Matsueda K, Inaba T, Kusumoto C, Imagawa A, Yamamoto K. Review of the diagnosis

and management of gastrointestinal bezoars. World J Gastrointest Endosc. 2015; 7:336-345.
5. de Toledo AP, Rodrigues FH, Rodrigues MR, Sato DT, Nonose R, Nascimento EF, Martinez CA. Diospyrobezoar as a cause of small bowel obstruction. Case Rep Gastroenterol. 2012; 6:596-603.
6. Quiroga S, Alvarez-Castells A, Sebastià MC, Pallisa E, Barluenga E. Small bowel obstruction secondary to bezoar: CT diagnosis. Abdom Imaging. 1997; 22:315-317.
7. Xu G, Guo Y. Computed tomography findings of small bowel obstruction due to bezoar impaction: A case series. Emergency Med. 2012; 2:130.
8. Fujimoto Y, Ohya Y, Hayashida S, Iizaka M, Maeda Y, Kumamoto S, Tsuji A, Shibata H, Kuramoto K, Hayashi H, Nakahara O, Tomiyasu S, Inomata Y. Laparoscopic surgery for two patients with strangulated transomental hernias. Surg Case Rep. 2020; 6:53.
9. Otani K, Ishihara S, Nozawa H, Kawai K, Hata K, Kiyomatsu T, Tanaka T, Nishikawa T, Yasuda K, Sasaki K, Murono K, Watanabe T. A retrospective study of laparoscopic surgery for small bowel obstruction. Ann Med Surg. 2017; 16:34-39.

Received February 8, 2023; Revised May 28, 2023; Accepted May 30, 2023.

Address correspondence to:
Yuki Ohya, Department of Surgery, Kumamoto Rosai Hospital, 1670 Takehara-machi, Yatsushiro, Kumamoto 866-8533, Japan
E-mail: pedsurg-oya@kumamotoh.johas.go.jp

Released online in J-STAGE as advance publication June 16, 2023.

DD&T
Drug Discoveries & Therapeutics

Guide for Authors

1. Scope of Articles

Drug Discoveries & Therapeutics (Print ISSN 1881-7831, Online ISSN 1881-784X) welcomes contributions in all fields of pharmaceutical and therapeutic research such as medicinal chemistry, pharmacology, pharmaceutical analysis, pharmaceutics, pharmaceutical administration, and experimental and clinical studies of effects, mechanisms, or uses of various treatments. Studies in drug-related fields such as biology, biochemistry, physiology, microbiology, and immunology are also within the scope of this journal.

2. Submission Types

Original Articles should be well-documented, novel, and significant to the field as a whole. An Original Article should be arranged into the following sections: Title page, Abstract, Introduction, Materials and Methods, Results, Discussion, Acknowledgments, and References. Original articles should not exceed 5,000 words in length (excluding references) and should be limited to a maximum of 50 references. Articles may contain a maximum of 10 figures and/or tables. Supplementary Data are permitted but should be limited to information that is not essential to the general understanding of the research presented in the main text, such as unaltered blots and source data as well as other file types.

Brief Reports definitively documenting either experimental results or informative clinical observations will be considered for publication in this category. Brief Reports are not intended for publication of incomplete or preliminary findings. Brief Reports should not exceed 3,000 words in length (excluding references) and should be limited to a maximum of 4 figures and/or tables and 30 references. A Brief Report contains the same sections as an Original Article, but the Results and Discussion sections should be combined.

Reviews should present a full and up-to-date account of recent developments within an area of research. Normally, reviews should not exceed 8,000 words in length (excluding references) and should be limited to a maximum of 10 figures and/or tables and 100 references. Mini reviews are also accepted, which should not exceed 4,000 words in length (excluding references) and should be limited to a maximum of 5 figures and/or tables and 50 references.

Policy Forum articles discuss research and policy issues in areas related to life science such as public health, the medical care system, and social science and may address governmental issues at district, national, and international levels of discourse. Policy Forum articles should not exceed 3,000 words in length (excluding references) and should be limited to a maximum of 5 figures and/or tables and 30 references.

Case Reports should be detailed reports of the symptoms, signs, diagnosis, treatment, and follow-up of an individual patient. Case reports may contain a demographic profile of the patient but usually describe an unusual or novel occurrence. Unreported or unusual side effects or adverse interactions involving medications will also be considered. Case Reports should not exceed 3,000 words in length (excluding references).

Communications are short, timely pieces that spotlight new research findings or policy issues of interest to the field of global health and medical practice that are of immediate importance. Depending on their content, Communications will be published as "Comments" or "Correspondence". Communications should not exceed 1,500 words in length (excluding references) and should be limited to a maximum of 2 figures and/or tables and 20 references.

Editorials are short, invited opinion pieces that discuss an issue of immediate importance to the fields of global health, medical practice, and basic science oriented for clinical application. Editorials should not exceed 1,000 words in length (excluding references) and should be limited to a maximum of 10 references. Editorials may contain one figure or table.

News articles should report the latest events in health sciences and medical research from around the world. News should not exceed 500 words in length.

Letters should present considered opinions in response to articles published in *Drug Discoveries & Therapeutics* in the last 6 months or issues of general interest. Letters should not exceed 800 words in length and may contain a maximum of 10 references. Letters may contain one figure or table.

3. Editorial Policies

For publishing and ethical standards, *Drug Discoveries & Therapeutics* follows the Recommendations for the Conduct, Reporting, Editing, and Publication of Scholarly Work in Medical Journals issued by the International Committee of Medical Journal Editors (ICMJE, *https://icmje.org/recommendations*), and the Principles of Transparency and Best Practice in Scholarly Publishing jointly issued by the Committee on Publication Ethics (COPE, *https://publicationethics.org/resources/guidelines-new/principles-transparency-and-best-practice-scholarly-publishing*), the Directory of Open Access Journals (DOAJ, *https://doaj.org/apply/transparency*), the Open Access Scholarly Publishers Association (OASPA, *https://oaspa.org/principles-of-transparency-and-best-practice-in-scholarly-publishing-4*), and the World Association of Medical Editors (WAME, *https://wame.org/principles-of-transparency-and-best-practice-in-scholarly-publishing*).

Drug Discoveries & Therapeutics will perform an especially prompt review to encourage innovative work. All original research will be subjected to a rigorous standard of peer review and will be edited by experienced copy editors to the highest standards.

Ethical Approval of Studies and Informed Consent: For all manuscripts reporting data from studies involving human participants or animals, formal review and approval, or formal review and waiver, by an appropriate institutional review board or ethics committee is required and should be described in the Methods section. When your manuscript contains any case details, personal information and/or images of patients or other individuals, authors must obtain appropriate written consent, permission and release in order to comply with all applicable laws and regulations concerning privacy and/or security of personal information. The consent form needs to comply with the relevant legal requirements of your particular jurisdiction, and please do not send signed consent form to *Drug Discoveries & Therapeutics* to respect your patient's and any other individual's privacy. Please instead describe the information clearly in the Methods (patient consent) section of your manuscript while retaining copies of the signed forms in the event they should be needed. Authors should also state that the study conformed to the provisions of the Declaration of Helsinki (as revised in 2013, *https://wma.net/what-we-do/medical-ethics/declaration-of-helsinki*). When reporting experiments on animals, authors should indicate whether the institutional and national guide for the care and use of laboratory animals was followed.

Reporting Clinical Trials: The ICMJE (*https:// icmje.org/recommendations/browse/publishing-and-editorial-issues/clinical-trial-registration.html*) defines a clinical trial as any research project that prospectively assigns people or a group of people to an intervention, with or without concurrent comparison or control groups, to study the relationship between a health-related intervention and a health outcome. Registration of clinical trials in a public trial registry

at or before the time of first patient enrollment is a condition of consideration for publication in *Drug Discoveries & Therapeutics*, and the trial registration number will be published at the end of the Abstract. The registry must be independent of for-profit interest and publicly accessible. Reports of trials must conform to CONSORT 2010 guidelines (*https://consort-statement.org/consort-2010*). Articles reporting the results of randomized trials must include the CONSORT flow diagram showing the progress of patients throughout the trial.

Conflict of Interest: All authors are required to disclose any actual or potential conflict of interest including financial interests or relationships with other people or organizations that might raise questions of bias in the work reported. If no conflict of interest exists for each author, please state "There is no conflict of interest to disclose".

Submission Declaration: When a manuscript is considered for submission to *Drug Discoveries & Therapeutics*, the authors should confirm that 1) no part of this manuscript is currently under consideration for publication elsewhere; 2) this manuscript does not contain the same information in whole or in part as manuscripts that have been published, accepted, or are under review elsewhere, except in the form of an abstract, a letter to the editor, or part of a published lecture or academic thesis; 3) authorization for publication has been obtained from the authors' employer or institution; and 4) all contributing authors have agreed to submit this manuscript.

Initial Editorial Check: Immediately after submission, the journal's managing editor will perform an initial check of the manuscript. A suitable academic editor will be notified of the submission and invited to check the manuscript and recommend reviewers. Academic editors will check for plagiarism and duplicate publication at this stage. The journal has a formal recusal process in place to help manage potential conflicts of interest of editors. In the event that an editor has a conflict of interest with a submitted manuscript or with the authors, the manuscript, review, and editorial decisions are managed by another designated editor without a conflict of interest related to the manuscript.

Peer Review: *Drug Discoveries & Therapeutics* operates a single-anonymized review process, which means that reviewers know the names of the authors, but the authors do not know who reviewed their manuscript. All articles are evaluated objectively based on academic content. External peer review of research articles is performed by at least two reviewers, and sometimes the opinions of more reviewers are sought. Peer reviewers are selected based on their expertise and ability to provide quality, constructive, and fair reviews. For research manuscripts, the editors may, in addition, seek the opinion of a statistical reviewer. Every reviewer is expected to evaluate the manuscript in a timely, transparent, and ethical manner, following the COPE guidelines (*https://publicationethics.org/files/cope-ethical-guidelines-peer-reviewers-v2_0.pdf*). We ask authors for sufficient revisions (with a second round of peer review, when necessary) before a final decision is made. Consideration for publication is based on the article's originality, novelty, and scientific soundness, and the appropriateness of its analysis.

Suggested Reviewers: A list of up to 3 reviewers who are qualified to assess the scientific merit of the study is welcomed. Reviewer information including names, affiliations, addresses, and e-mail should be provided at the same time the manuscript is submitted online. Please do not suggest reviewers with known conflicts of interest, including participants or anyone with a stake in the proposed research; anyone from the same institution; former students, advisors, or research collaborators (within the last three years); or close personal contacts. Please note that the Editor-in-Chief may accept one or more of the proposed reviewers or may request a review by other qualified persons.

Language Editing: Manuscripts prepared by authors whose native language is not English should have their work proofread by a native English speaker before submission. If not, this might delay the publication of your manuscript in *Drug Discoveries & Therapeutics*.

The Editing Support Organization can provide English proofreading, Japanese-English translation, and Chinese-English translation services to authors who want to publish in *Drug Discoveries & Therapeutics* and need assistance before submitting a manuscript. Authors can visit this organization directly at *https://www.iacmhr.com/iac-eso/support.php?lang=en. IAC-ESO* was established to facilitate manuscript preparation by researchers whose native language is not English and to help edit works intended for international academic journals.

Copyright and Reuse: Before a manuscript is accepted for publication in *Drug Discoveries & Therapeutics*, authors will be asked to sign a transfer of copyright agreement, which recognizes the common interest that both the journal and author(s) have in the protection of copyright. We accept that some authors (*e.g.*, government employees in some countries) are unable to transfer copyright. A JOURNAL PUBLISHING AGREEMENT (JPA) form will be e-mailed to the authors by the Editorial Office and must be returned by the authors by mail, fax, or as a scan. Only forms with a hand-written signature from the corresponding author are accepted. This copyright will ensure the widest possible dissemination of information. Please note that the manuscript will not proceed to the next step in publication until the JPA Form is received. In addition, if excerpts from other copyrighted works are included, the author(s) must obtain written permission from the copyright owners and credit the source(s) in the article.

4. Cover Letter

The manuscript must be accompanied by a cover letter prepared by the corresponding author on behalf of all authors. The letter should indicate the basic findings of the work and their significance. The letter should also include a statement affirming that all authors concur with the submission and that the material submitted for publication has not been published previously or is not under consideration for publication elsewhere. The cover letter should be submitted in PDF format. For an example of Cover Letter, please visit: Download Centre (*https://www.ddtjournal.com/downcentre)*.

5. Submission Checklist

The Submission Checklist should be submitted when submitting a manuscript through the Online Submission System. Please visit Download Centre (*https://www.ddtjournal.com/downcentre)* and download the Submission Checklist file. We recommend that authors use this checklist when preparing your manuscript to check that all the necessary information is included in your article (if applicable), especially with regard to Ethics Statements.

6. Manuscript Preparation

Manuscripts are suggested to be prepared in accordance with the "Recommendations for the Conduct, Reporting, Editing, and Publication of Scholarly Work in Medical Journals", as presented at *http://www.ICMJE.org*.

Manuscripts should be written in clear, grammatically correct English and submitted as a Microsoft Word file in a single-column format. Manuscripts must be paginated and typed in 12-point Times New Roman font with 24-point line spacing. Please do not embed figures in the text. Abbreviations should be used as little as possible and should be explained at first mention unless the term is a well-known abbreviation (*e.g.* DNA). Single words should not be abbreviated.

Title page: The title page must include 1) the title of the paper (Please note the title should be short, informative, and contain the major key words); 2) full name(s) and affiliation(s) of the author(s), 3) abbreviated names of the author(s), 4) full name, mailing address, telephone/fax numbers, and e-mail address of the corresponding author; 5) author contribution statements to specify the individual contributions of all authors to this manuscript, and 6) conflicts of interest (if you have an actual or potential conflict of interest to disclose, it must be included as a footnote on the title page of the manuscript; if no conflict of interest

exists for each author, please state "There is no conflict of interest to disclose").

Abstract: The abstract should briefly state the purpose of the study, methods, main findings, and conclusions. For article types including Original Article, Brief Report, Review, Policy Forum, and Case Report, a one-paragraph abstract consisting of no more than 250 words must be included in the manuscript. For Communications, Editorials, News, or Letters, a brief summary of main content in 150 words or fewer should be included in the manuscript. For articles reporting clinical trials, the trial registration number should be stated at the end of the Abstract. Abbreviations must be kept to a minimum and non-standard abbreviations explained in brackets at first mention. References should be avoided in the abstract. Three to six key words or phrases that do not occur in the title should be included in the Abstract page.

Introduction: The introduction should provide sufficient background information to make the article intelligible to readers in other disciplines and sufficient context clarifying the significance of the experimental findings.

Materials/Patients and Methods: The description should be brief but with sufficient detail to enable others to reproduce the experiments. Procedures that have been published previously should not be described in detail but appropriate references should simply be cited. Only new and significant modifications of previously published procedures require complete description. Names of products and manufacturers with their locations (city and state/country) should be given and sources of animals and cell lines should always be indicated. All clinical investigations must have been conducted in accordance with the Declaration of Helsinki (as revised in 2013, *https://wma.net/what-we-do/medical-ethics/declaration-of-helsinki*). All human and animal studies must have been approved by the appropriate institutional review board(s) and a specific declaration of approval must be made within this section.

Results: The description of the experimental results should be succinct but in sufficient detail to allow the experiments to be analyzed and interpreted by an independent reader. If necessary, subheadings may be used for an orderly presentation. All Figures and Tables should be referred to in the text in order, including those in the Supplementary Data.

Discussion: The data should be interpreted concisely without repeating material already presented in the Results section. Speculation is permissible, but it must be well-founded, and discussion of the wider implications of the findings is encouraged. Conclusions derived from the study should be included in this section.

Acknowledgments: All funding sources (including grant identification) should be credited in the Acknowledgments section. Authors should also describe the role of the study sponsor(s), if any, in study design; in the collection, analysis, and interpretation of data; in the writing of the report; and in the decision to submit the paper for publication. If the funding source had no such involvement, the authors should so state.

In addition, people who contributed to the work but who do not meet the criteria for authors should be listed along with their contributions.

References: References should be numbered in the order in which they appear in the text. Citing of unpublished results, personal communications, conference abstracts, and theses in the reference list is not recommended but these sources may be mentioned in the text. In the reference list, cite the names of all authors when there are fifteen or fewer authors; if there are sixteen or more authors, list the first three followed by *et al*. Names of journals should be abbreviated in the style used in PubMed. Authors are responsible for the accuracy of the references. The EndNote Style of *Drug Discoveries & Therapeutics* could be downloaded at **EndNote** (*https://www.ddtjournal.com/examples/Drug_Discoveries_Therapeutics.ens*).

Examples are given below:

Example 1 (Sample journal reference):

Nakata M, Tang W. Japan-China Joint Medical Workshop on Drug Discoveries and Therapeutics 2008: The need of Asian pharmaceutical researchers' cooperation. Drug Discov Ther. 2008; 2:262-263.

Example 2 (Sample journal reference with more than 15 authors):

Darby S, Hill D, Auvinen A, *et al*. Radon in homes and risk of lung cancer: Collaborative analysis of individual data from 13 European case-control studies. BMJ. 2005; 330:223.

Example 3 (Sample book reference):

Shalev AY. Post-traumatic stress disorder: Diagnosis, history and life course. In: Post-traumatic Stress Disorder, Diagnosis, Management and Treatment (Nutt DJ, Davidson JR, Zohar J, eds.). Martin Dunitz, London, UK, 2000; pp. 1-15.

Example 4 (Sample web page reference):

World Health Organization. The World Health Report 2008 – primary health care: Now more than ever. *https://apps.who.int/iris/handle/10665/43949* (accessed September 23, 2022).

Tables: All tables should be prepared in Microsoft Word or Excel and should be arranged at the end of the manuscript after the References section. Please note that tables should not in image format. All tables should have a concise title and should be numbered consecutively with Arabic numerals. If necessary, additional information should be given below the table.

Figure Legend: The figure legend should be typed on a separate page of the main manuscript and should include a short title and explanation. The legend should be concise but comprehensive and should be understood without referring to the text. Symbols used in figures must be explained. Any individually labeled figure parts or panels (A, B, *etc*.) should be specifically described by part name within the legend.

Figure Preparation: All figures should be clear and cited in numerical order in the text. Figures must fit a one- or two-column format on the journal page: 8.3 cm (3.3 in.) wide for a single column, 17.3 cm (6.8 in.) wide for a double column; maximum height: 24.0 cm (9.5 in.). Please make sure that artwork files are in an acceptable format (TIFF or JPEG) at minimum resolution (600 dpi for illustrations, graphs, and annotated artwork, and 300 dpi for micrographs and photographs). Please provide all figures as separate files. Please note that low-resolution images are one of the leading causes of article resubmission and schedule delays.

Units and Symbols: Units and symbols conforming to the International System of Units (SI) should be used for physicochemical quantities. Solidus notation (*e.g*. mg/kg, mg/mL, mol/mm^2/min) should be used. Please refer to the SI Guide *www.bipm.org/en/si/* for standard units.

Supplemental data: Supplemental data might be useful for supporting and enhancing your scientific research and *Drug Discoveries & Therapeutics* accepts the submission of these materials which will be only published online alongside the electronic version of your article. Supplemental files (figures, tables, and other text materials) should be prepared according to the above guidelines, numbered in Arabic numerals (*e.g*., Figure S1, Figure S2, and Table S1, Table S2) and referred to in the text. All figures and tables should have titles and legends. All figure legends, tables and supplemental text materials should be placed at the end of the paper. Please note all of these supplemental data should be provided at the time of initial submission and note that the editors reserve the right to limit the size

and length of Supplemental Data.

7. Online Submission

Manuscripts should be submitted to *Drug Discoveries & Therapeutics* online at *https://www.ddtjournal.com/login*. Receipt of your manuscripts submitted online will be acknowledged by an e-mail from Editorial Office containing a reference number, which should be used in all future communications. If for any reason you are unable to submit a file online, please contact the Editorial Office by e-mail at *office@ddtjournal.com*

8. Accepted Manuscripts

Page Charge: Page charges will be levied on all manuscripts accepted for publication in *Drug Discoveries & Therapeutics* (Original Articles / Brief Reports / Reviews / Policy Forum / Communications: $140 per page for black white pages, $340 per page for color pages; News / Letters: a total cost of $600). Under exceptional circumstances, the author(s) may apply to the editorial office for a waiver of the publication charges by stating the reason in the Cover Letter when the manuscript online.

Misconduct: *Drug Discoveries & Therapeutics* takes seriously all allegations of potential misconduct and adhere to the ICMJE Guideline (*https://icmje.org/recommendations*) and COPE Guideline (*https://publicationethics.org/files/Code_of_conduct_for_journal_editors.pdf*). In cases of suspected research or publication misconduct, it may be necessary for the Editor or Publisher to contact and share submission details with third parties including authors' institutions and ethics committees. The corrections, retractions, or editorial expressions of concern will be performed in line with above guidelines.

(As of December 2022)

Drug Discoveries & Therapeutics
Editorial and Head Office
Pearl City Koishikawa 603,
2-4-5 Kasuga, Bunkyo-ku,
Tokyo 112-0003, Japan.
E-mail: office@ddtjournal.com